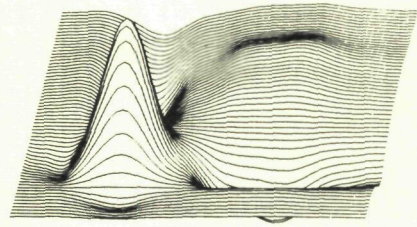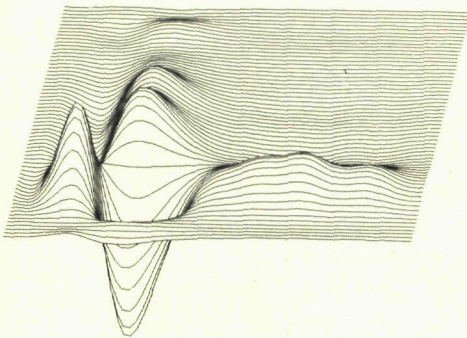# SPATIO-TEMPORAL AND CHROMATIC

PROPERTIES OF VISUAL NEURONES

IN THE RHESUS MONKEY

GENICULATE NUCLEUS

CCAM GIELEN

SPATIO-TEMPORAL AND CHROMATIC PROPERTIES OF VISUAL NEURONES IN THE RHESUS MONKEY GENICULATE NUCLEUS

SPATIO-TEMPORAL AND CHROMATIC PROPERTIES OF VISUAL NEURONES IN THE RHESUS MONKEY GENICULATE NUCLEUS

PROEFSCHRIFT

TER VERKRIJGING VAN DE GRAAD VAN DOCTOR
IN DE WISKUNDE EN NATUURWETENSCHAPPEN AAN DE
KATHOLIEKE UNIVERSITEIT TE NIJMEGEN, OP GEZAG
VAN DE RECTOR MAGNIFICUS PROF. DR. P.G.A.B. WIJDEVELD
VOLGENS BESLUIT VAN HET COLLEGE VAN DECANEN
IN HET OPENBAAR TE VERDEDIGEN OP
DONDERDAG 11 SEPTEMBER 1980
DES NAMIDDAGS OM 16.00 UUR

DOOR:

CONSTANTINUS CORNELIS ADRIANUS MARIA GIELEN
GEBOREN TE BREDA

SEPTEMBER 1980

Graag wil ik hier iedereen bedanken, die heeft bijgedragen aan de tot-
standkoming van dit proefschrift.

In de eerste plaats zijn dit de huidige en vroegere medewerkers van
het laboratorium voor Medische Fysica en Biofysica, die op velerlei wijzen
hun stempel gedrukt hebben op dit proefschrift. Daarnaast ben ik dhr.
Gelsing erkentelijk voor de precisie, waarmee hij de dia's maakte voor
mijn experimenten. Anneke Gielen-van den Broek wil ik bedanken omdat zij
het grootste deel van dit proefschrift op het Engels heeft doorgelezen
en, waar nodig, heeft gecorrigeerd.

C O N T E N T S

The retina in primates contains four receptor types: rods and red-, green-
and blue-sensitive cones, which contain different pigments and thus have
different spectral sensitivities. The signals from the receptors, elicited
by light falling on the retina, travel through the retina to the final
retinal cells: the retinal ganglion cells, undergoing a rather complex
neural processing, and from there along the axons of the retinal ganglion
cells to the lateral geniculate nucleus (LGN) and a number of other nuclei.
The retinal area, where light stimuli can influence the responses of a
neurone, is called the receptive field of that neurone. In 1953 Kuffler
showed that the receptive field of retinal ganglion cells is composed
of two regions: the centre and surround, which are concentrically organized
with a large spatial overlap. Stimulation of these two regions produces
antagonistic effects upon the activity of the neurone. This concentric
arrangement of receptive fields is a property, found in a majority of
retinal ganglion cells and neurones in the LGN in cat and monkey (Wiesel,
1960; Hubel and Wiesel, 1960; Rodieck and Stone, 1965; Wiesel and Hubel,
1966). The neural systems, that are concerned with the information process-
ing of centre and surround responses are called centre and surround
mechanism respectively. When centre and surround receive input from
different types of cone, the neurone will give antagonistic responses to
diffuse stimuli of different wavelength. These neurones are called colour-
opponent neurones.

In 1966 Enroth-Cugell and Robson demonstrated that cat retinal gan-
glion cells could be distinguished into two categories: if a position can
be found in the receptive field, where counterphase modulation of a spatial
sine wave or square wave grating does not influence the cell response, the
neurone is called X-type. If such a null-position cannot be found, the
neurone is classified as Y-type. This dichotomy has been demonstrated to
exist in retinal ganglion cells in cat and monkey (Hochstein and Shapley,

1976a; De Monasterio, 1978a) and in LGN neurones in cat and monkey (So
and Shapley, 1979; this thesis). The classification, based on the presence
or absence of a null-position, appeared to be no casual choice, since
X- and Y-cells have later been shown to differ in many more aspects, such
as response latency, receptive field size, distribution of receptive
fields over the retina, strength of the periphery effect and 'contrast
gain control' (Peichl and Wässle, 1979; Kratz et al., 1978; Derrington
et al., 1979; Dreher et al., 1976; Derrington and Fuchs, 1979; Shapley
and Victor, 1978) and, in monkey, also in the chromatic properties (De
Monasterio 1978a,b,c; this thesis).

X-cells

     In monkey, X-cells have colour-opponent properties (Dreher et al.,
1976; De Monasterio, 1978a,b; this thesis), which means that antagonistic
responses are elicited in different parts of the visible spectrum. This
property is a consequence of the fact, that the antagonistic mechanisms
in the receptive field, centre and surround, are mediated by different
types of cone (Wiesel and Hubel, 1966; De Monasterio, 1978a,b; De Mo-
nasterio et al., 1975). Because of the spatial overlap of centre and
surround and the overlap of the spectral sensitivity of the three types
of cone, it is impossible to measure responses, originating from a
single type of cone. The response contributions from a single type of
cone to centre and surround, mentioned above, are obtained by spectral
adaptation of one or two types of cone, while measuring responses from
the other type of cone. However, this adaptation also reduces the gain
and probably affects the time course of the responses of the cone type
under study. In chapter 1 two methods are described which enable the
measurement of response contributions of a single type of cone to X-cells
without adaptation techniques.

     The time course of the response contributions of a single type of
cone appeared to be remarkably similar over many neurones irrespective
of differences in other properties such as receptive field size, eccen-
tricity etc. Moreover, the three types of cone appeared to have equal
temporal properties, apart from the sign of the response (on/off), the
gain and the time delay of the response, which is somewhat longer (mean
value: 16 msec) for surround mediated cone type responses with respect
to the response latency of the centre mediating cone type contributions.

2

These results indicate, that a neurone is fully characterized by the
parameters sign, strength and time delay of the responses of the contri-
buting types of cone.

The property of X-cells that a position can be found where amplitude
modulation of a standing sine wave grating does not affect the firing rate
of the neurone, does not imply, that centre and surround responses
summate linearly. Other tests are necessary to investigate this point.
Enroth-Cugell and Lennie (1975) investigated this issue in cat retinal
ganglion cells with small spots and annuli. Their results suggest linear
summation. The nature of the combination of centre and surround responses
in X-cells is studied in chapter 1 and appeared to be linear within
experimental accuracy. Based upon these results a model was proposed to
describe the responses of LGN X-cells.

The sign and strength of the response contributions of the three types
of cone are determined in chapter 2. The responses to several stimuli were
predicted with the model proposed in chapter 1, in order to investigate the
validity of the assumptions which underly this model.

An interesting aspect in this investigation is the extent to which the
properties of LGN X-cells could be related to the results of psychophysical
measurements on chromatic and luminous flicker, especially since these
measurements have led many investigators to postulate two channels in the
visual system: one channel for luminance and one for chromatic information
processing (King-Smith and Carden, 1976; Tolhurst, 1977). Therefore re-
sponses of LGN neurones to chromatic and luminous flicker were investigated.

As a consequence of the small difference in latency between the re-
sponses of the opponent mechanisms, the transfer functions for chromatic
and luminous flicker appeared to be different in that the transfer function
for chromatic flicker has less low-pass and more high-pass attenuation than
the transfer function for luminous flicker. Although this difference is in
qualitative agreement with psychophysical measurements, a quantitative dis-
crepancy between psychophysical and electrophysiological results is caused by
the fact that the psychophysically determined high-frequency cut-off for
chromatic flicker is at a lower frequency than the high-frequency cut-off
for LGN colour-opponent neurones. The results are presented in chapter 2.

Y-cells

Until the work of Hochstein and Shapley (1976a,b) the investigations

on Y-cells were mainly qualitative in character and remained confined to
the report of the many aspects of nonlinear behaviour of Y-cells. Hoch-
stein and Shapley systematically investigated the temporal and spatial
properties with sinusoidally modulated spatial sine wave gratings. Second-
order harmonic responses, which form the clearest expression of nonlinear
behaviour in Y-cells, could be elicited over a larger spatial region than
the linear response contributions. Led by these results they proposed a
model, which consists of a centre and surround mechanism, as in X-cells,
and a nonlinear mechanism. This nonlinear mechanism contains a large
number of subunits, which each have a receptive field smaller than the
centre mechanism of the Y-cell and extend over a large part of the retina.
The responses from these subunits are rectified before the point of
summation, which explains the nonlinear second-order harmonic responses.
Elaborating the model Victor and Shapley (1979) demonstrated that the
nonlinear mechanism in Y-cells can be conceived of as a static non-
linearity, sandwiched between two linear systems. In another study Shapley
and Victor (1978) found that stimulation of the receptive field surround
in cat retinal ganglion cells reduced the responses of the receptive field
centre in a frequency selective way, which is a nonlinear effect. This
effect was small in X-cells in contrast to the effect in Y-cells. Their
results suggest that the mechanism, which modifies the responses from the
linear systems, is the same mechanism, which generates the second-order
harmonic responses.

Apart from the second-order harmonic responses to amplitude modulated
spatial sine wave gratings another way of nonlinear behaviour was reported
by Krüger and Fischer (1973) and Krüger et al. (1975), who showed that
a rapid displacement of a stimulus pattern far away from the classical
receptive field elicited responses in retinal ganglion cells (shift-effect).
However, Derrington et al. (1979) demonstrated that the mechanisms, which
generate the second-order harmonic responses and the shift-effect, have
similar spatial properties, at least in cat, suggesting that a single
mechanism underlies both phenomena.

The model, which is proposed for retinal ganglion cells in cat is
supported by the results from intracellular recordings in the mudpuppy
retina (Werblin, 1972). Recordings in bipolar cells have shown, that these
cells have a receptive field with a centre and surround as in X-cells, and
that the bipolar cell responses, which are sustained, are not influenced

4

by stimulation far from the receptive field centre (Werblin, 1972; Thibos and Werblin, 1978a,b). However, amacrine cells give transient responses to both intensity increments and decrements and are responsive to stimulation far from the receptive field.

Since most experiments on Y-cells are done on cat retinal ganglion cells it is interesting to investigate the properties of Y-cells in the rhesus monkey, which has a visual system very similar to the human. A model is proposed to describe the main response properties of LGN Y-cells. The model consists of a linear centre and surround mechanism, which responses are combined before a stage, where the combined centre and surround responses are modified by the responses from a nonlinear mechanism. This nonlinear subsystem also contributes to the cell response by a direct pathway. The gaussian white noise (GWN) crosscorrelation method was used to determine the temporal properties of the subsystems of the model. This method, that will be discussed in more detail below, has the advantage over the use of other methods, such as the use of sinusoidally modulated spatial sine wave gratings, that it offers the possibility to determine the sequence of linear and nonlinear systems. Sinusoidally modulated sine wave gratings were used to investigate the spatial properties of the linear and nonlinear systems in the model. Moreover, the temporal response properties to the sine wave stimuli were compared with the results, obtained with the GWN crosscorrelation method. The results indicate, that the centre mechanism behaves linearly indeed. The properties of the nonlinear mechanism are compatible with a static nonlinearity, sandwiched between two linear systems. The nonlinear mechanism responds to higher spatial frequencies and to lower temporal frequencies than the linear centre and surround mechanisms.

System identification with the GWN crosscorrelation method

As already described, the behaviour of LGN neurones may be very nonlinear. This implies that linear system theory will be inadequate to give a characterization of these neurones and a more general approach to system analysis was chosen.

Volterra (1959) showed, that in general for a system, that is nonlinear, time invariant, has infinite memory and is analytic, the relation between input $x(t)$ and output $y(t)$ is given by a summation of convolution integrals of the input $x(t)$ with the Volterra kernels. However, the calcu-

lation of the Volterra kernels of an unknown and in general nonlinear
system is a nearly impossible task with present analytical and computa-
tional means. This is mainly due to the fact, that the calculation of the
n-th order kernel depends on the other Volterra kernels: the kernels can-
not be calculated independently. Wiener (1958) solved this problem by the
introduction of a set of functionals $\{G_m\}$ of increasing order that are
orthogonal to each other with respect to a gaussian white noise input.
Moreover, the orthogonality gives the Wiener series a stronger convergence
than the Volterra series. Wiener showed, that the response $y(t)$ of a system
to the stimulus $x(t)$ with power level P_x can be written as

$$y(t) = \sum_{m=o}^{\infty} \{G_m(h_m(\tau_1, \tau_2, \ldots, \tau_m); x(t^l), t^l < t)\}$$

A gaussian white noise input is chosen since such a signal subjects a
system to all possible stimulus inputs, which sometimes gives the most
efficient way to investigate the system (Bendat and Piersol, 1966). With
a gaussian white noise input $x(t)$ the Wiener kernels $h_m(t_1, t_2, \ldots, t_m)$
can be calculated by

$$h_o = \lim_{T \to \infty} \frac{1}{T} \int_0^T y(t) \, dt$$

$$h_1(\tau) = \frac{1}{P_x} \lim_{T \to \infty} \frac{1}{T} \int_0^T y(t)x(t-\tau) dt$$

$$h_2(\tau_1, \tau_2) = \frac{1}{2P_x^2} \lim_{T \to \infty} \frac{1}{T} \int_0^T y(t) \, x(t-\tau_1)x(t-\tau_2)dt - \frac{1}{2P_x} \delta(\tau_1-\tau_2)$$

etc.

(Lee and Schetzen, 1965). The response $y(t)$ of neurones is not a continuous
signal but consists of a sequence of actionpotentials. It is generally
assumed, that the information of this signal is contained in the time of
occurence of the actionpotentials since their size and shape is in-
variably the same. Accordingly, the response or sequence of actionpoten-
tials $y(t)$ may be written as

$$y(t) = \sum_{i=1}^{N} \delta(t-t_i)$$

where t_i indicates the time of occurence of the i-th actionpotential.
Therefore the Wiener kernels are given by

$$h_o = \lim_{T\uparrow\infty} \frac{N(T)}{T}$$

$$h_1(\tau) = \frac{1}{P_x} \lim_{T\uparrow\infty} \frac{1}{T} \sum_{i=1}^{N(T)} x \ (t_i-\tau)$$

$$h_2\ (\tau_1,\tau_2) = \frac{1}{2P_x^2} \lim_{T\uparrow\infty} \frac{1}{T} \sum_{i=1}^{N(T)} x(t_i-\tau_1)x(t_i-\tau_2) - \frac{1}{2P_x} \delta\ (\tau_1-\tau_2)$$

etc.

where $N(T)$ is the number of actionpotentials in $[0,T]$. The zeroth order Wiener kernel only gives the mean firing rate of the neurone. The first order Wiener kernel gives a best linear approximation of the neurone in the sense of least square error. Nonlinear response properties are given by the contributions from the higher order Wiener kernels.

The response of the neurone to the stimulus $s(t)$ with the same power level P_x can be related to the calculated Wiener kernels by the formula

$$y(t) = h_o + \int h_1(\tau)\ s(t-\tau)d\tau + \int\int h_2(\tau_1,\tau_2)\ s(t-\tau_1)\ s(t-\tau_2)d\tau_1 d\tau_2$$

$$+\ \ldots.\ etc.$$

The response $y(t)$ to a stimulus $s(t)$, which is predicted on the base of the Wiener kernels is a continuous signal and is an estimator of the probability per unit of time of the generation of an actionpotential. Experimentally the probability density of the generation of an action-potential can be obtained by averaging the responses to a repeated presentation of the stimulus. As a matter of fact, the probability density function is a more interesting signal than the single sequence of action-potentials to a stimulus, since the generation of actionpotentials is a stochastic process, modulated by the stimulus.

Bendat, J. and Piersol, A. (1966), Measurement and analysis of random
    data. New York: Wiley.

De Monasterio,F.M., Gouras, P. and Tolhurst, D.J. (1975), Trichromatic
    colour opponency in ganglion cells of the rhesus monkey retina. J.
    Physiol. 251,197-216.

De Monasterio,F.M. (1978a), Properties of concentrically organised X and
    Y ganglion cells of macaque retina. J.Neurophysiol. 41,1394-1417.

De Monasterio, F.M. (1978b), Center and surround mechanisms of opponent-
    color X and Y ganglion cells of retina of macaques. J.Neurophysiol.
    41,1418-1434.

De Monasterio,F.M. (1979c), Properties of ganglion cells with atypical
    receptive-field organization in retina of macaques. J.Neurophysiol.
    41,1435-1449.

Derrington,A.M., Lennie,P. and Wright,M.J.(1979), The mechanism of
    peripherally evoked responses in retinal ganglion cells. J.Physiol.
    289,299-310.

Derrington,A.M. and Fuchs,A.F. (1979), Spatial and temporal properties of
    X and Y cells in the cat lateral geniculate nucleus. J.Physiol. 293,
    347-364.

Dreher,B., Fukada,Y. and Rodieck,R.W. (1976), Identification, classification
    and anatomical segregation of cells with X-like and Y-like properties in
    the lateral Geniculate nucleus of old-world primates. J.Physiol.
    258,433-452.

Enroth-Cugell,C. and Robson,J.G. (1966), The contrast sensitivity of retinal
    ganglion cells of the cat. J.Physiol. 187,517-552.

Enroth-Cugell, C. and Lennie,P. (1975), The control of retinal ganglion
    cell discharge by receptive field surrounds.J.Physiol. 247,551-578.

Hochstein,S. and Shapley,R.M. (1976a), Quantitative analysis of retinal
    ganglion cell classifications. J.Physiol. 262,237-264.

Hochstein,S. and Shapley,R.M. (1976b), Linear and nonlinear spatial sub-
     units in Y cat retinal ganglion cells. J.Physiol. 262,265-284.

Hubel,D.H. and Wiesel,T.N. (1960), Receptive fields of optic nerve fibers
     in the spider monkey. J.Physiol. 154, 572-580.

King-Smith, P.E. and Carden,D. (1976), Luminance and opponent-color
     contributions to visual detection and adaptation and to temporal and
     spatial integration. J.Opt.Soc.Am., 66,709-717.

Kratz,K.E., Webb,S.V. and Sherman,S.M. (1978), Electrophysiological classi-
     fication of X- and Y-cells in the cat's lateral geniculate nucleus.
     Vision Res. 18, 489-492.

Krüger,J. and Fischer,B. (1973), Strong periphery effect in cat retinal
     ganglion cells. Excitatory responses in On- and Off-center neurons
     to single grid displacements.Exp.Brain Res. 18,316-318.

Krüger,J., Fischer,B. and Barth,R. (1975), The shift-effect in retinal
     ganglion cells of the rhesus monkey. Exp.Brain Res. 23,443-446.

Krüger,J. (1977), The shift-effect in the lateral geniculate body of the
     rhesus monkey. Exp.Brain Res. 29,387-392.

Kuffler,S.W. (1953), Discharge patterns and functional organization of
     mammalian retina. J.Neurophysiol. 16,37-68.

Lee,Y.W. and Schetzen,M. (1965) Measurement of the Wiener kernels of a non-
     linear system by cross-correlation. J.Int.Control, 2,237-254.

Peichl,L. and Wässle,H. (1979), Size, scatter and coverage of ganglion cell
     receptive field centres in the cat retina. J.Physiol. 291,117-141.

Rodieck,R.W. and Stone,J. (1965), Analysis of receptive fields of cat
     retinal ganglion cells. J.Neurophysiol. 28, 833-849.

Shapley,R.M. and Victor,J.D. (1978), The effect of contrast on the transfer
     properties of cat retinal ganglion cells. J.Physiol. 285,275-298.

So,Y.T. and Shapley,R.M. (1979), Spatial properties of X and Y cells in
     the lateral geniculate nucleus of the cat and conduction velocities
     of their inputs. Exp.Brain Res. 36,533-550.

Thibos,L.N. and Werblin,F.S. (1978a), The response properties of the steady
     antagonistic surround in the mudpuppy retina. J.Physiol. 278,79-99.

Thibos,L.N. and Werblin,F.S. (1978b), The properties of surround antagonism
     elicited by spinning windmill patterns in the mudpuppy retina.
     J.Physiol. 278,101-116.

Tolhurst,D.J. (1977), Colour-coding properties of sustained and transient
     channels in human vision. Nature, 266,266-268.

Victor,J.D. and Shapley,R.M. (1979), The nonlinear pathway of Y ganglion
    cells in the cat retina. J.Gen.Physiol., 74, 671-689.
Volterra,V. (1959), Theory of functionals and of integral and integro-
    differential equations. Dover Publications, New York.
Werblin,F.S. (1972), Lateral interactions at inner plexiform layer of
    vertebrate retina: antagonistic responses to change. Science 175,
    1008-1010.
Wiener,N. (1958), Nonlinear problems in random theory. M.I.T. Press and
    John Wiley.
Wiesel,T.N. (1960), Receptive fields of ganglion cells in the cat's retina.
    J.Physiol. 153, 583-594.
Wiesel,T.N. and Hubel,D.H. (1966), Spatial and chromatic interactions in
    the LGB of the rhesus monkey. J.Neurophysiol. 29, 1115-1156.

CONTRIBUTIONS OF THE THREE CONE MECHANISMS TO RESPONSES OF COLOUR-
OPPONENT X-CELLS IN MONKEY LGN : A QUANTITATIVE STUDY

1.1. Introduction

Single unit studies in the primate visual system at the level of retinal
ganglion cells (De Monasterio et al., 1975a),LGN units (De Valois, 1965;
Wiesel and Hubel, 1966) and cortical units (Michael, 1978a; 1978b) have
demonstrated that differences in spectral sensitivity among neurones
reflect differences in sign and strength of the input signals from rods
and cones. The purpose of this study is to find out, how these various
receptor type inputs in monkey LGN colour-opponent neurones, combine
and to describe, at a quantitative level, the signal processing occurring
between each receptor type and the neurone.

The classification of neurones into X and Y type, based on the
property of linear or nonlinear spatial summation and first applied on
retinal ganglion cells (Enroth-Cugell and Robson, 1966) has been extended
recently to higher visual centres such as the lateral geniculate nucleus
(Shapley and Hochstein, 1975). As stressed by De Monasterio (1978a) the
existence of a null-position in the commonly used X-Y test, where reversal
of the contrast of a spatial sine wave grating in a range of spatial
frequencies does not elicit a change in firing, indicates only that these
neurones have linear spatial summation within the centre and surround
mechanism, prior to the stage of combination of centre and surround
responses. Enroth-Cugell and Lennie (1975) showed, that retinal ganglion
X-cells in cat also have linear summation of centre and surround responses.
If this linear summation of centre and surround responses occurs in monkey
LGN X-cells as well, it implies that the responses, originating from

different types of cone, summate linearly too, since centre and surround
of LGN colour-opponent units are mediated by input from different types
of cone (Wiesel and Hubel, 1966). In this paper it is shown that type
I (Wiesel and Hubel, 1966) colour-opponent neurones behave as X-cells and
combine signals from the various cone types linearly. The neural pathway
between the receptors of a single type of cone, which gives input to a
neurone, and the spike generating mechanism is called a cone mechanism.

It has also been investigated to what extent the neural signal
processing in the retinal and geniculate neural networks, which determines
how light absorption in a particular cone pigment ultimately contributes
to the response of the LGN neurone, can be characterized as linear. For
this purpose the Gaussian white noise (GWN) analysis is a useful tool,
since it provides a general characterization of the linear and non-
linear response contributions and can reveal the sequence of linear and
nonlinear mechanisms.

The results of this study have revealed that nonlinearities in the
response contributions from the three types of cone within a luminance
range of 0.5 logunit appear to be due to rectification at the spike
generating mechanism. Apart from this rectification the response contri-
butions are linear if the cell response remains below the level of satu-
ration. Moreover, it appeared that all cone mechanisms contribute to the
cell response with the same time course. This is related to the fact that
centre and surround have equal temporal properties apart from the sign,
the strength and a small time delay of the surround response with respect
to the centre response. The cell response appeared to be equal to the
linear addition of the response contributions from the three types of
cone. This enables the correct prediction of the cell response to various
stimuli if the sign, strength and time course of the contributions from
the types of cone are known.

In the alert monkey the strength of the responses and the maintained
activity were larger on the average than in the anaesthetized monkey. How-
ever, the time course of the responses was equal in both the alert and
anaesthetized monkey.

1.2. Methods

1.2.1. Animal preparation

Extracellular recordings were obtained in the lateral geniculate nucleus
(LGN) in chronic rhesus monkeys (Macaca mulatta). Prior to the recordings
a stainless steel chamber was fixed, under anaesthesia, on the skull
over a trephine hole aimed at the LGN. The dura was left intact. A light
aluminium crown was attached to the skull with dental cement to provide
for a painless head fixation during the experiments (modified after Friend-
lich, 1973). After a recovery period of some weeks experiments began,
each session lasting up to twenty hours once every two weeks for each
animal. The monkey was anaesthetized with ketamine hydrochloride (1 mg/kg)
and subsequently paralyzed with an initial shot of 30 µg/kg pancuronium
(Organon; The Netherlands) followed by a continuous infusion of 30 µg/kg/
hour under artificial respiration (20 strokes/min.) with a mixture of
N_2O and $O_2 (2 : 1)$. Rectal temperature was maintained at 37.5^o C. Expired
CO_2 was monitored with an infant capnograph (Type MO 1, Godart, The
Netherlands) and kept between 4-5%.

Mydriasis and cycloplegia were obtained with atropine sulphate and
phenylephrine hydrochloride. A contact lens with an artificial pupil of
3 mm diameter and well chosen radius (6.3-6.5 mm) protected the cornea.
Usually only one contact lens was used on either the right or left eye,
dependent on the layer of the LGN where the recording was made. The other
eye was closed. A 2% methylcellulose solution was used as a contact lens
cushioning fluid. The optical quality of the eyes was carefully checked
at regular intervals during the experimental session. When the optical
quality began to deteriorate to the extent that tiny bloodvessels could no
longer clearly be seen, the eye was closed and recordings were continued
in a layer of the LGN, which received its inputs from the other eye.
Additional spectacle lenses were placed to focus the stimuli on the retina.
The power of the required spectacle lenses was determined by retinoscopy
with an accuracy of 0.5 diopter.

To reduce residual drift eye movements, the eye was glued at four
points on the limbus with a small amount of dura glue (Hystoacril; Braun-
Melsungen) to a mechanically stabilized semicircular holder. This method
reduced the eye movements for many hours to small oscillations of not
more than 1 minute of arc, due to heart beat. In a few initial experiments

13

these small residual eye movements were measured with a small beam, aimed
at a small mirror,   glued onto the eye. The reflected beam was projected
onto a screen, which enabled the measurement of eye movements within 0.1
min. of arc. A local anaesthetic (Novesine) was dropped into the eye, but
in fact no clear signs of discomfort or irritation were seen during or
after the experiment.

    Before recording began, four or five retinal landmarks, oftenest
bifurcations of bloodvessels, were projected on the tangent screen by
means of a reversible ophthalmoscope. Receptive field position was measured
with respect to the known fixed points on the retina. Comparing these
points with a fundus photograph of the same retina, made earlier, receptive
field position with respect to the fovea could be reconstructed within 0.5
deg. To reduce tangential distortion the monkey could be rotated about a
vertical and a horizontal axis so that even for peripheral receptive
fields tangential distortion could be kept minimal.

    The alert monkey was trained to fixate within a small rectangular
square on the screen and received a reward of apple juice, when fixation
within the square exceeded a certain duration. The monkey was sitting in
a primate chair and the head was fixated to the chair with the aluminium
crown attached to the skull. In an operation under anaesthesia, several
months before the experiments, a coil was implanted under the conjunctiva
thus enabling the measurement of eye movements with two perpendicular
alternating magnetic fields (Fuchs and Robinson, 1966). The eye movements
of the monkey, which was used previously in experiments on the oculomotor
system, provide a good indication of the state of alertness, since the
maximum velocity in saccadic eye movements is reduced and the amplitude
of drift eye movements increases during drowsiness. Diffuse stimuli, which
homogeneously illuminated a square of 120x120 deg. in front of the monkey,
were modulated on and off at regular intervals of 1 sec. or were modulated
by gaussian white noise. The pupils were dilated by atropine. Responses
obtained during saccades or blinks or when the monkey fixated near the
edge of the stimulus square, were excluded from the analysis.

1.2.2. Data_recording

Single unit activity was recorded with tungsten micro-electrodes (1.0-2.5 MΩ)
measured at 1000 Hz. In the experiments both with the anaesthetized and the

alert monkey a closed chamber system was used for stabilization and a guard
tube was used to penetrate the dura. Signals were amplified with a pre-
amplifier (Grass P16) and monitored on an oscilloscope to insure single
cell recording. Action potentials were level discriminated and their moments
of occurrence were sent to a PDP 11/45 computer with a precision of 0.1
msec. Data were stored on disc for off-line analysis.

1.2.3. Stimulus generation

Spatial counterphase sine wave gratings for the classification of units
into X or Y type were generated on an oscilloscope (HP 1321 A) with a
repetition rate of 200 images/sec. The spatial frequency of the sine wave
pattern could be varied from 0.0625 to 24 cycles/deg. by a combination of
changing the spatial frequency on the oscilloscope and varying the distance
between the monkey and the screen. The spatial sine wave grating was
temporally modulated by a 5 Hz sinusoid. The phosphor P31 had a yellowish-
green hue. The horizontal axis was generated by a triggered ramp generator;
the vertical axis by a 3 MHz triangle generator. Intensity modulation was
performed with a programmable synthesizer (Rockland, model 5100). Mean
stimulus luminance on the oscilloscope was 10 cd/m^2. Modulation depth
could be varied and was usually < 30%. Linearity of the oscilloscope
luminance as a function of the input voltage was better than 10%.

Other stimuli could be rear projected on a screen with a Kodak
caroussel projector (S-RA 2000). Slides, including very small slits for
the investigation of the size and shape of the receptive field and spots
and annuli for stimulation of centre or surround (e.g. 50 μm on the slide,
corresponding to 1.5 min. of arc on the screen when at 171 cm. from the
monkey) were fabricated using techniques applied in electronic circuit
design. Stimuli could be moved using two mirrors, driven by two optical
scanners (G 300-PDT, General Scanning) controlled by two driver amplifiers
(CCX-102-T, General Scanning). The tangent screen (a stiff translucent
screen) could be placed at various distances from the monkey in a range
from 1-3 meter. Usually a distance of 1.71 meter was used (1 mm = 2 min.
of arc). Stimuli were projected on a background, which was obtained using
a tungsten lamp with a DC power supply. Unless stated otherwise the back-
ground had a luminance of 1 cd/m^2.

In order to be able to modulate the luminance of the stimuli on the

translucent screen the light source of the slide projector was replaced by an OSRAM 450 W xenon arc lamp. This could be modulated up to 90% from 0 to 150 Hz with a flat amplitude spectrum within 1% and with a maximum phase delay of 1.2 deg. at 150 Hz (TNO-450 Heinzinger modulation unit). For on/off modulation a shutter was used, driven by a G-100-PD scanner(General Scanning) with a rise time of 1 msec. Energy and wavelength of the beam were varied by means of neutral density filters (Gevaert) in steps of 0.1 log units and with narrow-band interference filters (centre wavelengths ranging from 440 to 656 nm; Schott) with 11 nm bandwidth. The Schott interference filters were checked for secondary transmission bands in the visible part of the spectrum. During the experiments the on- and offset of the stimulus modulation was continuously monitored on an oscilloscope using a photodiode (TIL-77 Texas Instruments). Stimulus luminance was measured with a telephotometer (UDT-11C) and an optometer (UDT-80X; United Detector Technology) with a calibrated photometric filter to match all stimulus wavelengths to the human photopic sensitivity curve, which equals the macaque photopic sensitivity curve (De Valois et al.,1974). To determine the number of quanten at the receptor level the data from van Norren and Vos (1974) were used to correct for absorption by the ocular media. The absorption spectrum of the macular pigment, which is equal for man and macaques (De Monasterio, 1978b), was taken from Wyszecki and Stiles (1967).

The stimuli, used to silence one type of cone and to study pure cone type responses from another type of cone were generated by two 450 W Xenon arc lamps, each with a 450 W Heinzinger modulation unit. In each light beam a Kodak Wratten filter (No. 61 and 29) was inserted.

During the crosscorrelation experiment the stimulus luminance was modulated with noise with a standard variation of 9% modulation depth. Use was made of low-pass filtered (6 dB/octave) GWN with the -3 dB point at 50 or 150 Hz. During the experiments a crude impression of the cross-correlation result was obtained using a digital delay line (sample rate 16 kHz) and an averager (Biomac 1000, Data Laboratories Ltd., London). In an off-line analysis the first order kernel was calculated on a PDP 11/45 computer. The pseudo random noise stimulus was stored on magtape with a 10 WT sample rate.

The pseudo random gaussian white noise stimulus was obtained by low-

pass filtering of a binary signal with a sequence length of 1048575 steps. A thorough check of the noise demonstrated a correlation between the amplitude and frequency distribution, in that higher frequencies tended to have higher amplitude values than lower frequencies, especially in the beginning of the sequence. Therefore the noise generator (HP 3722-A) was modified by the addition of 2 feedback loops from the 20-th bit to the 15-th and 11-th bit of the shift register. For the 50 Hz (150 Hz) GWN stimulus the sequence duration was about 15(5) minutes. Spurious results, due to the pseudo random character of the noise (Swerup, 1978) were excluded with this long period, since the experiment duration was usually less than the sequence duration.

1.3. Results

The data concern 70 X-type colour-opponent units from 3 anaesthetized rhesus monkeys, which were classified as type I (Wiesel and Hubel, 1966) because of the presence of two opponent mechanisms with a different spatial extent, and 9 colour-opponent units from 1 alert rhesus monkey. With regard to the data from the anaesthetized monkeys the centre received input exclusively from the red-sensitive type of cone in 35 units, from the green-sensitive type of cone in 28 units and from the blue-sensitive type of cone in 7 units. They received antagonistic input, in their surrounds, from the green-sensitive type of cone, the red-sensitive type of cone and both the red- and green-sensitive types of cone respectively. Classification according to Wiesel and Hubel (1966) was not attempted in the alert monkey. Of these units, 8 had RG antagonism. The other unit received excitatory input from the blue-sensitive type of cone and inhibitory input from the red- and green-sensitive types of cone.

Based on their responses to spatial counterphase gratings all units from anaesthetized animals were classified as X-type according to the criterion of linear spatial summation (Enroth-Cugell and Robson, 1966; Hochstein and Shapley, 1976). A similar result for type I units in retinal ganglion cells was found by De Monasterio (1978a).

Receptive field eccentricities were found up to 45 degrees, but most units (70%) had a receptive field within 10 degrees from the fovea.

1.3.1. Statement of the problem

The main purpose of this paper is to describe in terms of system theory
the neural signal processing which determines how light, absorbed by each
of the three cone pigment systems in the retina, influences the responses
of primate colour-opponent LGN units. A model representation of such a
neurone is given in Fig. 1.1. where the filter preceding the spike
generating mechanism comprises both the spectral properties of the pigment
systems in the retina as well as the further neural information processing
in the networks connected with the neurone. The spike generating mechanism,
which has a treshold and saturates for large input signals, is proposed to
be a static nonlinearity. Of course, we are aware that another rectifying
stage occurs at the level of retinal ganglion cells. However, the simple
model in Fig. 1.1. appears to be sufficient to explain the second order
kernel results, which contain information about nonlinearities in the
system (see appendix). We can think of several reasons why this result
was obtained: first, the retinal rectifier may be relatively unimportant
because retinal ganglion cells, at least in cat, have higher mean firing
rates (Cleland et al., 1971); secondly, almost all temporal filtering may
occur in the retina, rather than in the LGN, so that the two rectifying
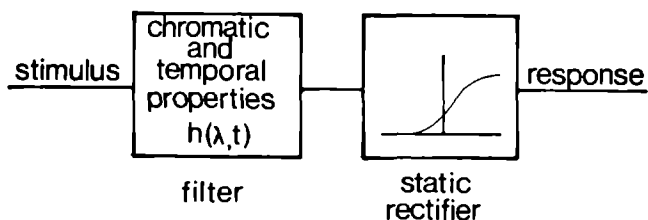stages can be lumped together.

Fig. 1.1. Schematic representation of LGN X-cell. Static nonlinearity represents
the spike generating mechanism of the neurone. Neural filter represents
the chromatic, spatial and temporal information processing of the
neural system before the spike generating mechanism.

One purpose of this paper is to determine how the response of an LGN neurone is determined by the responses from the three different types of cone and, possibly, also by the responses from the rods. For this purpose it is useful to make a further subdivision of the spectro-temporal filter (Fig. 1.1.) into four chromatic filters, $V(\lambda)$, representing the absorption spectra of the rod and cone pigment systems, each followed by a neural filter, $f(t)$, representing the sign, strength and time course of the response contributions of each receptor type to the cell response, and, finally, a stage where the signals from the rods and the three cone channels are combined (Fig. 1.2.).
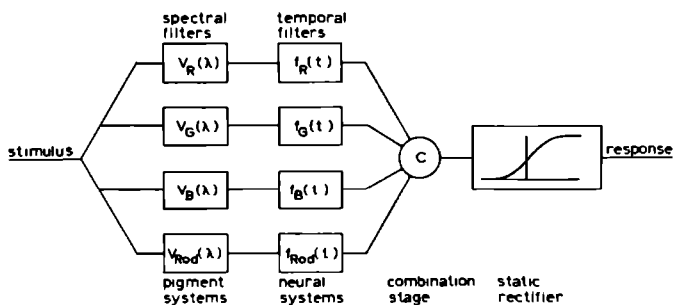

Fig. 1.2. More detailed model to describe functional properties of LGN type I units. $V_R(\lambda)$, $V_G(\lambda)$, $V_B(\lambda)$ and $V_{ROD}(\lambda)$ represent the spectral sensitivity of the red-, green- and blue-sensitive type of cone and of the rod system. $f_R(t)$, $f_G(t)$, $f_B(t)$ and $f_{ROD}(t)$ represent the temporal properties of the neural filter belonging to each receptor system. The responses of the neural filters combine at a stage before the spike generating mechanism.

The spectral absorption of each cone type mechanism can be found in the literature (Bowmaker et al., 1978; van Norren and Padmos, 1973) but the neural filter, which characterizes the temporal properties of the cone mechanism is unknown and will be investigated in this paper.

A valuable method to demonstrate input from a particular type of cone is selective adaptation of the other types of cone. However, for the following reason this method is not adequate for the purpose of this study. By the spectral overlap of the absorption curves (especially of the

red- and green-sensitive types of cone) adaptation of a particular
type of cone will also adapt the type of cone under study and thus change
the temporal properties of the corresponding cone type mechanism. More-
over, after partial adaptation an accurate determination of the strength
of the contribution of responses from this type of cone to the LGN
neurone is not possible anymore. Therefore other methods were used to
obtain the strength and time course of the response contributions of a
particular cone mechanism to the response of LGN neurones.

Led by the result of Enroth-Cugell and Lennie (1975), who found a
linear summation of centre and surround responses in cat retinal ganglion
X-cells, we hypothesize, that the responses from the cone type mechanisms
summate linearly in LGN neurones. This hypothesis will be investigated
later on (Figure 1.5.).

By the nature of linear addition, each response of the neurone at a
given wavelength is a linear combination of the responses of the receptor
mechanisms:

$$h(\lambda,t) = V_r(\lambda)f_r(t) + V_g(\lambda)f_g(t) + V_b(\lambda)f_b(t) + V_{rod}(\lambda)f_{rod}(t) \qquad (1)$$

where $h(\lambda,t)$ denotes the wavelength dependent impulse response of the
spectro-temporal filter in Fig. 1.1., $V(\lambda)$ indicates the spectral sensitiv-
ity of the receptor type and $f(t)$ denotes the impulse response of the
neural filter.

The wavelength dependent impulse response, $h(\lambda,t)$, was determined
with the method of GWN crosscorrelation (Lee and Schetzen, 1965), which
has been used earlier in the visual system of the goldfish (Schellart and
Spekreijse, 1972) and catfish (Marmarelis and Naka, 1973a; 1973b; 1973c).
Apart from a constant the first order kernel gives the shape of the
impulse response of the linear filters for a system, consisting of some
linear filters followed by a static nonlinearity (Marmarelis and Marmarelis,
1978). For example, if the spike generating mechanism in Figure 1.2. has
a sigmoid relationship between input and output, and if the neural filter
is linear the first order kernel characterizes the linear system (see
appendix), whereas with other stimuli such as a step-increment of stimulus
intensity, the output of the neural filter is distorted by the sigmoid
function and the response depends on the dc level of the input signal.
Unless this nonlinearity is known, it is hard to obtain the filter char-
acteristics with light flashes, intensity increments, etc.

20

The absorption spectra, $V(\lambda)$, of the various pigment systems are
known from the literature (Bowmaker et al., 1978; van Norren and Padmos,1973).
The strength of the input from a receptor type is defined as the strength
of the response contribution of the receptor type at the optimally sensi-
tive wavelength. Since the time course of the cell response $h(\lambda,t)$ is
known from measurement and the spectral sensitivity of each receptor
type is known at each wavelength, the time course of the neural filters
can be found by solving a set of n equations with n unknown variables.
Because the number of known pigment systems is 4, the responses of the
LGN neurone at 4 properly chosen wavelengths would suffice. However, since
the system also adds noise to the response, a better estimation of the
time course of the responses of the neural filters is obtained when more
than 4 cell responses are considered. In our case we observed the cell
responses at 8 wavelengths. The first order kernel of each neural filter
was calculated with the computer program BMDP1R (Biomedical Computer
Programs, developed by Health Sciences Computing Facility, UCLA), which
performed a linear regression on corresponding individual sample points.
This method does not demand each neural filter being linear, but only
assumes a linear addition of the responses from the neural filters.

1.3.2. Temporal properties of neural filters

Figure 1.3A. shows a first order kernel for an R^+G^- unit, obtained with
a diffuse narrow band red (656 nm) stimulus, modulated by filtered GWN with
a mean luminance of 280 td.

     If the temporal properties at this wavelength are linear, the first
order kernel equals the response to a light flash of 656 nm and the
response to a step increment should be equal to the integral of the kernel.
This is valid only for teststimuli falling in the linear range of the
rectifier. The good agreement between predicted and measured responses
Figure 1.3B.) indicates that LGN type I units, except for response rectifi-
cation, behave linearly in good approximation. The transfer function to
luminous flicker at 656 nm (Figure 1.3C.) is obtained by Fourier trans-
formation of the first order kernel.

     The shape of the first order kernel varies with stimulus wavelength
(Figure 1.4. and 1.5.). The response to stimulus increments and decrements
can again be predicted accurately with the first order kernel for all

stimulus wavelengths. These results indicate, that the neurone may be
modelled by a linear filter followed by a spike generating mechanism
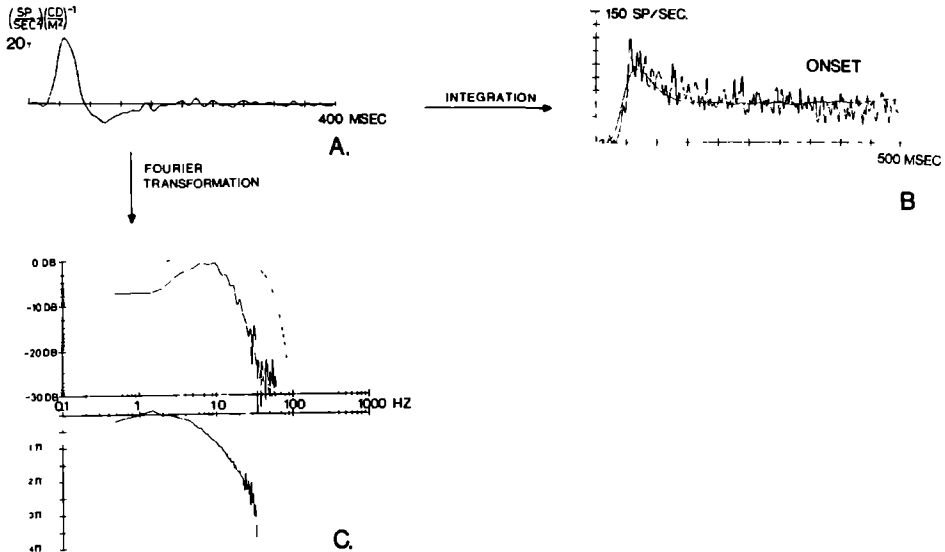(Figure 1.1.).

Fig. 1.3. A.An example of a first order kernel, obtained by GWN stimulation of
an R^+G^- type I unit with a diffuse 656 nm narrow band stimulus. The
modulation signal consisted of GWN,low-pass filtered at 50 Hz.B. The
fit between the measured response (PSTH) to intensity steps of 0.7 log
unit around a mean luminance of 280 td and the predicted response,
obtained by averaging the responses to 100 stimulus presentations and
by smoothing the averaged response with a filter with a gaussian
waveform ($\sigma = 3$ msec). C.The amplitude and phase characteristics,
obtained by Fourier transformation, revealing a maximum sensitivity
at about 9 Hz. The dashed curve in the amplitude spectrum gives the
spectrum of the GWN stimulus. In both A and B the stimulus had a
luminance of 280 td and covered the whole receptive field. Centre size
of 0.08 deg. at 1/e of the peak sensitivity. Eccentricity: 5 deg.

However, the linearity of the total system (neural filter and rectifier) is limited to specific stimulus conditions. When the stimulus modulation depth exceeds 30%, the cell response may saturate. Another nonlinear phenomenon is expressed by the fact, that the transfer function of the neurone changes, when the luminance is changed. This was found earlier by Spekreijse et al.(1971) who showed, that at lower modulation frequencies the amplitude of the response is related to relative modulation depth ($\Delta I/I$), whereas at higher modulation frequencies the response is related to absolute modulation depth (ΔI). This explains why the responses become larger and more high frequency tuned (faster) to stimuli with increasing mean luminance and equal relative modulation depth. Although most units appear to have no significant higher order nonlinear kernels, some units demonstrated second order kernels. However, these nonlinear response contributions can be attributed to the rectifying spike generating mechanism (see appendix).

This idea is supported by the fact, that neurones with strong responses and a low rate of maintained activity demonstrate the largest second order kernels. When stimulus intensity increases the second order kernels often increase especially at mean luminances above 400 td. Below 400 td nonlinear responses due to rectification contribute less than 5% of the total cell response.

In order to determine the temporal properties of LGN neurones at several wavelengths, the first order kernel was calculated at eight different wavelengths. The stimulus was diffuse, covering the whole receptive field. The flash response of a neurone changed continuously with change in wavelength as shown in Figure 1.4A for an B^+Y^- unit and in Figure 1.4B for an R^+G^- unit. The response contributions from the opponent mechanisms to $h(\lambda,t)$ differ not only in the initial sign of their kernel contribution, simply reflecting their response antagonism, but also in the delay (latency). Similarly to findings of Gouras and Zrenner (1979) in retinal ganglion cells, we found that the centre responses (blue- and red-sensitive type of cone in Fig. 1.4A and 1.4B respectively) in LGN units, too, always have a shorter latency than the surround responses (see below; Fig. 1.7.). In the spectral range where the opponent mechanisms strongly overlap (RG unit: $\lambda < 600$ nm; BY unit: $503 < \lambda < 529$ nm), the kernels have a triphasic shape which arises because stimuli here excite two opponent
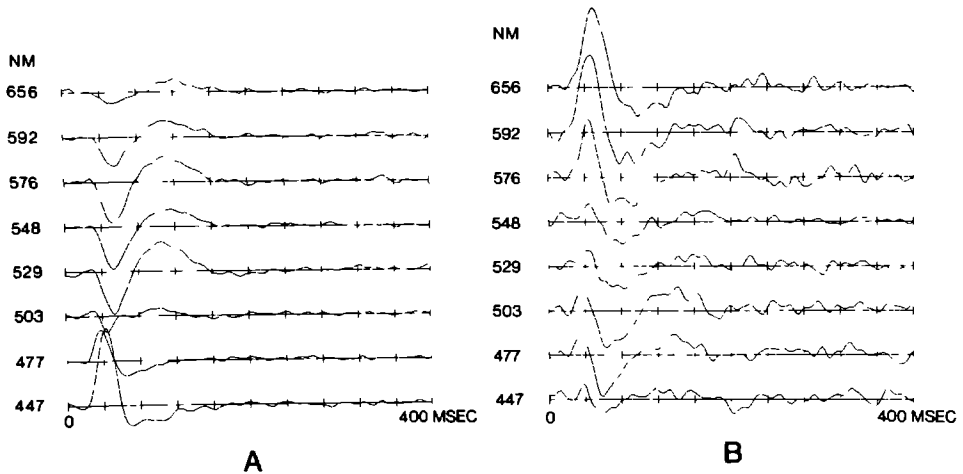
23

Fig. 1.4. A.The first order kernels at different wavelengths for a B^+Y^- unit are shown. The wavelength,where the sign of the response to a low frequency modulated narrow band stimulus reverses, is at about 500 nm. Below this wavelength the blue-sensitive type of cone dominates the cell responses. The on-response at the short wavelengths is due to the centre. The surround response at the long wavelengths has a small delay of about 15 msec with respect to the centre response. All narrow band stimuli were set at the same luminance (280 td) based on the photopic luminosity curve. Centre size of 0.13 deg at 1/e value of the peak sensitivity. Ecc.: 9 deg. B. First order kernels at different wavelengths for an R^+G^- unit. The first order kernel at 656 nm is almost completely due to the red-sensitive type of cone,which dominates the centre response. At lower wavelengths the responses from the red- and green-sensitive types of cone are intermingled. The neutral point of this unit was at about 548-576 nm. Stimulus luminosity was 280 td. Centre size: 0.04 deg at 1/e value of the peak sensitivity. Ecc.: 4 deg.

24

mechanisms with a difference in time delay. Also because of this difference
in latency, a true neutral wavelength was never found (Fig. 1.4A, B; see
below). For a correct interpretation of the results it should be kept in
mind that all stimuli were matched to the photopic luminosity curve.

Data such as in Fig. 1.4A, B were analysed in the computer with the
regression method. That is, the computer has calculated the four signals
$f_r(t)$, $f_g(t)$, $f_b(t)$ and $f_{rod}(t)$, which represent sign, gain and time course
of the four basic receptor mechanisms (see above), which give the best fit,
within the constraints of equation (1), to the $h(\lambda,t)$ data of that neurone.

Figure 1.5. shows how the contributions from the red- and green-
sensitive types of cone in the R^+G^- neurone, shown in Fig. 1.4B, vary with
wavelength (A) and, when summed, fit nicely with the first order kernels
measured at various wavelengths (B). This demonstrates that the response
to a narrow band chromatic stimulus is determined, in line with equation
(1), by a linear addition of the response contributions from the types of
cone, each weighed by a coefficient, determined by the spectral absorption
of the type of cone in the particular chromatic range of the stimulus.
Fig. 1.5. shows no contributions from rods and the blue-sensitive type of
cone since the strengths attributed to these receptor mechanisms by the
regression computation drowned completely in the noise so that they were
either absent or very weak (i.e. -30 dB relative to the dominant cone
input). The regression analysis to determine the four receptor type
contributions to the neurone was applied to 16 cells. The goodness of fit
is expressed by the correlation coefficient between the measured first
order kernel and the predicted first order kernel, based upon the calcu-
lated first order kernels for the four receptor types, at each of the eight
different wavelengths. Mean correlation coefficient is 0.85 (range:
0.57-0.95), indicating that the good fit in Fig. 1.5. was not atypical.
These results demonstrate that responses from different types of cone
summate linearly and, therefore, that the condition, on which the determi-
nation of the time course of the responses from the three types of cone
by the regression method was based, is satisfied.

All units were tested for rod input in the photopic luminance range.
No rod input could be demonstrated. Even units, which after 20 minutes
dark adaptation gave clear responses, which because of their spectral
sensitivity and the fact that stimulus intensity was below cone treshold,
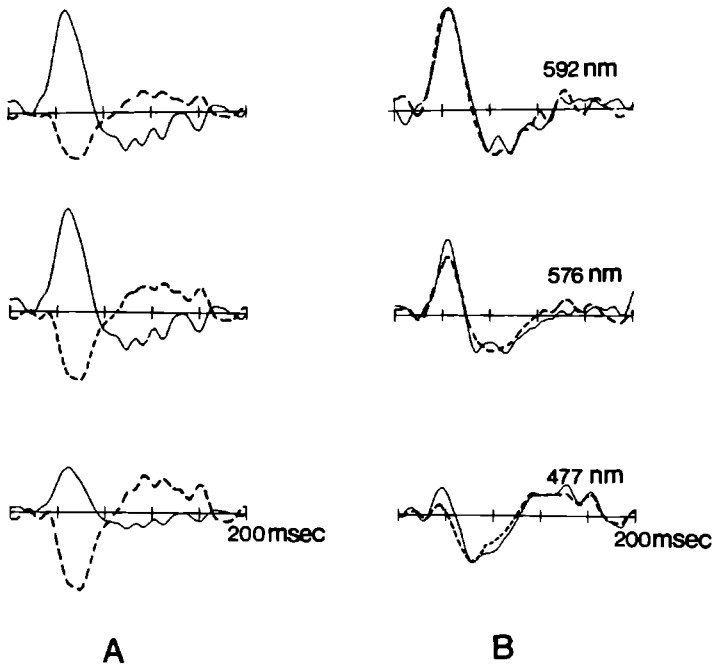were ascribed to rod input, failed to demonstrate rod input in the photopic

Fig. 1.5. A.Contributions of red and green cone mechanisms to responses at three
different wavelengths of an R^+G^- neurone as computed with the linear
regression method. Same neurone as in Fig. 1.4B. The regression
computation did not reveal any significant response contributions from
rods and from the blue-sensitive type of cone in this neurone. Note that
the response from the centre mediating red-sensitive type of cone has a
latency which is shorter and a polarity which is reversed with respect
to the surround contribution (green-sensitive type of cone). Note also,
that apart from these differences the time course of the signals from
the red- and green-sensitive types of cone are very much alike.
B. Illustrating that when the signals from the red- and green-sensitive
types of cone, shown in A, are added algebraically as suggested by
equation (1) which underlies the method to compute them, their sum
accurately matches the first order kernel, which was actually measured
at various wavelengths. Dashed curves are predicted kernels.

range. The results of the linear regression method indicated that rod input, if present at all, did not exceed the noise level of 30 dB in all neurones at about 200 td. Moreover, none of the RG units appeared to receive any significant input from the blue-sensitive type of cone (con- tributions less than 5%).

1.3.3. Time course of response contributions of cone mechanisms to LGN neurones.

Figure 1.6A shows the time course of the impulse responses of the neural filter for each of the cone mechanisms, determined in many neurones. All responses are scaled and the sign of the response is made positive. The upper set gives the time course for cone mechanisms mediating the centre; surround mediated responses are given in the lower set.

The temporal properties of the cone mechanisms were also investigated by another method in 9 units in order to have an independent check on the results in Figure 1.6A. This method, the spectral compensation method (Estévez and Spekreijse, 1974) does not require the assumption of linear addition of the responses from the three types of cone. Due to the overlap of the spectral sensitivity of the pigment systems a chromatic stimulus, aimed to stimulate a particular pigment system, will also stimulate another pigment system, be it much weaker. Therefore, a second stimulus of different wavelength was modulated in counterphase with the former stimulus in order to silence the response of the unintendedly modulated pigment system. The ratio of the modulation depths of both counterphase modulated stimuli, at which a given type of cone is silenced, was calculated from the spectra of the light source, the transmittance of the chromatic filters and the absorption spectrum of the pigment systems. With this method, first used in psychophysics by Estévez and Spekreijse (1974) it is possible to obtain responses from a single type of cone without any assumption about the nature of the interaction between responses from different types of cone (i.e. the combination stage in Fig. 1.2.). The compensation method results (Fig. 1.6B) were identical with the regression method results (Fig.1.6A).

Since both methods demand exact knowledge of the spectral sensitivity of the types of cone, we wondered whether some uncertainty in the bluish part of the spectrum due to absorption by the lens and the macular pigment might have caused us to attribute, erroneously, what were in fact con-
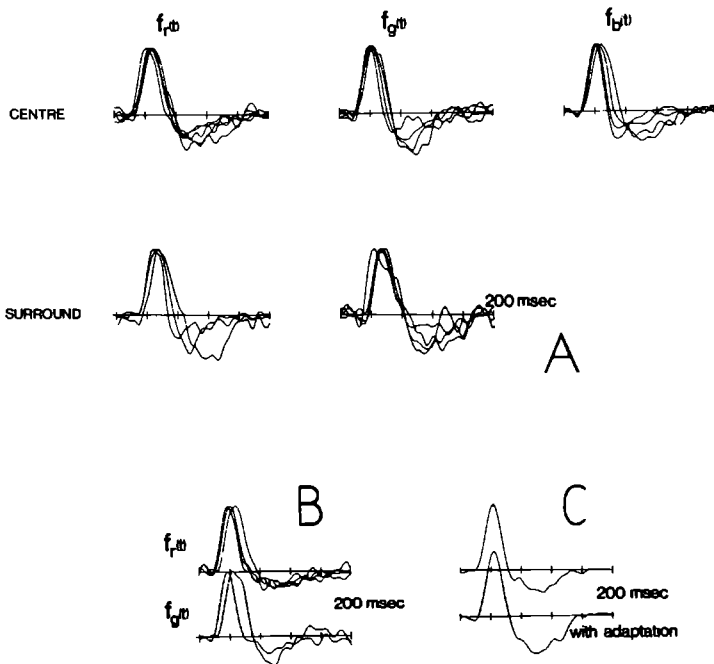
Fig. 1.6. A.Neural filter impulse responses for the three types of cone as
computed for LGN units. All impulse responses are scaled to have equal
sign and gain. The temporal properties of all neural filters appear to
be roughly the same apart from the small difference in time delay related
to whether the response is mediated by the centre or the surround
mechanism. All data were obtained at a luminance of 280 td. No blue
off-centre cells or cells with blue cone type input to the surround were
seen. The signal to noise ratio in the cone kernels giving input to the
surround is somewhat smaller due to the fact, that the gain of the
centre mechanism usually exceeds that of the surround mechanism. B. Neural
filter impulse responses for the red and green cone mechanisms, obtained
with the spectral compensation technique (see text). C.First order
kernels of a B^+Y^- type I unit at 447 nm, obtained without and with
a strong yellow background of 13000 td (Wratten filter No. 15).

tributions from the green-sensitive type of cone to the blue cone mechanism. Therefore we also determined the temporal properties with a strong yellow background (Wratten No. 15). The responses at 447 nm before and after yellow adaptation remained the same, indicating that the measured response originated from the blue-sensitive type of cone (Figure 1.6C) and demonstrating the reliability of the regression method results.

The results in Figure 1.6. demonstrate that all three cone mechanisms have equal temporal properties: peak latency or duration of the excitatory part of the impulse response of the neural filter of a particular cone type mechanism does not differ significantly ($P<0.05$) from that of another cone type mechanism. However, since the chromatic stimuli were matched to the photopic luminosity curve, the spectral density is more intense in the bluish part of the spectrum than in the range from 500 to 620 nm. Therefore, if we should have used an equal energy spectrum, the blue cone mechanism should have appeared somewhat more low-frequency tuned than the red and green cone mechanisms. Based upon measurements at lower intensities it can be predicted that in that case the optimal temporal frequency shifts from about 9 Hz to 6 Hz and the flicker fusion frequency from 30 Hz to about 20 Hz.

In accordance with results of Malpeli and Schiller (1978), who demonstrated a lack of blue-off centre cells in the visual system of the monkey, all cells, which centre received input from the blue-sensitive type of cone, gave on-centre responses. Since all B^+Y^- units had a blue-sensitive centre mechanism and since RG units appeared to receive negligible input from the blue-sensitive type of cone, Figure 1.6A shows no flash responses for the blue cone type mechanism, mediating the surround of LGN X-cells.

In summary the results in Figure 1.6. permit three conclusions. First, the time course of the response contributions of a particular cone type mechanism is independent of the sign (on/off). Secondly, the time course is independent on whether the cone mechanism gives input by the centre or surround apart from a small time delay. The third conclusion is that all three cone mechanisms give input to LGN X-cells with a similar time course.

The question whether the neural filters in the cone channels are linear was approached by comparing first order kernels and increment/decrement responses of RG neurones to stimuli designed to stimulate just one cone system (either R or G; spectral compensation method, see above). As there

was generally good agreement (such as in Fig.1.3B) between step responses and integrated first order kernels, the evidence is that neural filters, at least in RG cells, behave linearly.

1.3.4. Centre-surround responses

The results in Figure 1.6. already indicate that centre and surround of monkey LGN type I units have equal temporal properties apart from the sign of the response (on/off) and a small time delay. This point has been investigated in a more direct way with chromatic spots and annuli, which stimulate one mechanism while the other is adapted.

Figure 1.7. shows the temporal characteristics of centre and surround of a B^+Y^- type I unit. The only difference between the first order kernels of centre and surround pertains to the sign of the kernels and the mutual time delay Δt. The different phase characteristics can be understood from these two differences by a phase shift π and by a frequency dependent phase shift $\exp(-i\omega\Delta t)$. The time delay between centre and surround responses has a mean value of 16 msec. with a standard deviation of 5 msec. (n=31), which is close to values obtained for cat LGN units (20-30 msec.) by Singer and Creutzfeldt (1970). The fact, that centre and surround responses of type I units in monkey LGN have a similar time course agrees with results of Poggio et al. (1969) in cat LGN neurones.
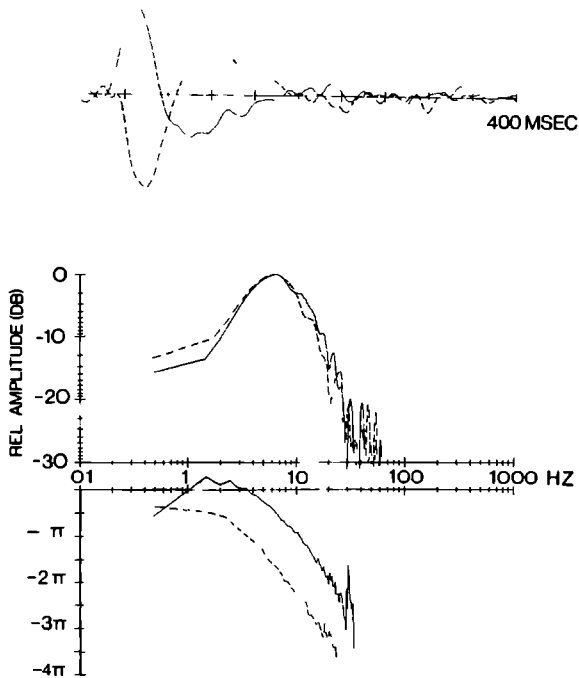
Fig. 1.7. The first order kernel and amplitude and phase characteristics for the centre and surround of a B^+Y^- type I cell. Both centre and surround (dashed curve) have equal temporal characteristics apart from a difference in pure time delay and the opposite sign of the responses, which results into a phase shift of the surround response with respect to the centre response. The centre was stimulated with a 447 nm spot; the surround with a 576 nm annulus. Both stimuli had a luminance of 280 td.

1.3.5. LGN neurone responses at the neutral point

Due to the differences in time delay between the antagonistic responses from the cone mechanisms there is no wavelength, where the responses of the antagonistic mechanisms cancel exactly. The same applies to the response to intensity increments. Figure 1.8A shows the responses to intensity increments and decrements for an R^+G^- type I unit. When both antagonistic inputs are equally strong (at about 576 nm for this unit) the

31

neurone responds with a transient burst due to the mutually delayed
antagonistic inputs. This implies that the neurone will not respond to
low-frequency modulated stimuli of 576 nm, but will respond at higher
modulation frequencies (Figure 1.8B). A similar result was found by Gouras
and Zrenner (1979) in monkey colour-opponent retinal ganglion cells.
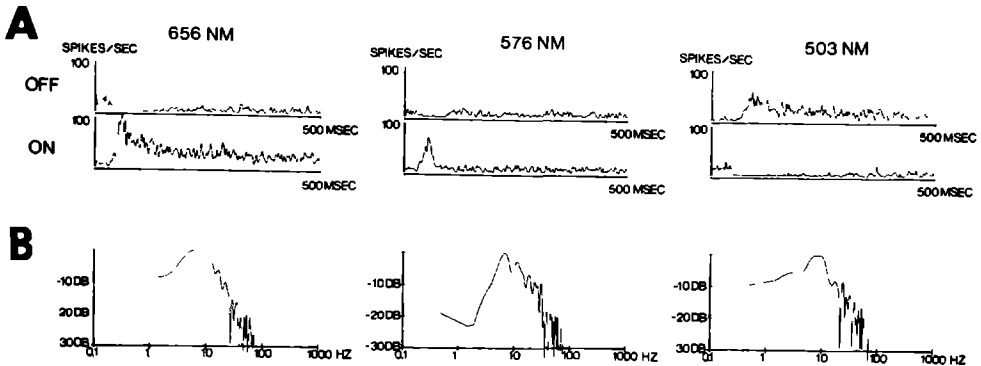

Fig. 1.8. A. PSTHs to intensity steps at 656 nm and 503 nm for an R^+G^- unit. The
response at 656 nm shows sustained firing in the on-period, the response
at 503 nm shows sustained firing in the off-period. At 576 nm the response
does not contain a sustained component, but shows only a short transient
burst at onset and a short lasting inhibition at offset due to the fact
that the centre response preceeds the surround response. B.Amplitude-
frequency characteristics at 656 nm, 576 nm and 503 nm. The amplitude
characteristics at 576 nm show low-frequency attenuation corresponding
with the transient responses at stimulus onset and offset.

The same can be stated, more rigorously, in mathematical terms. Suppose
a neurone receives input from two opponent chromatic systems. Then the
wavelength dependent impulse response is given by

$$h(\lambda,t) = V_1(\lambda)f_1(t) - V_2(\lambda)f_2(t)$$

where $V_1(\lambda)$ and $V_2(\lambda)$ is the spectral sensitivity of the centre and
surround mediating mechanism respectively

32

$f_1(t)$ and $f_2(t)$ is the impulse response of the centre and surround
mediating mechanism respectively

Since the centre and surround responses are equal apart from a time delay
Δt equation (2) becomes

$$h(\lambda,t) = V_1(\lambda)f_1(t) - V_2(\lambda)f_1(t-\Delta t)$$

The transfer function to luminous flicker at wavelength λ is obtained by
Fourier transformation:

$$H(\lambda,\omega) = V_1(\lambda)F_1(\omega) - V_2(\lambda)F_1(\omega)e^{-i\omega\Delta t}$$

$$= F_1(\omega)\left[V_1(\lambda) - V_2(\lambda)e^{-i\omega\Delta t}\right]$$

At the neutral point λ_n, where $V_1(\lambda_n) = V_2(\lambda_n)$, $H(\lambda_n,\omega)$ approaches zero
for small ω values, but at higher frequencies, where $\omega\Delta t > \pi$, the neurone
may give more vigorous responses than at other wavelengths λ.

1.3.6. Influence of anaesthesia

As described by Maffei et al. (1965) and Coenen and Vendrik (1971),
LGN neurones exhibit fluctuations in their responsiveness, related to sleep
and wakefulness. During the experiments with anaesthetized monkeys,
fluctuations in responsiveness were often observed, which could be pre-
vented by making noise, stroking the animal, etc. This motivated us to do
some experiments with an alert monkey. Fluctuations as observed in the
anaesthetized monkey were not observed. The time course of the response
contributions to LGN colour-opponent units from the three cone mechanisms
were calculated with the linear regression method. The time course of the
responses from the cone mechanisms in the alert monkey appeared to be the
same as in the anaesthetized monkey. Small differences between responses
in anaesthetized and alert monkey exist in that the responses to diffuse
stimuli seemed to be larger in the alert monkey and in that the mean firing
rate to a diffuse stimulus covering the complete receptive field, was
significantly higher ($p < 0.001$) in the alert monkey (mean firing rate is
24.2 sp/sec; range: 8.8 - 57.5 sp/sec) than in the anaesthetized monkey
(mean firing rate 7.5 sp/sec; range: 0.86 - 26.1 sp/sec).

1.4. Discussion

The results of this study show that it is possible to determine the strength,

sign and time course of the response contributions of the three cone
type mechanisms and to corroborate the model (Fig. 1.2.). Especially because
the temporal properties of the neural filters appear to be so stereotyped
(Fig. 1.6.), it is possible to characterize many of the differences among
colour-opponent LGN type I units accurately with just a few parameters
(chapter 2). The model predicts accurately the responses
to stimulus increments and decrements and explains the different temporal
properties of LGN neurones at various stimulus wavelengths. It also
explains why at the neutral wavelength, where the antagonistic chromatic
systems are equally strong, the responses cancel at low temporal fre-
quencies, but become less antagonistic at higher temporal frequencies
(Gouras and Zrenner, 1979). The model, so far, does not include the
spatial distribution of the different chromatic systems.

    One goal of this paper is to determine the sign, strength and time
course of the contributions from the three types of cone to the responses
of type I units in the monkey LGN. In contrast to electrophysiological
(van Norren and Padmos, 1973; Boynton and Baron, 1975) and psychophysical
evidence (Kelly, 1974),that signals from the blue-sensitive type of cone are
slower than those of red- and green-sensitive cones, all three cone
mechanisms appear to contribute to the responses of type I units with
equal time courses in this study. A methodological aspect which may partly
explain this discrepancy, but probably cannot completely account for the
difference, concerns the fact that in this study the intensities of the
small band chromatic stimuli were matched to the macaque photopic lumin-
osity curve, whereas usually equal energy spectra are used. Because the
macaque visual system is optimally sensitive at about 560 nm and much less
at wavelengths below 500 nm and above 620 nm (De Valois et al., 1974) our
narrow band stimuli, matched to the photopic luminosity curve, below 500
nm and above 620 nm contain more energy than those in the range from 500
to 620 nm. This choice of stimulus intensities causes responses from the
blue-sensitive type of cone at higher stimulus intensities than would have
been obtained with an equal energy spectrum. Since responses of LGN
neurones become more high frequency tuned at higher stimulus intensities
(Spekreijse et al., 1971; this study) the choice of an equal energy spec-
trum would have led to slower responses for the blue cone mechanism. Our
results demonstrate that, dependent on stimulus luminance, responses of the
blue cone mechanism can be as fast as the responses of the red and green

cone mechanisms. After correction for the different intensities that were used, the temporal properties for the blue cone mechanism – found in this study – are much in line with other electrophysiological results. The higher fusion frequency, found by De Monasterio (1979) and Gouras and Zrenner (1979) must – at least partly – be due to the high stimulus intensity they used. However, there remains a discrepancy with psychophysical results since Kelly (1974) finds an optimal sensitivity at about 3 Hz at an retinal illuminance of 1000 td., whereas we find an optimal sensitivity at about 8 Hz even at a lower retinal illuminance of about 250 td.

One aspect of nonlinear behaviour in B^+Y^- units is that responses to incremental short wavelength stimuli show an initial discharge, followed by a prolonged afterdischarge extending into the off–phase of these stimuli (De Monasterio, 1979). This lack of mirror symmetry in responses to onset and offset of stimuli, however, is pronounced only at high luminances, just like the nonlinear phenomenon of transient tritanopia in retinal ganglion cells (De Monasterio, 1979). This may well explain why in none of the 8 B^+Y^- neurones in our sample, where on/off stimulation data were available, any of these nonlinearities could be observed.

The model (Fig.1.2.), explaining the responses of monkey LGN type I and type II units is rather similar to the model proposed by Sirovich and Abramov (1977). This model, too, assumes pooling of input from receptors with a common pigment. After filtering and pooling of the responses from the receptors, the responses from different types of receptors are summated linearly. The latter assumption could be verified experimentally (Fig. 1.5B). We did not attempt to model adaptation phenomena.

Nonlinear responses of LGN neurones could be attributed to the limited linear range of the neural filters and to the rectifying spike generating mechanism. Due to these nonlinear aspects the linear description provided by the model gives only a good approximation of the responses of type I units of the anaesthetized and alert monkey in a luminance range of 0.3 logunit. Larger modulation of stimuli causes saturation and rectification of the responses in the spike–generating mechanism. Moreover, the temporal characteristics of the neural filters change with stimulus luminance (Spekreijse et al., 1971). Another nonlinearity, not incorporated in the model, is the transition from rod dominated responses at scotopic intensities to cone dominated responses at photopic intensities. Our data reveal no

evidence for rod input at luminances of about 200 td, although several
of these neurones did reveal rod input after 20 minutes of dark adaptation.

Recently a nonlinear interaction in X and Y cells was described in cat
retinal ganglion cells: the contrast gain control mechanism (Shapley and
Victor, 1978). The effect of contrast gain control in X-cells was not
measurable in contrast to the effect in Y-cells, which demonstrate a clear
suppression of responsiveness after stimulation of the visual field far
away from the receptive field (chapter 3).

We also studied some concealed colour-opponent units (De Monasterio
et al., 1975b). Antagonistic chromatic responses could only be obtained
after selective chromatic adaptation of the neurone. The time course of
the responses from the type of cone, mediating the centre (without centre
adaptation) and from the type of cone, mediating the surround (with centre
adaptation) appeared to be equal apart from the sign of the response and
apart from a small time delay. These units appeared to have a null-
position for a spatial counterphase grating, in accordance with the
behaviour of concealed colour-opponent ganglion cells (De Monasterio,
1978a). The behaviour of concealed colour-opponent units is not described
by the model in Fig. 1.2., because the colour-opponent properties of these
units suggest a nonlinear interaction between cone type mechanisms. On
account of the small number of concealed units in our sample, namely 4,
not enclosed in the 70 units, which are mentioned earlier in this paper,
more detailed conclusions could not be drawn.

1.5. Appendix

For a system, consisting of a sequence of linear and static nonlinear
mechanisms the first order kernel equals the impulse response of the
cascade of linear mechanisms, apart from a constant (Price, 1958). Thus, if
the filter in Fig.1.1. is linear and its impulse response is given by
h(t), it can be shown with the theorem of Price (1958), that the first
order Wiener kernel $h_1(t)$ can be written as:

$$h_1(t) = \beta \left[\tfrac{1}{2} - erf(\theta/\sigma) \right] \, h(t) \tag{3}$$

where β = slope of the rectifying mechanism

θ = treshold of the rectifying mechanism

erf(z) = errorfunction of z, which is given by $\frac{1}{\sqrt{2\pi}} \int_0^z exp(-u^2/2) \, du$

σ = standard deviation of the gaussian noise input signal $x(t)$ after filtering by the filter $h(t)$

Thus equation (3) indicates, that the shape of the first order kernel $h_1(t)$ equals the shape of the impulse response of the linear filter. If the treshold θ is far below zero ($\theta<<0$), the rectifying mechanism becomes a multiplying system (multiplication by β) and the first order kernel only differs from $h(t)$ by the multiplying constant β. If the neurone has a high maintained activity and if the modulation of the response is small, the rectification has virtually no influence on the response and the system may be considered as being linear.

The same theorem of Prince (1958) can be used to show, that the second order Wiener kernel $h_2(t_1,t_2)$ between input stimulus $x(t)$ and response $y(t)$ is related to the impulse response $h(t)$ by the relation

$$h_2(t_1,t_2) = \alpha h(t_1)h(t_2)$$
$$= \alpha\gamma^2 h_1(t_1)h_1(t_2) \tag{4}$$

where α depends again on β,θ and σ
and $\gamma = \{\beta[\frac{1}{2} -\text{erf}(\theta/\sigma)]\}^{-1}$.

This equation (4) gives the relation between first and second order Wiener kernels for the model in Fig.1.1. and 1.2. Figure 1.9. shows the measured second order Wiener kernel and the second order Wiener kernel, predicted by equation (4) for an R^-G^+ unit. The agreement between predicted and measured kernels in Fig.1.9. indicates that the model of Fig.1.1. is compatible with the behaviour of LGN type I units, and also indicates that nonlinearities in cell responses, as apparent in the second order Wiener kernel, are due to the spike-generating mechanism and do not reflect a nonlinearity in the neural filter.
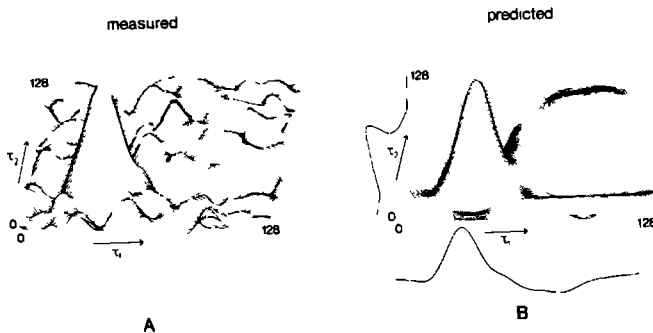
Fig. 1.9. Measured (A) and predicted (B) second order Wiener kernels. The first
order Wiener kernels, on which the prediction of the second order kernel
was based, are shown along the time axes. The results are from an R^-G^+
type I unit, stimulated with a diffuse (5x5 deg.) stimulus of 656 nm.

1.6. References

Bowmaker, J.K., Dartnall, H.J.A., Lythgoe, J.N., Mollon, J.D. (1978), The
visual pigments of rods and cones in the rhesus monkey, Macaca mu-
latta. J. Physiol. Lond. 274, 329-348.

Boynton, R.M. and Baron, W.S. (1975), Sinusoidal flicker characteristics
of primate cones in response to heterochromatic stimuli. J. Opt.Soc.
Am. 65, 1091-1100.

Cleland, B.G., Dubin, M.W. and Levick, W.R. (1971), Sustained and transient
neurones in the cat's retina and lateral geniculate nucleus. J.Physiol.
Lond. 217, 473-496.

Coenen,A.M.L. and Vendrik, A.J.H. (1971), The influence of sleep and wake-
fulness on the input-output relation of lateral geniculate neurons.
Pflügers Archiv. 324, 84-85.

De Monasterio,F.M., Gouras,P., Tolhurst,D.J. (1975a), Trichromatic colour opponency in ganglion cells of the rhesus monkey retina. J.Physiol. Lond. 251, 197-216.

De Monasterio,F.M., Gouras,P., Tolhurst,D.J. (1975b), Concealed colour opponency in ganglion cells of the rhesus monkey retina. J.Physiol. Lond. 251, 217-229.

De Monasterio,F.M. (1978a), Properties of concentrically organized X and Y ganglion cells of macaque retina. J.Neurophysiol. 41, 1394-1417.

De Monasterio,F.M. (1978b), Macular pigmentation and the spectral sensitivity of retinal ganglion cells of macaques. Vision Res. 18, 1273-1277.

De Monasterio,F.M. (1979), Asymmetry of on- and off-pathways of blue-sensitive cones of the retina of macaques. Brain Res. 166, 39-48.

De Valois,R.L. (1965), Analysis and coding of colour vision in the primate visual system. Cold Spring Harbor Symposia on Quantitative Biology, vol.30, 567-579.

De Valois,R.L., Morgan,H.C., Polson,M.C., Mead,W.R., Hull,E.M. (1974), Psychophysical studies of monkey vision - I. Macaque luminosity and color vision tests. Vision Res. 14, 53-67.

Enroth-Cugell,C., Robson,J.G. (1966), The contrast sensitivity of retinal ganglion cells of the cat. J. Physiol. Lond. 187, 517-552.

Enroth-Cugell,C., Lennie,P. (1975), The control of retinal ganglion cell discharge by receptive field surrounds. J. Physiol. Lond. 247, 551-578.

Estévez, O., Spekreijse,H. (1974), A spectral compensation method for determining the flicker characteristics of the human colour mechanisms. Vision Res. 14, 823-830.

Friendlich, A.R. (1973), Primate head restrainer using a nonsurgical technique. J. Appl. Physiol. 35, 934-935.

Fuchs,A.F. and Robinson,D.A. (1966), A method for measuring horizontal and vertical eye movements chronically in the monkey. J.Appl. Physiol. 21, 1068-1070.

Gouras,P. and Zrenner,E.(1979), Enhancement of luminance flicker by color-opponent mechanisms. Science, 205, 587-589.

Hochstein,S., Shapley,R.M. (1976), Quantitative analysis of retinal ganglion cell classifications. J. Physiol. Lond. 262, 237-264.

Kelly,D.H. (1974), Spatio-temporal frequency characteristics of color-vision

mechanisms. J. Opt.Soc.Am., 64, 983-990.

Lee,Y.W. and Schetzen,M. (1965), Measurement of the Wiener kernels of a non-linear system by crosscorrelation. Int.J.Control., 2, 237-254.

Maffei,L., Moruzzi,G. and Rizzolatti, G.(1965), Influence of sleep and wakefulness on the response of lateral geniculate units to sinewave photic stimulation. Arch.Ital.Biol.,103, 596-608.

Malpeli,J.G., Schiller,P.H. (1978), Lack of blue off-centre cells in the visual system of the monkey. Brain Res., 141, 385-389.

Marmarelis,P.Z. and Marmarelis,V.Z. (1978), Analysis of physiological systems. Plenum Press, New York, 1978.

Marmarelis,P.Z. and Naka, K.-I. (1973a), Nonlinear analysis and synthesis of receptive-field responses in the catfish retina I. Horizontal cell ganglion cell chain. J.Neurophysiol., 36, 605-618.

Marmarelis,P.Z. and Naka, K.-I. (1973b), Nonlinear analysis and synthesis of receptive-field responses in the catfish retina II. One-input white-noise analysis. J. Neurophysiol., 36, 619-633.

Marmarelis,P.Z. and Naka, K.-I. (1973c), Nonlinear analysis and synthesis of receptive-field responses in the catfish retina III. Two-input white-noise analysis. J. Neurophysiol., 36, 634-648.

Michael,C.R. (1978a), Color vision mechanisms in monkey striate cortex: dual-opponent cells with concentric receptive fields. J.Neurophysiol., 41, 572-588.

Michael,C.R. (1978b), Color vision mechanisms in monkey striate cortex: simple cells with dual opponent-color receptive fields. J.Neurophysiol., 41, 1233-1249.

Norren,D. van, Padmos, P. (1973), Human and macaque blue cones studied with electroretinography. Vision Res., 13, 1241-1254.

Norren,D. van, Vos,J.J. (1974), Spectral transmission of the human ocular media. Vision Res., 14, 1237-1244.

Poggio,G.F., Baker,F.H., Lamarre,Y. and Riva Sanseverino,E. (1969), Afferent inhibition at input to visual cortex of the cat, J.Neurophysiol., 32, 892-915.

Price,R. (1958), A useful theorem for nonlinear devices having gaussian inputs. IEEE Trans Inf. Theory, IT-4, 69-72.

Schellart,N.A.M., Spekreijse,H. (1972), Dynamic characteristics of retinal ganglion cell responses in goldfish. J.Gen.Physiol, 59, 1-21.

Shapley,R. and Hochstein, S. (1975), Visual spatial summation in two
      classes of geniculate cells. Nature, 256, 411-413.

Shapley,R.M. and Victor, J.D. (1978), The effect of contrast on the transfer
      properties of cat retinal ganglion cells. J.Physiol. Lond., 285,
      275-298.

Singer,W., Creutzfeldt, O.D. (1970), Reciprocal lateral inhibition of on-
      and off-centre neurones in the lateral geniculate body of the cat.
      Exptl.Brain Res., 10, 311-330.

Sirovich,L. and Abramov, I. (1977), Photopigments and pseudo-pigments.
      Vision Res., 17, 5-16.

Spekreijse,H., Norren,D. van, Berg,T.J.T.P.van den,(1971), Flicker responses
      in monkey lateral geniculate nucleus and human perception of flicker.
      Proc.Natl.Acad·Sci. U.S., 68, 2802-2805.

Swerup,C. (1978), On the choice of noise for the analysis of the
      peripheral auditory system. Biol.Cybernetics, 29, 97-104.

Wiesel,T.N., Hubel,D.H. (1966), Spatial and chromatic interactions in the
      LGB of the rhesus monkey. J.Neurophysiol., 29, 1115-1156.

Wyszecki,G. and Stiles,W.S. (1966), Color Science. J.Wiley & Sons Inc.,
      New York.

STRENGTH OF CONE TYPE RESPONSES IN MONKEY LGN COLOUR-OPPONENT X-CELLS AND
IMPLICATIONS FOR CELL RESPONSES TO LUMINOUS AND CHROMATIC FLICKER

2.1. Introduction

The receptive field of X and Y type neurones in the visual system of
mammals is built up by two mechanisms, which give antagonistic contri-
butions. Centre and surround of type I units in monkey, which belong to
the category of X-cells (De Monasterio, 1978a; this thesis: chapter 1)
receive input from different types of cone (Wiesel and Hubel, 1966;
De Monasterio, 1978a). This underlies the antagonistic responses of these
neurones to chromatic stimuli in different parts of the visible spectrum.
Adaptation studies have shown that different spectral properties are due
to differences in the combination of antagonistic cone-type inputs
and in the strengths of the input from the cone-type mechanisms (De
Monasterio et al., 1975a,b). However, the strength of the response contri-
butions of the three types of cone to neurones in the visual system has
never been determined quantitatively, which is due to the difficulty to
obtain pure responses from a single type of cone without adaptation.

In the previous chapter I reported two different methods to determine
quantitatively the response contributions of the individual cone-type
mechanisms in type I units. The study demonstrated that the response
contributions from the different types of cone summate linearly in colour-
opponent X-cells and that the temporal properties of the response contri-
butions of a single cone-type are equal, except for small differences in
the time delay between centre and surround mediating cone-type responses.
Therefore, according to this model, LGN X-cells are completely characterized
by the sign, strength and time delay of the response contributions from
each of the three types of cone. This study gives a survey of the strength

at which different types of cone impinge upon LGN X-cells for a population
of units. The results are used to predict the neutral wavelength of these
units which is in fact also another test on the linear summation of cone-
type responses. Moreover, based upon the model presented in chapter 1, the
cell-specific parameters – such as the sign, strength and time course of
the response contributions of the single types of cone – are used to
predict the cell responses to luminous and chromatic flicker, which are
in good agreement with measured responses.

This model explains, in a similar way as has been done by Gouras and
Zrenner (1979) that these neurones respond better to chromatic changes at
low temporal frequencies and respond better to luminous changes at higher
temporal frequencies. The extent to which the responses to luminous and
chromatic flicker differ depends on the relative strength of the
antagonistic responses and on the difference in time delay.

The difference in temporal behaviour to luminous and chromatic flicker
of these units appears to be in qualitative agreement with psychophysical
measurements (De Lange, 1958). However, a marked quantitative discrepancy
remains between psychophysical and electrophysiological results in that
the high frequency cut-off for chromatic flicker is at a lower frequency
in psychophysical measurements than it is in LGN X-cells.

2.2. Methods

2.2.1. Animal preparation

The experimental methods were similar to those described in the previous
chapter. Briefly, single unit recordings were obtained from LGN neurones
in three chronic monkeys (Macaca mulatta). On the day of the experiment
the monkey was anaesthetized with ketamine hydrochloride (1 mg/kg) and
subsequently paralyzed with an initial shot of 30 µg/kg pancuronium
(Organon; The Netherlands) followed by a continuous infusion of 30 µg/kg/
hour under artificial respiration (20 strokes/min) with a mixture of
N_2O and O_2 (2:1). Pupils were dilated with atropine sulphate and well-
fitting contact lenses with an artificial pupil of 3 mm protected   the
cornea. Additional spectacle lenses were placed to focus the stimuli on the
retina.

After a guard tube had penetrated the dura, tungsten microelectrodes
(1.0 - 2.5 MΩ at 1000 Hz) were lowered into the brain in a closed chamber

system. Action potentials were amplified and after level discrimination their moments of occurrence were fed into a PDP 11/45 computer for off-line ana-lysis with a precision of 0.1 msec.

2.2.2. Stimulation

Two XBO 450W xenon-arc lamps, which could be modulated independently by two TNO-450W Heinzinger modulation units, created two optical beams, mixed by a beamsplitter. Stimuli were rear projected on a translucent screen. Chromatic stimuli for the spectral compensation method (see below) were obtained with Kodak Wratten filters No. 29 (red) and 61 (green). The chromatic small-band filters, used to elicit cell responses at several wavelengths for the linear regression analysis (chapter 1) were obtained with Schott interference filters at 8 wavelengths, rather equally spaced in the range from 440 to 656 nm. The chromatic stimuli were spots with a diameter of 5 deg., covering the complete receptive field. Background stimuli were obtained with a tungsten-halide light source (150 W, 24 V) with a DC power supply (colour temperature ca. 3200 K). Luminance of the stimuli was measured with a calibrated tele-photometer (United Detector Technology 11C) and an optometer (United Detector Technology 80X).

2.2.3. Spectral compensation method

Two methods are used for the determination of the contributions of the different types of cone to the response of a neurone. One is the linear regression method by which the cone-type responses can be determined from the cell responses at several wavelengths (chapter 1). The other is the spectral compensation method, adopted from psychophysics (Estévez and Spekreijse, 1974; Kelly and Van Norren, 1977). Using the known absorption spectra of the ocular media and the pigment systems, this method enables the stimulation of only one class of cones. This is achieved by strongly stimulating one class of cones with a stimulus, which, unavoidably, also stimulates another class of cones. This unintended response contribution is cancelled by a simultaneous modulation in counterphase of a different chromatic stimulus, which compensates for the unintended stimulation in such a way, that the effective quantum catch of the latter class of cones remains unchanged.

From the spectral radiance $E(\lambda)$ of the light sources, the spectral transmittance $T_r(\lambda)$ and $T_g(\lambda)$ of the red and green Wratten filters and the photopic luminosity function $V(\lambda)$, being the same for man and monkey (De Valois et al., 1974), the luminance of the two coloured beams was calculated by $\int V(\lambda)E(\lambda)T_g(\lambda)d\lambda$ and $\int V(\lambda)E(\lambda)T_r(\lambda)d\lambda$. Neutral density filters were added to the Wratten filters to equalise the luminance of the two chromatic beams. The result was verified psychophysically by flicker photometry with human observers. The luminance of the two beams was carefully checked before each experiment with luminous and chromatic modulated stimuli.

The responses of a neurone could be studied in the range from purely red luminous flicker, through chromatic flicker to purely green luminous modulation by variation of the modulation depths of the counterphase modulated red and green chromatic beams (compare Kelly and Van Norren, 1977). Given the spectral sensitivity of the red sensitive cones ($V_r(\lambda)$) and the green sensitive cones ($V_g(\lambda)$), pure cone-type responses from the green cone-type are obtained when the responses from the red cones are silenced. This is obtained when the red and green chromatic beams are modulated by modulation depths m_r and m_g respectively such, that

$$m_g \int E(\lambda) T_g(\lambda) V_r(\lambda)d\lambda = -m_r \int E(\lambda) T_r(\lambda) V_r(\lambda)d\lambda.$$

Just as in the psychophysical experiments (Kelly and Van Norren, 1977) the sum of modulation depths $m_g + m_r$ remained constant; only the balance ratio's $\dfrac{m_g}{m_r + m_g}$ and $\dfrac{m_r}{m_r + m_g}$ were changed. Using the spectral sensitivity functions for $V_r(\lambda)$ and $V_g(\lambda)$ from Bowmaker et al. (1978) and evaluating the integrals in the equation above at 10 nm increments, the balance ratio

$\dfrac{m_g}{m_r + m_g}$, where the red cones are silenced, was calculated to be 0.62.

The balance ratio $\dfrac{m_g}{m_r + m_g}$ where the green cones are silenced, appeared to be 0.28.

Due to the different spectral transmittance of the red and green Wratten filters, affecting the red and green sensitive cones in a different way, the effective modulation depth of the green cones in the 'red cone silencing' condition differs from the effective modulation depth of the red cones, when the green cones are silenced. Therefore, the size of the responses in the silencing conditions have to be scaled to correct for the

different effective modulation of the red and green cones in the two
silencing conditions, which was done for the data in Table 2.1 (see also
Fig. 2.5a).

For brevity the terms 'blue', 'green' and 'red' cones refer to the
macaque cone-types, having maximal sensitivity in the 440-450 nm, 535-
540 nm and 570-580 nm bands (Marks et al., 1964; Bowmaker et al., 1980).
The classification of colour-opponent units in RG and BY units refers to
the cone-type inputs and is not primarily based on the sign and strength
of the responses in the different spectral regions.

2.3. Results

Recordings were obtained from 70 colour-opponent X-cells. Enough data
were obtained from 22 units to calculate the strength, sign and time
course of the response contributions of all three types of cone to the
neurone with the methods described in the Introduction. The data from
the other 48 units were incomplete to calculate the strength and time
course of the response contributions for all three types of cone. As far
as available, however, the data from these units confirmed the picture on
LGN X-cells as described in this paper.

It was shown (chapter 1), that the responses of LGN X-cells to
intensity increments and decrements could be predicted with the first
order Wiener kernel. This result implies that the first order kernel in
LGN X-cells equals the impulse response i.e. the response to a short light
flash.Therefore the size of the first order kernel is related to the strength
of the cell response. Since the shape of the first order kernel is equal
for all three types of cone in all LGN X-cells in the same experimental
conditions (chapter 1), the peak value of the first order kernel of a
given type of cone is related to the strength of the response contributions
of that type of cone to a particular neurone. In this study the strength
of the response contribution of a given type of cone to a neurone is
defined as the peak value of the first order kernel of the cone type
contributions to that neurone response.

In all units, the centre mechanism appeared to mediate responses from
only one cone mechanism, which was also found in LGN units by Wiesel and
Hubel (1966) and by De Monasterio et al. (1975a) in retinal ganglion
cells. When the centre was mediated by the red or green cone-type the

47

surround mechanism appeared to receive input only from the green or red cone-type respectively (Table 2.1). With our experimental accuracy of 5%, this implies that if the blue cone-type gave input to these units, the strength of the response contributions is less than 5% of the strength of the centre dominating type of cone. De Monasterio et al. (1975b) demonstrated that in 6% of monkey retinal ganglion cells the red or green cone-type responses through the centre are opposed by blue cone-type responses through the surround. Since adaptation stimuli were used, accurate quantitative data about the strength of the blue cone-type input are not available. However, the data in their paper (De Monasterio et al., 1975b) and in the paper of Padmos and Van Norren (1975) suggest a blue cone-type input to some RG units, which is about two log units weaker than the red or green cone-type input. These weak contributions cannot be detected by our methods.

In units, where the centre was dominated by the blue cone-type, the surround response revealed input from the red and green cone-type (Table 2.1). The sign of the responses from the red and green cone-types was always antagonistic to the excitatory centre responses from the blue cone-type. A similar result was found by De Monasterio et al. (1975b) in monkey retinal ganglion cells.

2.3.1. Strength of cone-type input

Only RG units were investigated with the compensation technique (Fig.2.5). The data of BY units and of part of the RG units were obtained with the linear regression method. The strengths of the response contributions from the three types of cone are given in Table 2.1 for each of the 22 units.

One striking result is that the mean ratio of centre and surround strength for the population of red-centre green-surround units (R_cG_s) (R/G = 1.0/0.9 = 1.1; range 0.66 to 2.5) is lower than for green-centre red-surround units (G_cR_s) (G/R = 1/0.54 = 1.85; range 1.3 to 3.45). The absolute strength of the centre of R_cG_s and G_cR_s units does not deviate significantly but the surround of G_cR_s units is significantly weaker ($p < 0.05$; t-test) than the strength of the surround mechanism in R_cG_s units.

In BY type I units the blue cone mechanism gives excitatory responses

48

CEL TYPE		STRENGTH OF CONE-TYPE INPUT $(SP/SEC^2) / (CD/M^2)$			RELATIVE STRENGTH			CENTRE SIZE 1/e value	ECCENTR.
C	S	R	G	B	R :	G :	B	(min.arc)	(deg.)
R+	G−	30.6	23.4		1.00	0.76		1.7	4.0
		16.4	11.4		1.00	0.70		2.7	15.8
		39.4	37.9		1.00	0.98		3.7	3.5
		87.6	134.0		1.00	1.50		4.2	4.8
		38.6	15.4		1.00	0.40		3.5	−
R−	G+	44.8	41.9		1.00	0.93		2.2	6.7
		42.9	34.9		1.00	0.81		2.5	13.8
		22.9	20.9		1.00	0.91		1.5	7.4
		52.6	45.0		1.00	0.86		3.0	0.2
		53.9	49.7		1.00	0.92		5.0	2.0
		40.6	44.6		1.00	1.10		2.2	5.2
		53.5	56.9		1.00	1.07		7.0	5.1
G+	R−	35.7	74.7		0.48	1.00		3.0	4.6
		6.2	22.1		0.29	1.00		4.5	12.0
		27.2	45.5		0.75	1.00		3.5	11.8
		30.6	49.9		0.77	1.00		5.0	5.3
		40.6	85.5		0.48	1.00		5.5	5.5
G−	R+	8.5	16.8		0.51	1.00		4.0	12.5
		46.6	97.3		0.50	1.00		10.0	6.5
B+	Y−	23.6	23.6	40.7	0.58	0.58	1.00	−	6.5
		16.6	22.7	40.7	0.49	0.67	1.00	6.2	9.3
		21.2	28.2	21.2	1.00	1.40	1.00	8.0	11.0

Table 1

to the centre mechanism (Malpeli and Schiller, 1978). The strength of
the responses from the blue cone-type is weaker than the strenght of the
combined responses from the red and green cone-types in each of the three
BY type I units, for which enough experiments were done to determine the
strengths of cone-type input. This implies that the strength of the centre
mechanism is weaker in these B^+Y^- units than that of the surround mechan-
ism. The same phenomenon was observed in three R_cG_s units from the sample
of 12 R_cG_s units. In G_cR_s units (N = 7) the strength of the centre mechan-
ism considerably exceeded that of the surround mechanism. In conclusion,
the strength of the centre mechanism does not always exceed that of the
surround mechanism.

The strength of the cone-type response contribution to centre or
surround of LGN units varies considerably (see Table 2.1). It was in-
vestigated whether any relation could be found between the strength of
cone-type responses and the eccentricity of the receptive field or the
size of the centre or surround mechanism. Since the density of cone-type
receptors decreases towards the retinal perifery, at least in man
(Österberg, 1935), owl monkey (Ogden, 1975) and cat (Steinberg et al.,
1973), the number of receptors, impinging upon a unit with a given
receptive field size, will decrease with the eccentricity of the receptive
field. For units with the same retinal eccentricity the number of receptors,
influencing the response of a neurone, will increase with receptive field
size. However, the strength of the response contributions will also
depend on the synaptic strengths in the neural pathway from the receptor
to the LGN neurone.

In Fig. 2.1 the strength of the response contribution of the cone-type,
governing the centre response, is plotted vs centre area. Since the number
of units in our sample was too small to include only units in a small
eccentricity range, we pooled the data from all units. Fitting the data
points by a straight line reveals a weak but significant correlation
(ρ = 0.58) between the area of the receptive field centre and the strength
of the cone-type responses.

Fig. 2.2 shows the relation between the strength of the cone-type
input per unit retinal area and the retinal eccentricity of the receptive
field. Since the data set did not include a sufficiently large number of
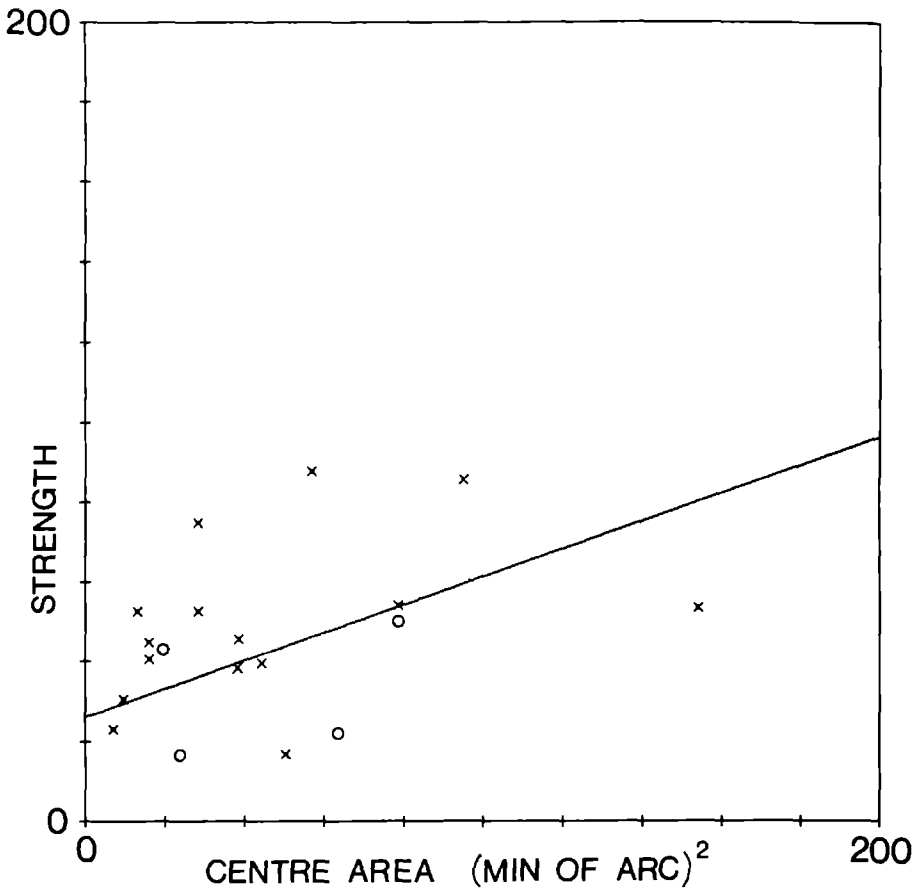units with a receptive field size within a small range and with different

Fig. 2.1. Strength of R and G cone-type responses, mediating the centre mechanism, for RG units as a function of centre area. o indicates data points of units at a retinal eccentricity exceeding 10 deg. The regression line is based on a linear regression of data points. One unit in table 2.1. with a large centre area is left out in this figure.

eccentricities to obtain reliable statistics, all data were incorporated in Fig. 2.2. Therefore the strength of cone-type input was divided by the area of the centre mechanism, which results into a strength of cone-type input per unit retinal area. Since only the centre size was determined accurately in most units, the data in Figs. 2.1 and 2.2 merely refer to the
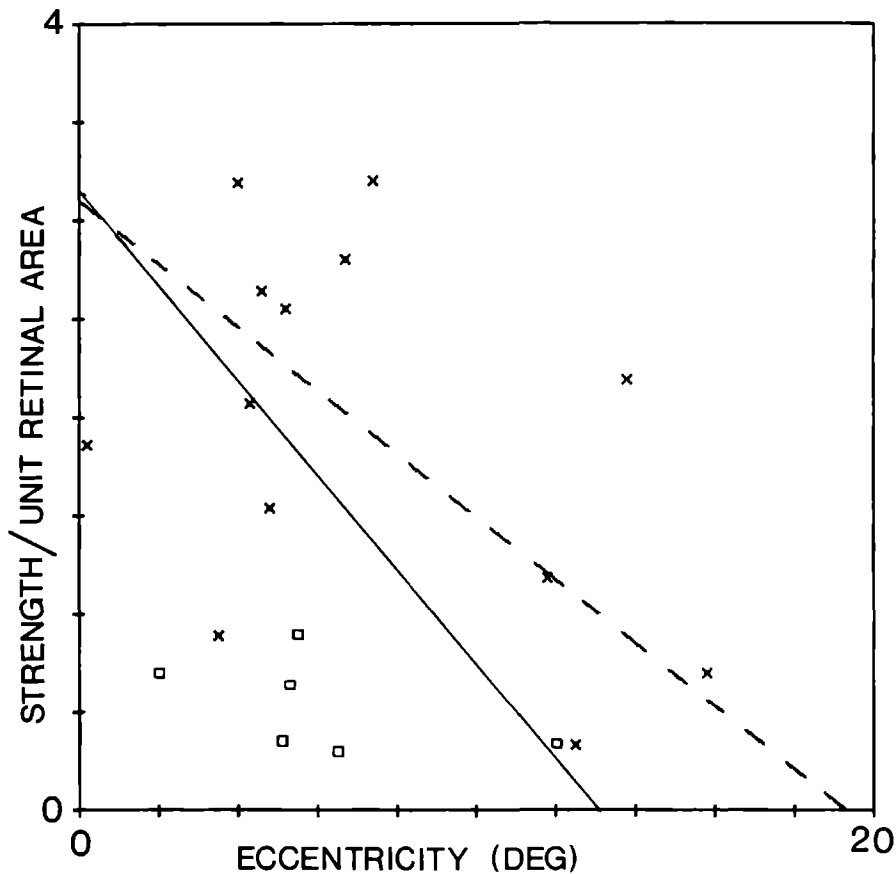
Fig. 2.2. Strength per unit retinal area of R and G cone-type responses, mediating the centre, as a function of retinal eccentricity of the receptive field. Data points of units with a 1/e value centre size exceeding 5 min. of arc are indicated by □. The regression line (————) is based on a linear regression. The dashed line gives the regression line, when the units with large centre sizes (1/e value ≥ 5 min. of arc) are left out.

type of cone which mediates through the centre. Taking all units into consideration, it results in a weak and insignificant correlation (ρ = -0.23) between relative strength of cone-type responses and receptive field eccentricity. However, closer scrutiny reveals that the data points in Fig. 2.2 at small eccentricities and small relative strength belong to units with large receptive fields. When the data from units with 1/e

centre size exceeding 5 min. of arc were left out, the correlation improves
to $\rho = -0.47$, which is significant ($p < 0.05$). A possible explanation for
the fact that the contribution of a unit retinal area is reduced in units
with large receptive fields, may be a cell specific gain attenuation,
aimed to prevent saturation of the cell response to physiologically
relevant stimuli.

The influence of centre size on the relation between strength of cone-
type responses per unit retinal area and eccentricity led us to investi-
gate the relation between strength of cone-type responses per unit
retinal area and centre area. Fig. 2.3 shows the correlation between these
two quantities ($\rho = -0.73$), confirming the suggestion from the data in
Fig.2.2, that the relative strength of the responses from a unit retinal
area is weaker in neurones with large centre sizes. Fig. 2.2 and 2.3.
indicate, that the strength per unit retinal area of cone-type responses
to the centre of LGN RG-units is negatively correlated with the eccen-
tricity of the receptive field, reflecting the decrease of the density
of cones/mm^2 on the retina with eccentricity, and with centre area
reflecting a neural attenuation of the strength of cone-type responses
per unit retinal area. Although mean receptive field size increases
with retinal eccentricity, at least in cat (Peichl and Wässle, 1979), the
correlation in Fig. 2.3 is not an implicit consequence of the different
eccentricities of the receptive fields alone, since, as already mentioned,
our sample of units also contains some units with large receptive fields
and small eccentricities.

A measure of the statistical significance of the relation between
several cell parameters is expressed by the correlation coefficient,
obtained with a linear regression. The linear regression was chosen,
because the scatter in the data don't permit an accurate curve fitting,
even though the data sometimes suggest a nonlinear relationship (e.g. in
Fig. 2.3). As a matter of fact, the relationship between strength of
cone-type input and centre area and between strength per unit retinal
area cannot both be linear. One more argument against a linear relation-
ship between the strength of cone-type responses per unit retinal area
and eccentricity in monkey is suggested by the fact that the density of
cones/mm^2 in man (Österberg, 1935) and in cat (Steinberg et al., 1973)
decreases not linearly with retinal eccentricity. A more important
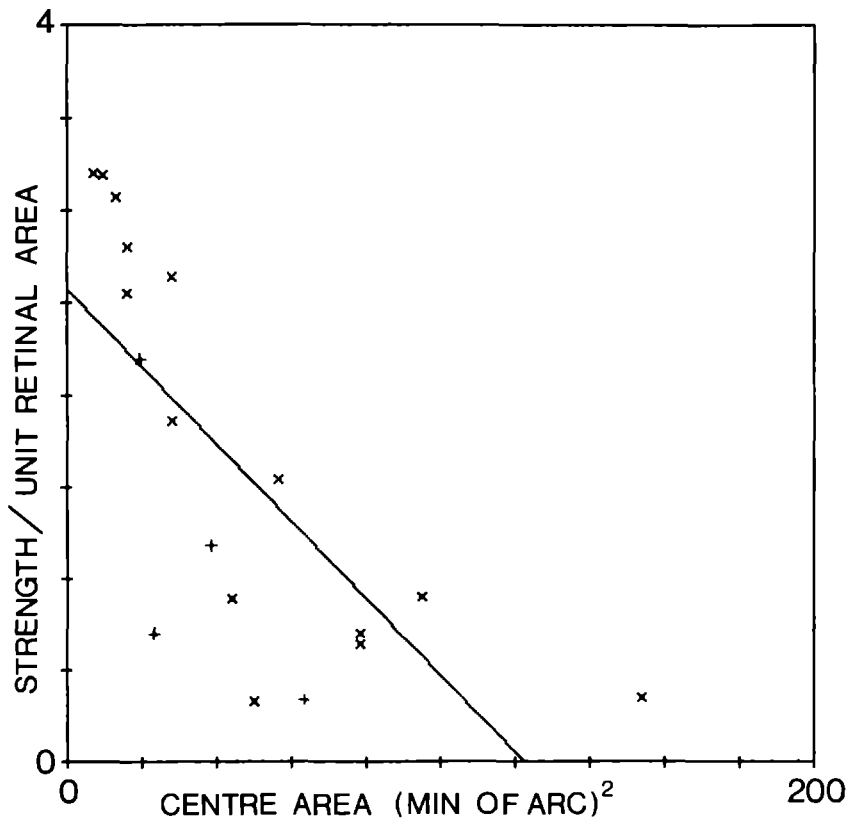
Fig. 2.3. Strength per unit retinal area of R and G cone-type responses, mediating the centre, as a function of centre area. Data points of units on a retinal eccentricity ≥ 10 deg are indicated by +. Regression line is based on a linear regression of data points. One unit, the same as in Fig. 2.1., is left out in this figure because of the large centre area.

parameter than cone density might be the quantity of pigment as a function of eccentricity or the coverage of the retinal area by cones. However, no data are available about these two quantities.

2.3.2. Prediction of neutral wavelengths

In chapter 1 we have demonstrated that the responses from the individual

54

cone-type mechanisms summate linearly in LGN units. This implies that the
neutral wavelength of a LGN neurone is completely determined by the
strength and sign of the response contributions of the cone-type mechanisms
and their spectral sensitivity. Fig. 2.4 shows the measured and predicted
neutral wavelengths for some LGN neurones. The regression line through
the data points is close to a straight line under 45 deg. with the X-axis
(slope = 0.95 + 0.34). The correlation coefficient of the data points is
0.91. This result confirms once more, that the response contributions from
the individual cone-type mechanisms add linearly (chapter 1). It is
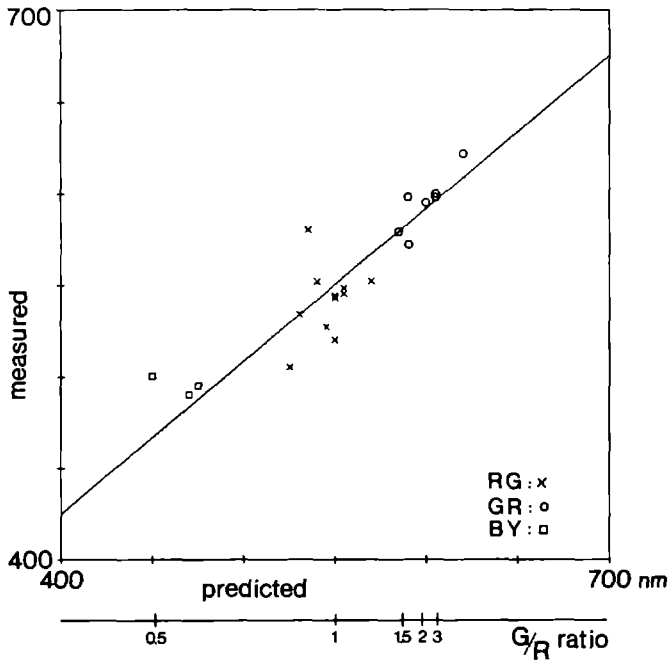interesting to note, that the position of the neutral wavelength is not

Fig. 2.4. Predicted and measured neutral wavelengths for $R_c G_s$, $G_c R_s$ and $B_c Y_s$
units. Horizontal scale, which indicates the relative strength of G
and R cone-type responses (G/R), equivalent with the predicted neutral
points on the abcissa, only applies to $R_c G_s$ and $G_c R_s$ units.

linearly related to the quotïent of the strengths of the antagonistic
systems, which is due to the asymmetric shapes of the absorption curves
of the cone-type systems. In fact, the experimental error in the values
of the strengths of the cone-type responses introduces a larger un-
certainty in the prediction of the neutral wavelengths at small G:R
ratios (i.e. at the shorter wavelengths) than it does for large G:R
ratios. With increasing G:R ratio the position of the neutral point is
less sensitive for errors in the G:R ratio.

The different distribution of ratios of centre and surround strength
in R_cG_s and G_cR_s units is reflected in the distribution of neutral wave-
lengths. For R_cG_s units the mean neutral wavelength is at 541 nm (s.d. =
19 nm); for G_cR_s units the mean neutral wavelength is at 595 nm (s.d. =
17 nm). The neutral wavelength of the R^+G^- in Table 2.1 with R:G = 1.:0.4
is left out in Fig. 2.4 since the predicted neutral wavelength is at 430
nm, which, in our set up, could not be verified experimentally.

2.3.3. Responses to chromatic flicker

The temporal properties of colour-opponent units in the monkey visual
system depend on the wavelength of the modulated stimulus (chapter 1).
When two chromatic stimuli are modulated in phase, the responses from
the antagonistic systems in colour-opponent retinal ganglion cells to a
low-frequency intensity modulation are almost 180 deg. out of phase.
The phase difference between the responses from the antagonistic systems
decreases with increase of modulation frequency. This is due to the small
difference in time delay between the antagonistic responses and results
into a larger modulation of the cell's discharge rate (Gouras and Zrenner,
1979). However, at chromatic flicker - when the chromatic stimuli are
modulated in counterphase - the responses from the opponent mechanisms
are in phase at lower modulation frequencies, but become gradually out
of phase with increase of modulation frequency. These considerations explain
the low frequency attenuation and the increased sensitivity at high fre-
quencies in the responses of colour-opponent X-cells to luminous flicker
with respect to the responses to chromatic flicker.

The results of Gouras and Zrenner (1979) in monkey retinal ganglion
cells led us to investigate the behaviour of LGN colour-opponent units
to luminous and chromatic flicker. The data were obtained only for RG
units with two chromatic beams (Wratten No. 61 and 29), and these two

were modulated in counterphase with different modulation depths for the green and red chromatic beams (see 2.2.3.). Fig. 2.5a shows the first order kernels in the different stimulus conditions for an R^-G^+ unit. This unit received no detectable input from the blue cone-type. At the modulation ratio $m_g:m_r$ = 0.28 : 0.72 and at 0.62 : 0.38 respectively the green and red cone mechanisms are silenced and the kernels are obtained consequently from pure red and green cone-type responses.

Since the red and green stimulus are modulated in counterphase the first order kernels of the antagonistic systems have equal sign. Therefore, to obtain the right sign of the first order kernels of the cone-types, the green cone-type kernel has to be inverted. Furthermore, the cone-type mechanisms are not equally strongly stimulated. The numbers at the right hand side indicate the strength of stimulation. In order to compare the gain of the responses from the green and red types of cone, the gain of the kernel of the green type of cone has to be multiplied by 0.59/0.31.

At green luminous modulation the first order kernel contains antagonistic response contributions from the red cone-type in addition to the green cone-type response, which is indicated by the effective stimulation of the cone-types at the right hand side of Fig. 2.5a. Since the red cone-type responses in this unit are mediated through the centre, the red cone-type responses precede the green cone-type responses by about 16 msec. (chapter 1), giving rise to the small positive peak at the start of the kernel (open arrow) for green luminous modulation. The green cone-type contribution to the kernel, obtained with red luminous modulation, is much weaker. However, the slightly more pronounced biphasic character of the first order kernel (solid arrow) is a consequence of this green cone-type contribution. It is generally found,that the first order kernels to luminous modulation are more biphasic or even triphasic in comparison with the pure cone-type kernels.

It was shown in chapter 1 that the first order kernel equals the impulse response or response to a short light flash. That is why the transfer function of a neurone to luminous or chromatic flicker can be obtained by Fourier transformation of the first order kernel to luminosity or chromaticity modulated stimuli. The result is shown in Fig. 2.5b.
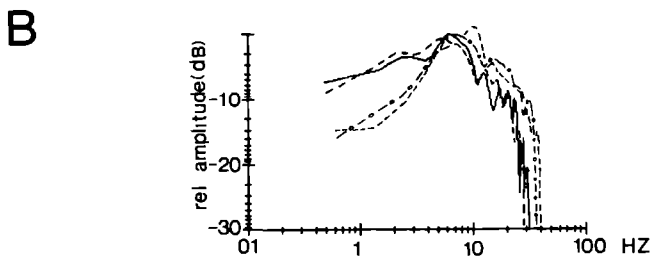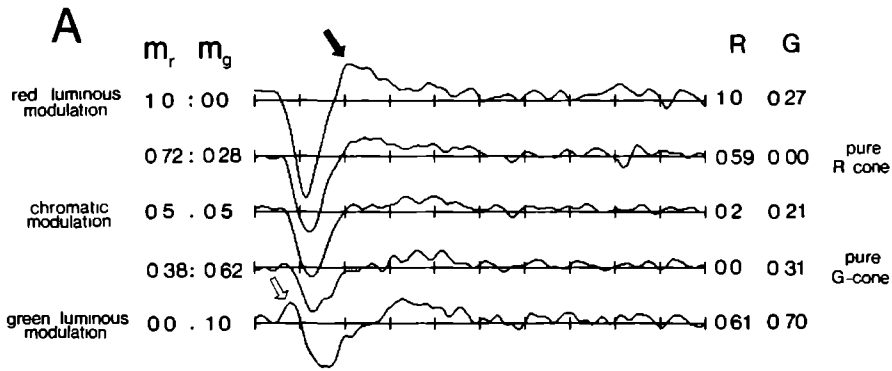
Fig. 2.5. A.First order kernels of an R⁻G⁺ unit to several modulation ratios
of the red (Wratten 29) and green (Wratten 61) stimulus. Red and
green chromatic stimuli are modulated such, that at each red/green
modulation ratio the sum of the modulation ratios is equal. Red/green
modulation ratio is shown at the left. First order kernels at R:G of
0.72 : 0.28 and 0.38 : 0.62 are from pure red and green cone-type
responses respectively. At the modulation ratio 0.5:0.5 the first
order kernel is shown for chromatic flicker. At the right the variation
in effective cone-type stimulation is shown. Further explanation is
given in text. B. Temporal transfer functions, predicted (dashed line)
and measured (full-line) for green luminous flicker (o o o o)
and chromatic flicker. All transfer functions are scaled independently
with the maximal sensitivity at 0 dB.

In line with the results of Gouras and Zrenner (1979) the transfer function to luminous flicker shows a decreased sensitivity at the lower frequencies and an increased sensitivity at the higher frequencies with respect to the transfer function to chromatic flicker. The increase of low-frequency sensitivity at chromatic flicker is small and the low-pass attenuation never disappeared completely. The high frequency cut-off (-3 dB) for chromatic flicker was somewhat lower than for luminous flicker, but it always exceeded 7Hz, which is far above the cut-off frequency for psychophysical responses to chromatic flicker (see Discussion).

In order to test the qualitative explanation of the different behaviour to luminous and chromatic flicker quantitatively, the transfer function to luminous and chromatic flicker was predicted by means of the responses from the single cone-types. The predicted transfer functions were obtained by Fourier transformation of a linear combination of the first order kernels of the red and green types of cone (see Appendix). The coefficients in the linear combination were calculated from the effective stimulation of the cone-types and correspond with the numbers at the right hand side of Fig. 2.5a.

The predicted and measured transfer functions were very close together, which is shown for a typical unit in Fig. 2.5b. This result also indicates, that the model, as presented in chapter 1 (Fig.1.2) and shown in a simplified way in Fig. 2.6a, describes the responses of monkey LGN colour-opponent X-cells to luminous and chromatic flicker.

Clearly, according to the model and to Gouras and Zrenner (1979), the extent, to which the temporal properties to chromatic flicker deviate from the pure cone-type responses, depends on the relative strengths of the opponent mechanisms and on the mutual time delay. In Fig. 2.6b the influence of the time delay on the cell responses to chromatic flicker is shown, when the response strength of each of the opponent mechanisms is equally strong. On the average the difference in time delay of the antagonistic responses in LGN colour-opponent X-cells is 16msec. (chapter 1). As shown in Figs. 2.5b and 2.6b a difference in latency in this order of magnitude causes only small differences between the transfer functions for luminous and chromatic flicker. In conclusion, the influence of the ratio between the strengths of the antagonistic chromatic mechanisms on the transfer functions to luminous and chromatic flicker is very small. The
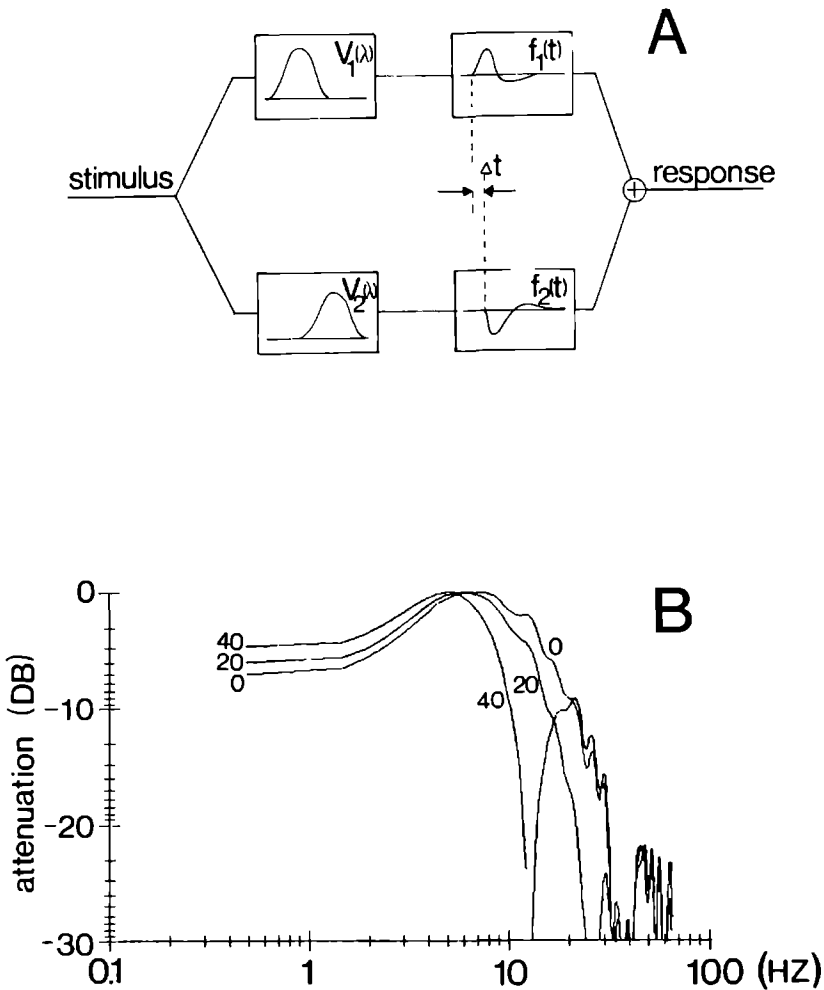
Fig. 2.6. A.Model to describe LGN X-cell responses. $V_1(\lambda)$ and $V_2(\lambda)$ indicate the spectral sensitivity and $f_1(t)$ and $f_2(t)$ the impulse responses of the centre and surround mechanism respectively. The spike generating mechanism, which may be represented by a one-sided rectifier, is omitted, since the results of the GWN crosscorrelation method for the centre and surround responses are independent on the presence of the spike generating mechanism. B.Predicted transfer functions of LGN colour-opponent X-cells to chromatic flicker for three values of delay Δt in msec between the centre and surround response. In the prediction the strengths of the antagonistic systems are supposed to be equal. The first order kernels for the cone-type responses in the response prediction are from a typical unit. All transfer functions are scaled independently with the maximal sensitivity at 0 dB.

60

most pronounced low-pass transfer function for chromatic flicker, however,
is obtained, when the opponent mechanisms respond equally strong. The
influence of time delay and relative strength of the antagonistic systems
is explained in mathematical terms in the Appendix.

2.4. Discussion

In chapter 1 we presented a model to describe the behaviour of monkey
LGN X-cells. In the present paper the parameters, which characterize a
neurone, are given for several units and with these parameters the
responses of a neurone to some stimuli are predicted. Predicted and measured
responses are in agreement within experimental error. These results show
that at a given luminance, where all cone-type systems have equal
temporal properties over many neurones, each neurone may be characterized
by a few parameters: the strength, sign and time delay of the responses
from the three types of cone, which contribute to the responses of the
neurone.

       One aim of this study is to determine the strength of the response
contributions of the individual types of cone to LGN colour-opponent X-cells.
In agreement with previous studies (De Monasterio, 1978a; Wiesel and Hubel,
1966) the centre mechanism appeared to receive input from only one type of
cone. The responses of units, where the centre received input from the
red-sensitive or green-sensitive type of cone, were opposed by responses
from the green-sensitive and red-sensitive type of cone respectively. A
particular kind of blue cone-type input to RG units, being expressed by
an attenuation of the direct signals from green- and red-sensitive cones
in monkey retinal ganglion cells (De Monasterio, 1979) was not to be seen,
no more than in other studies on colour-opponent units. As suggested by
De Monasterio, the reason of this is probably that the effect is only
seen with field action spectra (i.e. the treshold determination for a test
light of fixed intensity and wavelength on an adapting field of varying
wavelength and intensity).

       All cells receiving blue cone-type input appeared to be trichromatic.
In BY cells the blue cone-type opposed the red- and green-sensitive types
of cone, which is in conformity with results of De Monasterio et al. (1975,
1978a) in monkey retinal ganglion cells. As already described by De Mo-
nasterio (1978b) the strength of the combined red and green cone-type
response exceeds the strength of the blue cone-type responses on a white

background. A more powerful surround mechanism was also found in three R_cG_s units. This means, that the whole surround mechanism may be more sensitive than the whole centre mechanism, although the centre mechanism may have a higher sensitivity in the middle of the receptive field, due to the larger extent of the surround mechanism.

The experimental error in the determination of the strength of the responses from the blue type of cone is larger than it is for the red and green types of cone due to uncertainty in the lenticular absorption, which is considerable at the short wavelengths and which may vary in humans by as much as 1 log unit at 400 nm (Wyszecki and Stiles, 1965, page 216). Since the eccentricity of the BY units is more than six degrees, the absorption by the macular pigment may be neglected. In the prediction of the neutral wavelength for the BY units the predicted result is at a lower wavelength than the measured neutral wavelength, indicating, that the strength of the responses from the blue type of cone might be some-what larger than the value calculated from the experimental data. The data from the three BY units in Fig. 2.4 are obtained from one monkey. Bringing the predicted neutral wavelength into line with the experimentally determined neutral wavelength demands a blue cone-type response, which is 0.3 log unit stronger than the calculated strength. Since the density of the ocular media varies considerably, at least in man (Wyszecki and Stiles, 1965), this variation in density between individuals may explain this discrepancy.

Fig. 2.4 shows the neutral wavelength for those units, which are investigated quantitively with the proper experiments on their cone-type input. From measurements on the position of the neutral wavelength of other units, not shown in this figure, it appeared that the neutral wave-length of BY units scatters around 500 nm, but that the neutral wave-length of RG units ranges from 470 nm to 650 nm, be it that the position of the neutral wavelength of most RG units (78%) is between 530 and 610 nm. A similar scatter in neutral wavelengths for RG units is also found by Zrenner in monkey retinal ganglion cells (personal communication).

The temporal transfer function of LGN neurones to chromatic flicker appears to demonstrate less attenuation at low-frequencies and more attenuation at high-frequencies than the transfer function to luminous flicker, in agreement with results of Gouras and Zrenner (1979) in monkey retinal ganglion cells. However, the agreement with similar psycho-

physical results seems to be only qualitative. The transfer functions for chromatic flicker show a cut-off frequency at about 10 Hz at 150 td., whereas the psychophysical cut-off frequency (Fig. 1 in Kelly and Van Norren, 1977) is at about 5 Hz at 860 td. Therefore a considerable quantitative discrepancy remains between the temporal properties of LGN colour-opponent X-cells and psychophysical observations to chromatic flicker.

2.5. Appendix

As shown in chapter 1 LGN X-cells may be represented by the model in Fig. 2.6a, where

$V_1(\lambda)$ and $V_2(\lambda)$ is the spectral sensitivity of the centre and surround mediating mechanism respectively

$f_1(t)$ and $f_2(t)$ is the impulse response of the centre and surround mediating mechanism respectively.

With these definitions the wavelength dependent impulse response of the neurone is given by

$$h(\lambda,t) = V_1(\lambda)f_1(t) - V_2(\lambda)f_2(t) \qquad (1)$$

with $f_2(t)(:)f_1(t - \Delta t)$. With chromatic flicker the antagonistic systems are stimulated in counterphase (i.e. 180 deg. out of phase), which results into a chromatic impulse response

$$h_{ch}(\lambda,t) = V_1(\lambda) f_1(t) + V_2(\lambda)f_2(t). \qquad (2)$$

The transfer function of the neurone to chromatic flicker is obtained by a Fourier transformation of eq.(2), which results into

$$H_{ch}(\lambda,\omega) = V_1(\lambda)F_1(\omega) + V_2(\lambda)F_2(\omega). \qquad (3)$$

The predicted transfer functions in Fig. 2.5b are calculated according to eq.(3). Eq.(3) passes into

$$H_{ch}(\lambda,\omega) = V_1(\lambda)F_1(\omega) + gV_2(\lambda)F_1(\omega)e^{-i\omega\Delta t}$$

$$= F_1(\omega) \left[V_1(\lambda) + gV_2(\lambda)e^{-i\omega\Delta t} \right] \qquad (4)$$

since centre and surround responses have equal time courses, apart from a time delay Δt. The coefficient g indicates the ratio of the strengths of the surround and centre mechanism and is defined by

$$g = \frac{|F_2(\omega)|}{|F_1(\omega)|} \;.$$

If $V_1(\lambda) \neq 0$ and $V_2(\lambda) \neq 0$, which means that both the centre and surround contribute to the cell response to chromatic flicker, then the transfer

function will differ in shape from the transfer function of the centre
or surround mechanism. When both transfer functions are shifted with the
maximum at 0 dB, the transfer function for chromatic flicker has less
low-pass and more high-pass attenuation than the transfer function of the
centre and surround. The extent to which these transfer functions differ
depends on the relative strength of the antagonistic responses and also
depends on the time delay Δt. Fig.2.6b shows, that the difference is
small for Δt values in the range from 10 to 40 msec., which is common
to LGN X-cells.

Eq.(4) shows the dependence of the transfer function for chromatic
flicker upon the relative strength of the centre and surround mechanisms
g. If g = 0, i.e. the surround gives no responses at all, there are no
changes at all. The low frequency gain and the high frequency loss are
maximal if g = 1.

The transfer function for luminance flicker is given by

$$H_1(\lambda,\omega) = F_1(\omega) \left[V_1(\lambda) - gV_2(\lambda)e^{-i\omega\Delta t} \right]. \tag{6}$$

When the maximum is shifted to 0 dB, just like the transfer function of the
centre and surround, the responses to luminous flicker have more low-
pass and less high-pass attenuation than the centre and surround responses.
From the argumentation above about the relation between the transfer
function for chromatic flicker and that of the centre or surround follows,
that the responses to chromatic flicker have less low-pass attenuation
and more high-pass attenuation than the responses to luminous flicker
(see Fig. 2.5b).

2.6. References

Bowmaker, J.K., Dartnall,H.J.A., Lythgoe,J.N. and Mollon,J.D. (1978),
    Visual pigments of rods and cones in the rhesus monkey,Macaca mulatta.
    J.Physiol.Lond. 274, 329-348.
Bowmaker,J.K., Dartnall,H.J.A. and Mollon,J.D. (1980), Microspectrophoto-
    metric demonstration of four classes of photo receptor in an old
    world primate, Macaca fascicularis. J.Physiol. 298, 131-143.
De Monasterio,F.M. and Gouras, P. (1975a), Functional properties of ganglion
    cells of the rhesus monkey retina. J.Physiol.Lond. 251, 167-196.
De Monasterio, F.M., Gouras,P. and Tolhurst,D.J. (1975b), Trichromatic
    colour opponency in ganglion cells of the rhesus monkey retina.

J.Physiol.Lond. 251, 197-216.

De Monasterio,F.M. (1978a), Properties of concentrically organized X and Y ganglion cells of macaque retina. J.Neurophysiol. 41, 1394-1417.

De Monasterio,F.M. (1978b), Center and surround mechanisms of opponent-color X and Y ganglion cells of retina of macaques. J. Neurophysiol. 41, 1418-1434.

De Monasterio,F.M. (1979), Signals from blue cones in 'red-green' opponent-colour ganglion cells of the macaque retina. Vision Res. 19, 441-449.

Estévez,O. and Spekreijse,H. (1974), A spectral compensation method for determining the flicker characteristics of the human colour mechanisms. Vision Res. 14, 823-830.

Gouras,P. and Zrenner,E. (1979), Enhancement of luminance flicker by color-opponent mechanisms. Science 205, 587-589.

Kelly,D.H. and Van Norren,D. (1977), Two-band model of heterochromatic flicker. J. Opt.Soc.Am. 67, 1081-1091.

Lange,H. de (1958), Research into the dynamic nature of the human fovea-cortex systems with intermittent and modulated light. II. Phase shift in brightness and delay in color perception. J. Opt.Soc.Am. 48, 784-789.

Malpeli,J.G. and Schiller,P. (1978), Lack of blue OFF-centre cells in the visual system of the monkey. Brain Res. 385-389.

Marks,W.B., Dobelle,W.H. and MacNichol jr.,E.F. (1964), Visual pigments of single primate cones. Science 274, 329-348.

Ogden,T.E. (1975), The receptor mosaic of Aotes trivirgatus; distribution of rods and cones. J. Comp. Neurol. 163, 193-202.

Österberg, G. (1935), Topography of the layer of rods and cones in the human retina. Acta Ophthal. (Kbh.) Suppl. 6.

Peichl, L. and Wässle, H. (1979), Size, scatter and coverage of ganglion cell receptive field centres in the cat retina. J. Physiol. Lond. 291, 117-141.

Steinberg, R.H., Reid,M. and Lacey, P.L. (1973), The distribution of
    rods and cones in the retina of the cat. J. Comp. Neurol. 148,
    229-248.

Wiesel, T.N. and Hubel, D.H. (1966), Spatial and chromatic interactions
    in the lateral geniculate body of the rhesus monkey. J. Neuro-
    physiol. 29, 1115-1156.

CHAPTER 3

CHARACTERIZATION OF SPATIAL AND TEMPORAL PROPERTIES OF MONKEY LGN
Y-CELLS

3.1. Introduction

Several single unit studies in retina and LGN have classified neurones
into two separate classes: X-type and Y-type (Enroth-Cugell and Robson,
1965; Shapley and Hochstein, 1975). A neurone is defined as X-type if a
position (null-position) can be found in the receptive field of the
neurone, where reversal of the contrast of a bipartite field or of a
sine or square wave grating in a range of spatial frequencies does not
influence the firing rate of the neurone. In Y-cells such a null-
position cannot be found, but instead the response contains second order
harmonic responses. This points out to a nonlinear mechanism in the
receptive field of Y-cells. The second harmonic responses are most
prominent, when first order harmonic responses are absent. The presence
of first order harmonic responses in Y-cells depends on the position of
the grating in the receptive field, as in X-cells, suggesting a mechanism
with linear spatial summation besides the nonlinear mechanism, already
mentioned. Hochstein and Shapley (1976a,b) demonstrated that second order
harmonic responses were due to a mechanism, which extends far from the
receptive field centre of cat retinal ganglion cells. This classification
criterion appeared to be only one of several different properties, which
distinguish X and Y cells in retina and LGN (Enroth-Cugell and Robson,
1966; Shapley and Hochstein, 1975; Dreher et al., 1978; Kratz et al.,1978;
De Monasterio, 1978a,b).

Recently, Shapley and Victor (1978) reported another nonlinear
phenomenon in responses of cat retinal ganglion cells, viz. that the

67

temporal transfer function of neurones depends on the contrast of the stimulus. The mechanism, responsible for this effect appeared to be located in the receptive field surround and the best temporal frequencies for producing the contrast effect appeared to be also those frequencies, which produce the second harmonic responses (Shapley and Victor, 1978) suggesting that a single mechanism may underly both phenomena. Results of Derrington et al. (1979) give evidence, that another nonlinear phenomenon, the 'shift effect' (Krüger and Fischer, 1973; Barlow et al., 1977) is also due to the mechanism, which generates the second order harmonic responses.

Thibos and Werblin (1978a,b) have shown in mudpuppy retina, that responses of bipolar cells are sustained and that centre and surround of bipolar cells act antagonistically. The responses of amacrine cells are not affected by steady illumination but are affected by modulated or moving stimuli. It is suggested, that the centre-surround organization of the linear mechanisms is present in bipolar cells and that amacrine cells can be identified with the nonlinear mechanism in the receptive field of Y-cells (Shapley and Victor, 1978; Jakiela, 1978).

These results suggest a model (Fig. 3.1) which may explain, at least qualitatively, many properties of Y-cells. A similar model has already been suggested by Wunk and Werblin (1979) based upon intracellular recordings in bipolar and amacrine cells in the mudpuppy retina and by Shapley and Victor (1979) and by Jakiela (1978) to explain the response characteristics of cat retinal ganglion Y-cells. This model consists of a centre and surround mechanism, behaving linearly, and of a nonlinear system. The centre and surround mechanism show linear summation in a limited range of luminance and contrast, just as in X-cells (chapter 1). The nonlinear mechanism contributes to the cell response in two ways. An additive contribution from the nonlinear mechanism is responsible for the second order harmonic responses. The other contribution is a multiplicative action on the responses from the linear mechanisms. This multiplicative action does not simply attenuate all signals equally, but affects the linear responses in a complicated frequency selective way, at least in cat retinal ganglion cells (Shapley and Victor, 1978). The spike generating mechanism is represented by a one sided rectifier.

The goal of this study is to investigate the validity of this model and to quantify the characteristics of the linear and nonlinear systems for LGN Y-cells in the rhesus monkey. In order to study the spatial
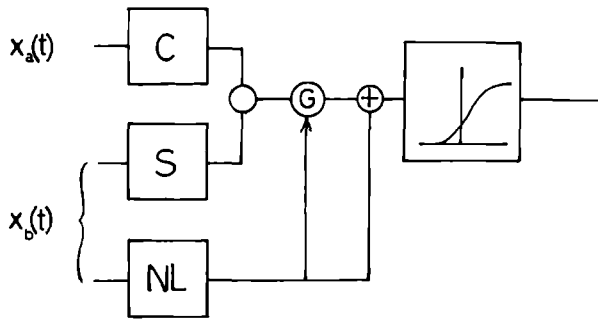
Fig.3.1. Model to describe LGN Y-cells. C and S indicate linear centre and
surround mechanisms and NL a nonlinear mechanism, which extends far
(at least 5 deg) from the centre of the receptive field. NL contributes
to the cell response in an additive way and also in a multiplicative
way at G, where the responses of the linear systems C and S are
modified in a frequency selective way. The spike generating mechanism
is represented by a static one-sided rectifier.

frequency characteristics of LGN Y-cells drifting and counterphase
modulated sine wave gratings were used. The temporal properties of the
elements in the model are investigated with the gaussian white noise
(GWN) crosscorrelation method (Lee and Schetzen, 1965; Marmarelis and
Marmarelis, 1978). Since the main goal is to characterize the linear and
nonlinear mechanisms C,S and NL (Fig. 3.1), the nonlinear parts of the
responses,expressed in the second and higher order kernels, are corrected
for the nonlinear response contributions by the spike generating mechanism,
which by itself behaves nonlinearly in several aspects.

The centre responses were studied by stimulating the centre with GWN
in the condition, that the surround was either dark, either steady
illuminated or also intensity modulated with uncorrelated GWN. From these
experiments the temporal characteristics of the centre mechanism can be

determined without and with the multiplicative action of the nonlinear mechanism. The experiment with the steady and modulated surround stimulus was designed to investigate, whether the nonlinear mechanism requires a steady or modulated stimulus to exercise it's multiplicative action, analogous to the experiments with a standing or moving windmill of Jakiela (1978) and Werblin (1972). In a similar way were the surround responses studied with the centre dark, steady illuminated or modulated in order to investigate a possible influence of centre stimulation on the surround responses. When the surround is stimulated without the stimulation of the centre the additive contributions from the nonlinear mechanism can be studied. Finally, when both centre and surround are stimulated with uncorrelated GWN, the nonlinear interaction between centre and surround is expected to be reflected in the crosskernels (Marmarelis and Marmarelis, 1978).

The results are compatible with the idea, that the centre mechanism behaves linearly and that the surround contains a linear and nonlinear mechanism. In line with results of Victor and Shapley (1979) in cat retinal ganglion cells we find that the characteristics of the nonlinear mechanism in monkey LGN Y-cells too are compatible with a sandwich model (two linear systems separated by a static nonlinearity). The dynamics of the multiplicative action on the responses from the linear systems by the responses from the nonlinear mechanism could not be characterized by the second order crosskernels. Nevertheless, the effect of the action by the nonlinear mechanism on the responses from the linear systems is clearly shown in the first order kernels of the centre and surround mechanism in the different stimulus conditions.

3.2. Methods

3.2.1. Animal preparation

The experimental methods were similar to those described in chapter 1. Briefly, single unit recordings were obtained from LGN neurones in 3 chronic monkeys (macaca mulatta). On the day of the experiment the monkey was anaesthetized with ketamine hydrochloride (1 mg/kg) and subsequently paralysed with an initial shot of 30 μg/kg pancuronium (Organon; The Netherlands) followed by a continuous infusion of 30 μg/kg/hour under

artificial respiration (20 strokes/min.) with a mixture of N_2O and O_2
(2:1). Pupils were dilated with atropine sulphate and well fitting contact
lenses with an artificial pupil of 3 mm protected the cornea. Additional
spectacle lenses were placed to focus the stimuli on the retina.

After penetration of the dura by a guard tube, tungsten micro-
electrodes (1.0-2.5 MΩ at 1000 Hz) were lowered into the brain in a closed
chamber system. Action potentials were amplified and after level discrimi-
nation their moments of occurrence were fed into a PDP 11/45 computer with
a precision of 0.1 msec. for off-line analysis.

3.2.2. Stimulation

Spatial counterphase sine wave gratings for the classification of units
into X or Y type were generated on an oscilloscope (HP 1321A with phosphor
P31) with a repetition rate of 200 images/sec. The spatial frequency of
the sine wave grating could be varied from 0.0625 to 12 cycles/deg. The
horizontal axis was generated by a triggered ramp generator; the vertical
axis by a 3 MHz triangle generator. Intensity modulation of the stimulus
on the oscilloscope could be performed with different temporal
frequencies by modulation of the z-axis of the oscilloscope with a
programmable synthesizer (Rockland, model 5100). Mean stimulus luminance
on the oscilloscope was 10 cd/m^2. Modulation depth could be varied and
usually was < 30%. Linearity of the oscilloscope luminance as a function
of the input voltage was better than 10%. Amplitude of first and second
order harmonic responses were calculated after Fourier transformation of
the cell response.

The two optical beams, used in the two-input experiment (see above),
were created by two XBO 450W xenon arc lamps. Slides, consisting of very
small spots and annuli for the stimulation of centre and surround,
respectively, fabricated using techniques applied in electronic circuit
design, were inserted in the optical beams, which were then combined with
a beamsplitter. Stimuli were projected on a translucent screen. A back-
ground obtained with a tungsten-halide lamp fed by a DC power supply was
continuously present during the experiments. Unless stated otherwise the
background had a luminance of 1 cd/m^2. Luminance of the stimuli was
measured with a calibrated telephotometer (United Detector Technology-
11C) and an optometer (United Detector Technology-80X). The two xenon arc
lamps could be modulated independently by two TNO-450 Heinzinger modulation

units up to 90% modulation depth with a flat amplitude spectrum within 1%
from 0 tot 150 Hz and with a maximum phase delay of 1.2 deg. at 150 Hz.
During the gaussian white noise (GWN) stimulation, the stimulus luminance
was modulated with noise with a standard deviation of 9% modulation depth.
The pseudo-random GWN signals were obtained from two HP 3722-A noise
generators, which were modified by the addition of 2 feedback loops from the
20-th bit to the 15-th and 11-th bit of the shift register in order to
improve the frequency characteristics of the noise sequence. For the 50
Hz (150 Hz) GWN stimulus the sequence duration was about 15 (5) minutes.
With this long period spurious results, due to the pseudo-random character
of the noise (Swerup, 1978) were excluded since the experiment duration
was usually less than the sequence duration.

3.2.3. Theoretical background of system analysis

To investigate the linear and nonlinear properties of Y-cells the Wiener
kernels were calculated up to second order for 32 cells. The characteriz-
ation of the model in Fig. 3.1. requires at least the calculation of the
zeroth, first and second order kernels. The zeroth order kernel, given by

$$h_0 = \lim_{T \uparrow \infty} \frac{1}{T} \int_{-T/2}^{T/2} y(t) \ dt \tag{1}$$

equals the mean of the response $y(t)$ of the neurone. The first order
kernels for the two input stimuli $x_a(t)$ and $x_b(t)$ with power levels or,
which is equivalent, power density spectra P_{x_a} and P_{x_b} are given by

$$h_{1,a}(\tau) = \frac{1}{P_{x_a}} \lim_{T \uparrow \infty} \frac{1}{T} \int_{-T/2}^{T/2} y(t) \ x_a(t-\tau) \ dt \tag{2}$$

and

$$h_{1,b}(\tau) = \frac{1}{P_{x_b}} \lim_{T \uparrow \infty} \frac{1}{T} \int_{-T/2}^{T/2} y(t) \ x_b(t-\tau) \ dt \tag{3}$$

and give the best linear description of the system in the sense of least
squares estimation. If the system is linear, the first order kernels give
a complete description and the temporal transfer function is obtained by
Fourier transformation of the first order kernels. If the system is non-
linear the characterization demands the calculation of higher order kernels.
The second order kernels are given by

$$h_{2,aa}(\tau_1,\tau_2) = \frac{1}{2P_{x_a}^2}\left[\lim_{T\uparrow\infty}\frac{1}{T}\int_{-T/2}^{T/2}y(t)x_a(t-\tau_1)x_a(t-\tau_2)dt - P_{x_a}\delta(\tau_1-\tau_2)\right] \quad (4)$$

$$h_{2,bb}(\tau_1,\tau_2) = \frac{1}{2P_{x_b}^2}\left[\lim_{T\uparrow\infty}\frac{1}{T}\int_{-T/2}^{T/2}y(t)x_b(t-\tau_1)x_b(t-\tau_2)dt - P_{x_b}\delta(\tau_1-\tau_2)\right] \quad (5)$$

$$h_{2,ab}(\tau_1,\tau_2) = \frac{1}{P_{x_a}P_{x_b}}\left[\lim_{T\uparrow\infty}\frac{1}{T}\int_{-T/2}^{T/2}y(t)x_a(t-\tau_1)x_b(t-\tau_2)dt\right] \quad (6)$$

Eq. (6) gives the nonlinear interaction between the two stimuli on the one hand and the response of the neurone on the other hand.

If these kernels characterize the neurone completely, the response of the neurone to stimuli $s_a(t)$ and $s_b(t)$ is given by

$$r(t) = h_0 + \int h_{1,a}(\tau)s_a(t-\tau)d\tau + \int h_{1,b}(\tau)s_b(t-\tau)\,d\tau +$$

$$\iint h_{2,aa}(\tau_1,\tau_2)s_a(t-\tau_1)s_a(t-\tau_2)d\tau_1 d\tau_2 +$$

$$\iint h_{2,bb}(\tau_1,\tau_2)s_b(t-\tau_1)s_b(t-\tau_2)\,d\tau_1 d\tau_2 +$$

$$\iint h_{2,ab}(\tau_1,\tau_2)\,s_a(t-\tau_1)s_b(t-\tau_2)\,d\tau_1 d\tau_2 . \quad (7)$$

An extensive and detailed survey of this analysis is given by Marmarelis and Marmarelis (1978).

3.3. Results

The data were obtained from 32 LGN Y-cells from 3 anaesthetized rhesus monkeys. Units were classified as Y-type on account of the presence of second order harmonic responses to spatial sine wave gratings.

3.3.1. First order kernels of LGN Y-cells

In order to determine the temporal properties of centre and surround, both mechanisms were investigated with the GWN crosscorrelation method. Fig. 3.2 shows the first order Wiener kernels for a Y-cell, obtained by stimulation with spots and annuli of different sizes. With increasing spot size the size of the first order kernel increases (Fig.3.2A). Fig.3.2B, which is obtained by Fourier transformation of the first order kernels, shows that the increasing size of the kernels is a consequence of an increase of sensitivity at higher frequencies at larger spot sizes. This change in size and shape may be explained by the increase of the response

contributions from the centre and from the surround. With small spots
mainly centre responses are elicited. Larger spots stimulate the centre
more effectively, but also stimulate the surround mechanism in an in-
creasing measure. These antagonistic surround responses cause a sensitivity
attenuation for low frequencies and, if the surround responses are some-
what delayed with respect to the centre responses, they may cause a
sensitivity increase at high frequencies (Ratliff et al., 1967; Maffei
et al., 1970; De Valois et al., 1977).
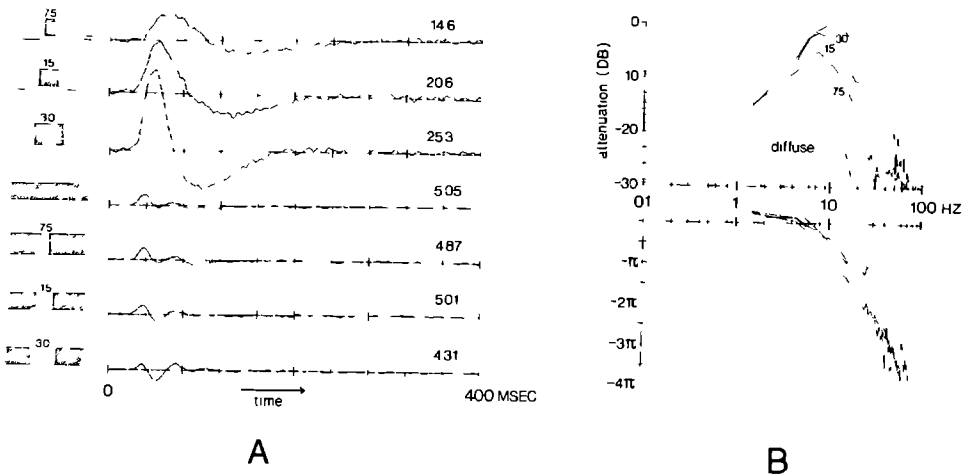
Fig.3.2. A.First order kernels, obtained with spots and annuli, for a typical
LGN Y-cell. The zeroth-order kernel h_0 [sp/sec] in each stimulus
condition is given with the first order kernels. Luminance: 420 td.
B.Amplitude spectra, obtained by Fourier transformation of the first
order kernels for different spot sizes and for diffuse light.

When the spot size exceeds about 30 min. of arc, the size of the first
order kernel decreases very rapidly in Y-cells. As in X-cells a possible
explanation could be a strong antagonistic response from the surround

mechanism. However, the first order kernel, obtained by stimulation of the complementary part of the receptive field with a large annulus is very small as well and therefore, the reduction of the first order centre-kernel to the size of the first order kernel, obtained with a diffuse stimulus cannot simply be explained by linear addition. This penomenon is found in all 8 units, which were investigated with spots and annuli with various dimensions.

The nonlinear phenomenon, described above, can be explained in different ways. One explanation could be, that by stimulation of the nonlinear mechanism in the surround the responses of the linear systems, which are reflected in the first order kernels, are attenuated in the multiplicative mechanism G (Fig. 3.1). Another explanation lays the origin of the nonlinearity in the presence of a spike generating mechanism. One might argue, that in an on-centre / off-surround cell an annulus or diffuse stimulus will inhibit the neurone, thus mimicking a rise in treshold. This would result into   smaller first order kernels and larger second order kernels for annuli and diffuse stimuli, due to the rectifi-cation of the responses in the spike generating mechanism. However, in off-centre / on-surround units stimulation of the surround would raise the mean firing rate of the neurone, thus mimicking a lower treshold, which in turn should predict larger first order kernels for diffuse stimuli than for small spots. In order to prevent the complex influence of the spike generating mechanism on the size of the first order kernels experiments were done, where centre and surround had the same mean luminance (Fig.3.3).

Many studies on Y-cells have reported, that pure surround responses are very difficult to obtain (Enroth-Cugell and Lennie, 1975; De Monasterio, 1978a). Also in LGN Y-cells it appeared nearly impossible to elicit pure surround responses by merely spatial arrangements of the stimuli. This is reflected in Fig.3.2A in that centre kernels are bifasic, like the first order kernels of the centre and surround of LGN X-cells (chapter 1), where-as kernels, obtained by stimulation of the surround are trifasic. However, after adaptation of the centre mechanism with a small intense spot the first order kernel appeared to become bifasic in shape, similar but antagonistic to the first order kernel of the centre.

75

3.3.2. Temporal properties of centre and surround and their mutual influence

Shapley and Victor (1978) demonstrated a nonlinear action of the non-linear mechanism on the responses of the linear systems in cat retinal ganglion Y-cells. In order to investigate this nonlinear action double noise experiments were done, where the intensities of centre and surround stimulus were modulated simultaneously with two uncorrelated noise sequences. Fig.3.3A shows the first order kernels for the stimulus situation, in which centre and surround were stimulated separately with GWN, while the intensity of the other stimulus remained unmodulated and for the stimulus situation that both centre and surround are stimulated independently with two uncorrelated noise sequencies. The first order centre kernel, obtained without modulation of the surround stimulus, $h_{1,c}(\tau)$ is larger than that, obtained when the surround stimulus is modulated as well ($h_{1,c/s}(\tau)$). Moreover, $h_{1,c/s}(\tau)$ has a shorter duration than $h_{1,c}(\tau)$. The responses of the centre mechanism are changed just by modulation of the intensity of the surround stimulus, while the mean luminance remained the same. This is typical for Y-cells and was never seen in X-cells. Modulation in the centre never influenced the first or second order kernels, obtained by stimulation of the surround, indicating a nonreciprocal influence of a mechanism in the surround on the centre mechanism. The transfer function of the centre mechanism in the steady and modulated surround condition, respectively, is obtained by Fourier trans-formation of the first order kernels $h_{1,c}(\tau)$ and $h_{1,c/s}(\tau)$ and is shown in Fig.3.3B. The first order surround kernels $h_{1,s}(\tau)$ and $h_{1,s/c}(\tau)$ are very much equal indicating no influence of modulation of the centre stimulus on the surround responses.

As already discussed above (Fig.3.2) linear summation of the kernels $h_{1,c}(\tau)$ and $h_{1,s}(\tau)$ overestimates the kernel $h_{1,c+s}(\tau)$, obtained with simultaneous in phase stimulation of centre and surround (i.e. with diffuse light). However, $h_{1,c+s}(\tau)$ is more accurately approximated by summation of the kernels $h_{1,c/s}(\tau)$ and $h_{1,s/c}(\tau)$. Apparently, when centre and surround are modulated, the first order kernels of the linear centre and surround mechanism add linearly.

To demonstrate that the nonlinear mechanism, which causes the fre-quency-selective gain attenuation of the responses of the linear mechanism,
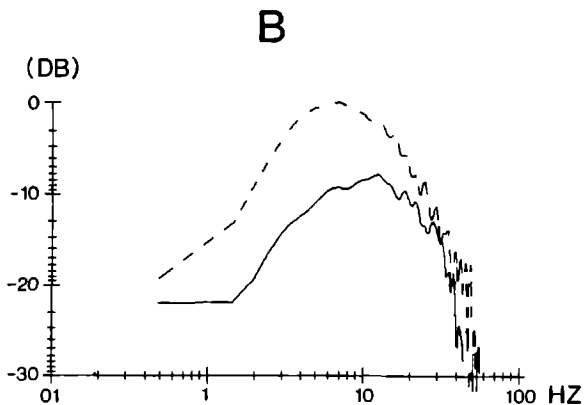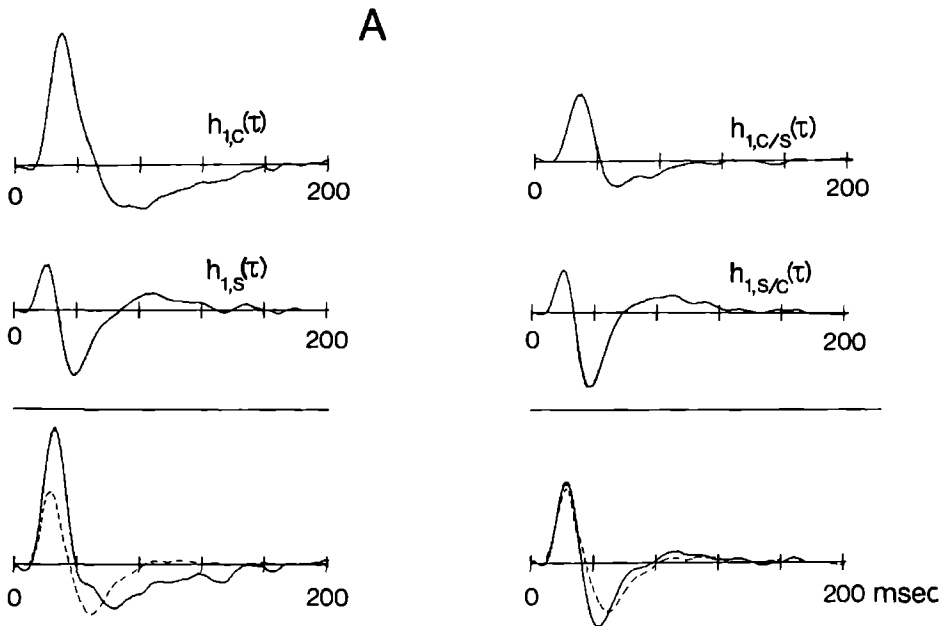
Fig.3.3. A.First order kernels of the centre mechanism without modulation of
the surround stimulus $(h_{1,c}(\tau))$ and with surround modulation $(h_{1,c/s}(\tau))$
and of the surround mechanism without centre modulation $(h_{1,s}(\tau))$ and
with centre modulation $(h_{1,s/c}(\tau))$. The linear summation of $h_{1,c}(\tau)$
and $h_{1,s}(\tau)$ and of $h_{1,c/s}(\tau)$ and $h_{1,s/c}(\tau)$ (full line) are compared
with $h_{1,c+s}(\tau)$ (dashed curve), being the first order kernel, obtained
by simultaneous and identical stimulation of centre and surround. Spot
diameter: 30 min. of arc. Inner diameter of annulus equals diameter of
spot. Outer diameter of annulus : 10 deg. Luminance 420 td. B.Amplitude
spectra of the centre mechanism with (full line) and without (dashed
line) surround modulation. Modulation in the surround attenuates
the centre responses in the low-frequency range, which results into a
smaller and faster first order centre kernel.

extends into the visual field far from the receptive field centre,
annuli were used with different outer diameters. Centre and surround were
stimulated with a spot and an annulus, which were modulated with in-
dependent noise signals. Fig.3.4A shows the first order centre kernel
obtained by stimulation of centre and surround for an off-centre Y-cell,
in the situation that the annulus had a very large outerdiameter (13 deg)
and with an annulus with an outerdiameter of 1.5 deg. In the latter
stimulus condition the first order kernel is larger than in the condition
with the large annulus. Fig.3.4B shows the Fourier transformed first
order centre kernels in the frequency domain, indicating that only the
low-frequency sensitivity is attenuated. Although stimulation in the
receptive field at a distance of 5 deg or further from the centre could
not elicit responses in this neurone, modulation of the stimulus intensity
in this part of the visual field did change the time course of the
responses of the linear systems. Apparently, the mechanism, which modifies
the responses of the linear mechanisms in a multiplicative and frequency-
selective way extends over a very large part of the visual field.

To investigate the nonlinear properties of Y-cells second order
Wiener kernels were calculated. However, the nonlinear rectification in
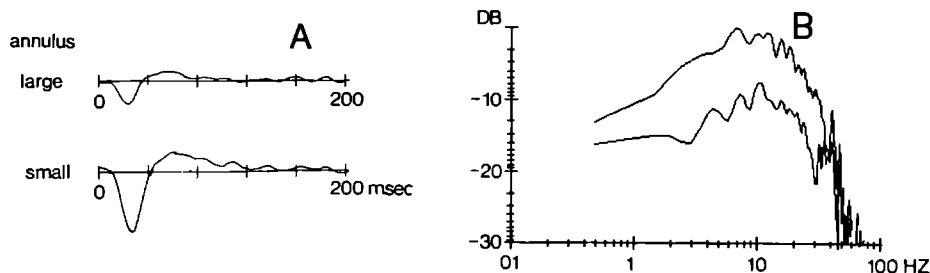the spike generating mechanism will give rise to contributions in the

Fig. 3.4. A.First order kernels, obtained by GWN stimulation of the centre with
a spot,while the surround is stimulated with an annulus, whioh outer
diameter is 13 deg. or 1.5 deg. Spot diameter is 0.42 deg.,which is
also the inner diameter of the annulus. Spot and annulus are
stimulated with uncorrelated GWN stimuli. B. Amplitude spectra, obtained
by Fourier transformation of the first order kernels in A. Luminance:
420 td.

second order kernels. Before presentation of the results of the second order kernels it will be discussed how the nonlinear response contributions, originating in the spike generating mechanism, can be separated from the contributions to the second order kernels from the mechanisms C,S and NL.

In order to explain the influence of the spike generating mechanism on the response characteristics of Y-cells, suppose the following model (Fig.3.5), which consists of two parallel linear systems, which are characterized completely by the impulse responses $h_c(\tau)$ and $h_s(\tau)$, followed by a static nonlinearity. Suppose, that the static nonlinearity,
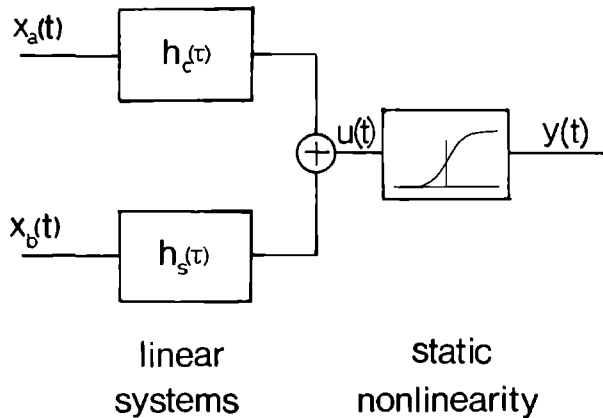

Fig.3.5. Model, consisting of two linear systems with impulse responses $h_c(\tau)$ and $h_s(\tau)$, which responses are summated before a static nonlinearity.

which represents the spike generating mechanism, may be approximated by the quadratic

$$y(t) = a_0 + a_1 u(t) + a_2 u^2(t) \qquad (8)$$

given the small range of the input stimuli $x_a(t)$ and $x_b(t)$, which implies an expansion of the responses of the spike generating mechanism up to second order. For this system the zeroth order kernel is given by

$$h_0 = a_0 + a_2 P_{x_a} \int d\sigma h_c^2(\sigma) + a_2 P_{x_b} \int d\sigma \, h_s^2(\sigma) \qquad (9)$$

The zeroth order kernel gives the mean response of the neurone. The first order kernels give the best linear approximation of the system in the sense of least-squares error and are given for this system by

$$
\begin{aligned}
h_{1,a}(\tau) &= a_1 h_c(\tau) \\
h_{1,b}(\tau) &= a_1 h_s(\tau)
\end{aligned}
\Bigg\} \qquad (10)
$$

This equation indicates that the first order kernels reflect the impulse responses of centre and surround apart from an unknown gain factor. Note, that because of the static nonlinearity $h_c(\tau)$ and $h_s(\tau)$ cannot be measured directly but can be determined apart from a constant. The second order kernels, which reflect nonlinear response contributions from the spike generating mechanism, are given by a product of the impulse responses apart from a constant:

$$h_{2,aa}(\tau_1,\tau_2) = a_2 h_c(\tau_1) h_c(\tau_2) \qquad (11a)$$

$$h_{2,bb}(\tau_1,\tau_2) = a_2 h_s(\tau_1) h_s(\tau_2) \qquad (11b)$$

$$h_{2,ab}(\tau_1,\tau_2) = a_2 h_c(\tau_1) h_s(\tau_2) \qquad (11c)$$

This indicates that second order kernels can be predicted with the first order kernels apart from an unknown gain factor a_2/a_1^2.

3.3.3. Interpretation of second order self-kernels

Fig.3.6 shows the measured and predicted second order self-kernels for a typical Y-cell. If the centre kernel $h_{2,aa}(\tau_1,\tau_2)$, predicted according to eq. (11a) with the first order centre kernel $h_{1,c/s}(\tau)$, is properly scaled, it is very close to the measured kernel. The difference between predicted and measured kernel is shown in Fig.3.6C. The fact, that the difference kernel is not significantly above the noise level, illustrates that the second order self-kernel of the centre mechanism can be ascribed entirely to the nonlinear spike generating mechanism and not to the centre mechanism itself. However the surround mechanism appears to behave differently. If the second order self-kernel of the surround mechanism is predicted with the first order kernel $h_{1,s/c}(\tau)$ according to equation (11b), the shape of

the predicted kernel differs markedly from the shape of the measured kernel.
If the predicted kernel is scaled with the same constant as the predicted
self-kernel of the centre and after that subtracted from the measured
kernel, the difference kernel betrays the presence of yet another
significant nonlinear contribution. According to the model in Fig.3.1 the
difference kernel reveals information on the nonlinear mechanism NL.
This nonlinearity can be expressed in the frequency domain after a two-
dimensional Fourier transformation. In this representation the second
order kernel shows peak responses near modulation frequencies of 5 Hz,
resulting into 10 Hz frequencies in the responses. Five Hz is a typical
optimal frequency for the nonlinear mechanism (mean value over 9
neurones: 4.9 Hz; range 2.6 - 7.2 Hz).

As suggested by Hochstein and Shapley (1976b), the origin of the
nonlinear mechanism in the receptive field of Y-cells may be a large
number of subunits, which responses are rectified before the point of
summation. This led Victor and Shapley (1979) to propose a sandwich model
for NL: a static nonlinearity, sandwiched between two linear filters
L_1 and L_2. According to the sandwich model, the second order frequency
kernel of this linear/static nonlinear/linear transduction can be written
by

$$H_2(f_1,f_2) = \text{constant.} \ H_{L_1}(f_1)H_{L_1}(f_2)H_{L_2}(f_1+f_2),$$

where $H_{L_1}(f)$ and $H_{L_2}(f)$ represent the transfer functions of the linear
systems L_1 and L_2 (Marmarelis and Marmarelis, 1978; Victor and Shapley,
1980).

The frequency kernel in Fig.3.6D shows significant response contri-
butions in both the sum and difference regions except for the frequencies,
when either f_1 or f_2 is near to zero. Therefore, $H_2(f_1,f_2)$ is large only
when neither frequency f_1 nor f_2 is close to zero, independent of f_1+f_2,
and for high values of f_1 and f_2. This indicates, that in LGN Y-cells the
filter L_1 has low-pass attenuation and is not a trivial all-pass filter.
The transfer function $H_{L_1}(f)$ can be obtained from the value $|H_2(-f,f)|$
on the diagonal of the frequency kernel. For these values $|H_2(-f,f)| =$
$|H_{L_1}(-f)H_{L_1}(f)|.|H_{L_2}(0)| = |H_{L_1}(f)|^2|H_{L_2}(0)|$. The transfer function
$|H_{L_1}(f)|$ is obtained apart from a constant and is shown in Fig.3.6E.
Filter L_1 appears to have similar properties in all LGN Y-cells: a
pronounced low-pass attenuation and a peak sentivity near 5Hz (mean value
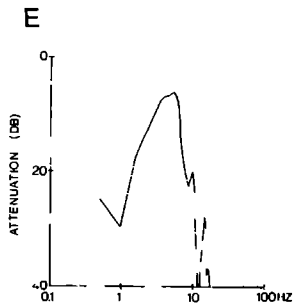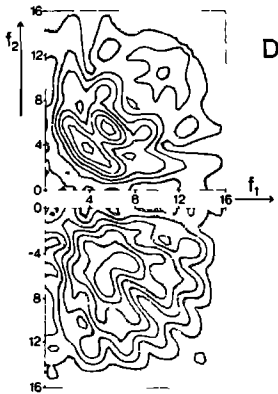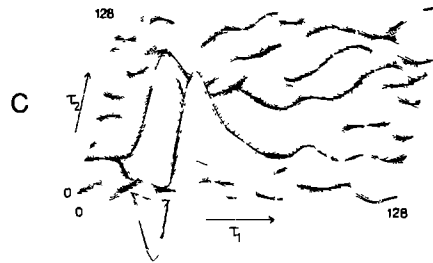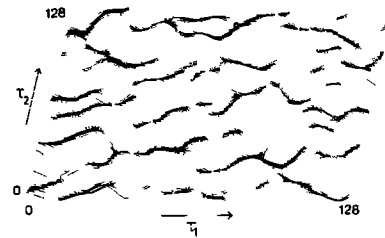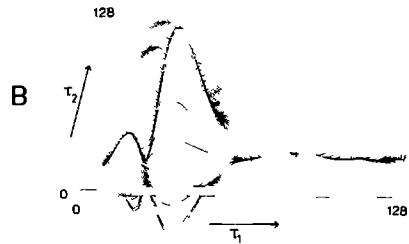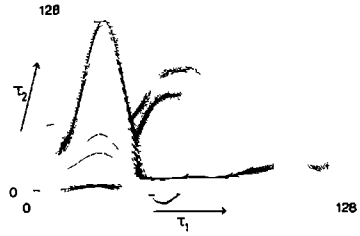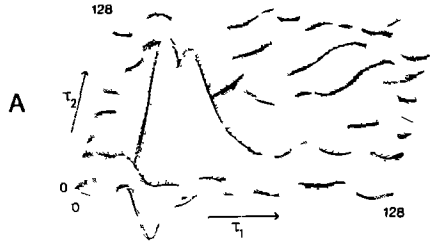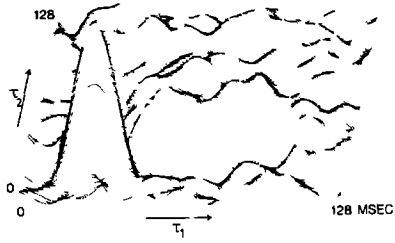
5.2 Hz; standard deviation 0.9 Hz, calculated from 9 neurones). Fig.3.6D
also shows, that the sum and difference regions are not equal. Just as
in cat retinal ganglion Y-cells (Victor and Shapley, 1979) the peak in the
sum region usually has a larger amplitude than the peak in the difference
region (factor of 1.17; range 0.84 - 1.64), indicating that the linear
filter L_2 has a slight band-pass character with a gentle low-frequency
attenuation. This weak low-pass attenuation is also seen in that the
frequency kernel in the difference region differs also in shape from that
in the sum region. In general the frequency kernel shows somewhat smaller
values on the diagonal $(-f,f)$ than just off the diagonal. The exact shape
of the transfer function of the filter L_2 is not shown, since the shape
of this filter varied considerably among different neurones. In some
units the low-pass attenuation was absent and in others it was very
clear. Moreover the shape of the frequency kernel in the sum-region
demonstrated, that the cut-off frequency at the high frequency side varied
considerably among several neurones.

3.3.4. Interpretation of cross-kernels

In order to characterize the action of the nonlinear mechanism on the
responses of the linear systems, the cross-kernel $h_{2,ab}(\tau_1,\tau_2)$ was
calculated. The kernel $h_{1,c/s}(\tau_1)h_{1,s/c}(\tau_2)$ was calculated in order to
correct the measured kernel for nonlinear response contributions from
the spike generating mechanism. The measured kernel $h_{2,ab}(\tau_1,\tau_2)$ and
the predicted kernel, originating from contributions from the spike
generating mechanism are shown in Fig.3.7. These kernels are very simi-

— — — — — — — — — — — — — — — — — — — —

Fig.3.6. Measured (A) and predicted (B) second order kernels for stimulation of
the centre and of the surround with a spot and annulus respectively.
Diameter of spot (0.5deg) equals inner diameter of annulus. Centre size
(1/e value):0.12deg. Kernels are calculated from data, obtained with a
two-input stimulus. C. shows the difference kernel of the surround
after a two dimensional Fourier transformation in the frequency domain.
Peak sensitivity is shown near the second harmonic of 5 Hz. E. shows
the temporal transfer function of the hypothetical filter L_1 (see text),
which is the first filter of the sandwich model. The optimal temporal
frequency of the filter L_1 is shown to be near 6 Hz. Stimulus luminance
250 td.

83

lar. The difference never contributed significantly in the response
prediction of Y-cells, indicating that the multiplicative action of the
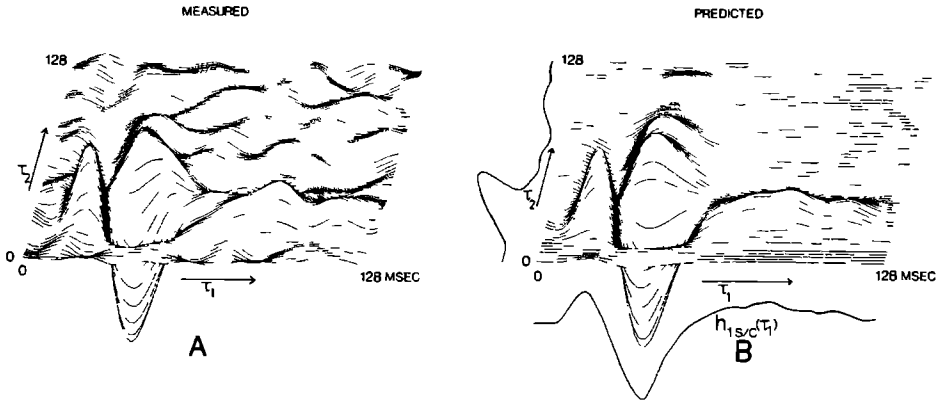nonlinear mechanism on the centre responses is not a simple second order
interaction.

Fig. 3.7. Measured (A) and predicted (B) crosskernels for an on-centre Y-cell.
Predicted crosskernel $h_{2,ab}(\tau_1,\tau_2)$ equals $h_{1,c/s}(\tau_1) \cdot h_{1,s/o}(\tau_2)$ apart
from a constant.

This result was found in all units (N=9), which were investigated. Since
it is known, that the nonlinear surround mechanism contains a second
order nonlinearity, because of the second order harmonic responses to
sinusoidal stimulation, this would suggest a nonlinear relation between
the centre stimulus and the power of the modulated signal in the surround
on the one hand and the response on the other hand. The quantitative
characterization of such an interaction suggests the calculation of
$h_{3,abb}(\tau_1,\tau_2,\tau_3)$. However, this kernel was equal in shape to
$h_{1,c/s}(\tau_1) h_{1,s/c}(\tau_2) h_{1,s/c}(\tau_3)$ apart from a constant, which can again be
explained as a nonlinear contribution from the spike generating mechanism
and not as an indication of a multiplicative action of the nonlinear
mechanism on the responses from the linear mechanisms.These results show,
that the multiplicative action of the nonlinear mechanism on the responses
from the linear mechanisms is difficult to characterize, at least with the
modulation depth, used in this study, and when the crosskernels are
calculated over 128 msec.

3.3.5. Responses to sine wave gratings

Also spatial sine wave gratings were used to investigate the spatial and temporal properties of the linear and nonlinear systems. In the receptive field of Y-cells a position can be found, where counterphase modulated sine wave gratings elicit no first harmonic responses but only second order harmonic responses (Hochstein and Shapley, 1976a). This enables one to investigate the spatial and temporal properties of the nonlinear mechanism. At other positions the counterphase modulated grating also elicits first order harmonic responses, whose amplitude depends on the position of the grating in the receptive field.

As in retinal ganglion cells (Hochstein and Shapley, 1976a) largest second order harmonic responses are obtained with counterphase gratings of high spatial frequency (Fig.3.8B), independent of the position of the grating in the receptive field, whereas lower spatial frequency gratings mainly elicit linear first order harmonics (Fig.3.8A). The spatial frequency which elicits maximum second order harmonic responses was between 6 and 12 cycles/deg (Fig.3.8E). Unfortunately the upper spatial frequency, which could be used in testing (12 cycles/deg), was still below the upper limit of the spatial resolution of Y-cells so that some units may have a nonlinear mechanism with a maximum spatial frequency sensitivity above 12 cycles/deg. The optimal spatial frequency of the linear systems was near 0.75 cycles/deg (mean over 12 neurones: 0.75 cycles/deg; range 0.1 - 2 cycles/deg).

The optimum temporal frequency of the linear responses varied between 4 and 8 Hz with a mean at 6.2 Hz over 12 neurones (Fig.3.8F). The optimum temporal frequency to elicit second order harmonics is near 4Hz (range: 0.5 - 6 Hz), indicating that the nonlinear mechanism is tuned to lower temporal frequencies than the linear mechanisms. This result also followed from the crosscorrelation results (Fig.3.6D). The fact that the nonlinear mechanism in Y-cells has higher spatial and lower temporal resolution than has the linear centre/surround portion of the receptive field is also found by Derrington et al. (1979) and by Lehmkuhle et al. (1980) in cat retinal ganglion cells and LGN neurones.

The increase of mean firing rate of Y-cells to moving gratings, which is found in cat (Enroth-Cugell and Robson, 1965) and monkey (De Monasterio, 1978a) retinal ganglion cells, was absent or very weak in monkey LGN
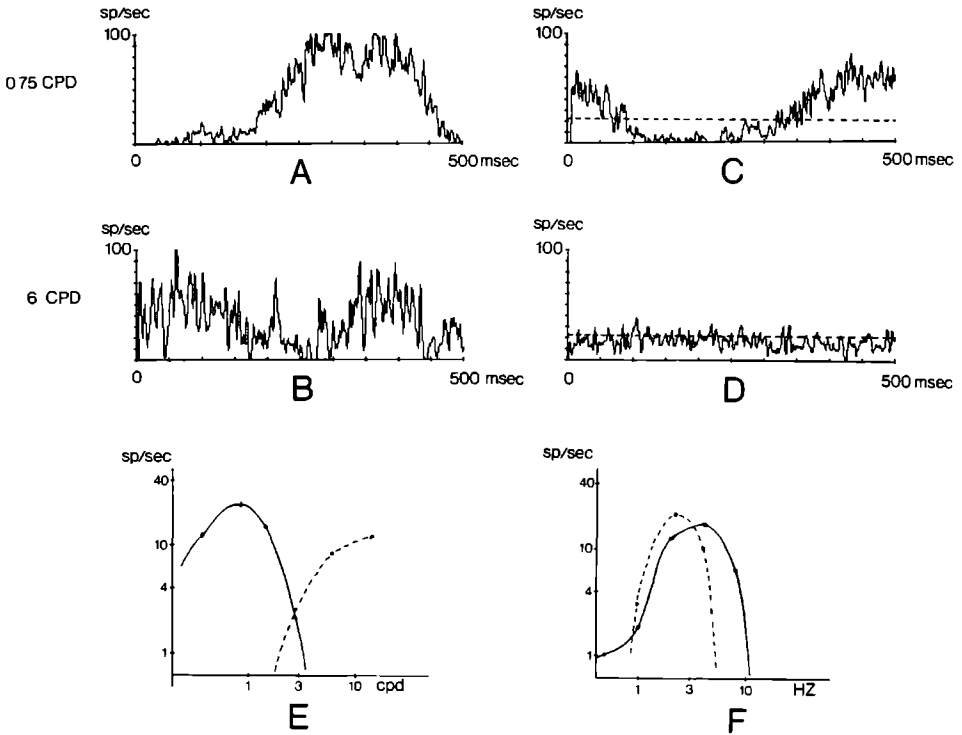
Fig.3.8. Responses to counterphase (A,B) and drifting (C,D) sine wave gratings
for a typical Y-cell. Contrast of gratings: 10%; temporal modulation:
2 Hz. First harmonic responses are elicited by 0.75 cycles/deg gratings
(A,C). Second harmonic responses are elicited by a 6 cycles/deg
counterphase grating (B). A 6 cycles/deg drifting grating gives no
modulation of firing rate nor does it increase the mean firing rate.
Dashed curve in C and D indicates the mean response of the neurone to
a diffuse steady stimulation at 30 td, which is the mean luminance of
the spatial sine wave gratings. Spatial transfer function at 4 Hz (E)
and temporal transfer function for the linear responses (at 1.5 cpd)
(full line) and for the second harmonic responses (dashed line) at
12 cpd, measured with counterphase gratings with several spatial
phases. Full and dashed lines are drawn by hand. Centre size: 7 min.
of arc (1/e value).

Y-cells (Fig.3.8C, D). This is also found in monkey and cat LGN Y-cells by Dreher et al. (1976) and So and Shapley (1979) and may be characteristic for LGN Y-cells. In some Y-cells, which gave very large second order harmonic responses to counterphase gratings, second order harmonic responses werd observed to drifting gratings. This was only seen for 12 cycles/deg gratings moving with 4 periods/sec over the receptive field. This was not a stimulus artefact since a photocell indicated a pure 4 Hz modulation and since X-cells never demonstrated this phenomenon.

3.3.6. Response prediction

In order to verify to what extent the results obtained with the GWN crosscorrelation method are sufficient to describe the responses of LGN Y-cells, the results were used to predict the responses to several stimuli.

The picture of the centre mechanism as a linear system was confirmed by the results of the response prediction to intensity increments and decrements of small spots (Fig. 3.9A). Within narrow limits the predicted response, based upon the kernels h_0, h_1 and h_2, and the measured response were equal; a representative example is shown in Fig.3.9A. The main effect of this second order response contribution is to nullify the negative responses predicted by the linear model. Similar results were observed in all 11 units which were investigated with small spots. However, this result only applies to small spots, e.g. 15 min. of arc. For larger spot sizes the measured response often is more transient than the predicted response based upon the first and second order kernels. This discrepancy can be explained by the fact, that large spot sizes also stimulate the nonlinear mechanism, which in its turn, acts on the centre responses by the multiplicative system. The time course of this nonlinear action could not be characterized by the second order Wiener kernels. Therefore a difference between predicted and measured responses could be expected for large stimuli. Probably small spots are too weak to stimulate the nonlinear mechanism effectively.

Fig.3.9B shows the predicted and measured responses to a short GWN stimulus. If the quadratic difference $\int(y(t) - h_0)^2 \, dt$ between measured response $y(t)$ and the average response h_0 during the GWN experiment is set to 100% (Marmarelis and Naka, 1974), the predicted response, based upon the kernels h_0, h_1 and h_2, deviates from the measured response with 31%.
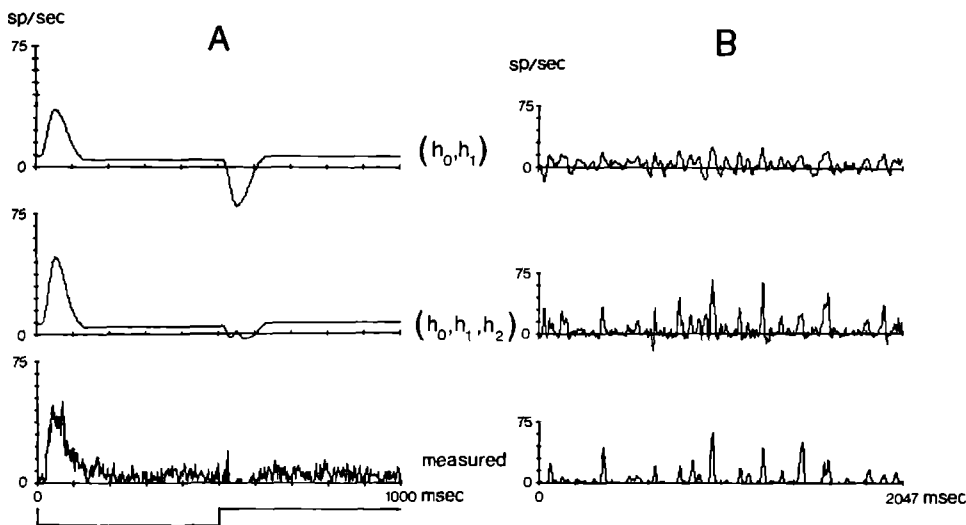
Fig. 3.9. A.Measured and predicted responses, based upon the linear model $\{h_0,h_1\}$ and nonlinear model $\{h_0,h_1,h_2\}$ for an off-centre Y-cell to intensity increments and decrements of 0.7 logunit. Stimulus is a spot (diameter: 15 min. of arc) in the centre. B.Measured and predicted responses, based on the linear $\{h_0,h_{1,c/s},h_{1,s/c}\}$ and nonlinear model $\{h_0,h_{1,c/s},$ $h_{1,s/c},h_{2,c/s,c/s},h_{2,s/c,s/c},h_{2,c/s,s/c}\}$ for on-centre Y-cell in a two-input experiment : a spot (15 min. of arc) and annulus were modulated with 50 Hz Low-pass filtered and uncorrelated GWN. Measured response is PSTH, obtained by averaging the responses to 100 stimulus presentations.

The linear model deviates from the measured response with 61%. The differences between measured and predicted responses to a short GWN-stimulus are mean values from the results of 3 neurones. Again the large difference of 31% between predicted and measured responses may be ascribed to the failure to characterize the time course of the multiplicative action on the responses from the linear systems.

3.4. Discussion

The results in this paper reveal several properties of Y-cells, which just as in retinal ganglion cells (De Monasterio, 1978a,b; Hochstein and Shapley, 1976a,b; Shapley and Victor, 1978) distinguish these neurones from X-cells. Apart from the second order harmonics, which were used as the classification criterion, Y-cells differ from X-cells in a clear attenuation of centre responses by independent stimulation in the surround, which we never saw in LGN X-cells. The first order kernel of the centre in X-cells does not differ within experimental error whether the surround is modulated or not. Moreover, LGN Y-cells have shorter response latencies than X-cells, which is reflected in the first order centre kernels of Y-cells (Figs.3.2 and 3.3) and X-cells (Fig.1.6). Mean response latency of the first order kernel is 18 msec (standard deviation: 5 msec) for Y-cells and 28 msec (standard deviation: 6msec) for X-cells, for stimulus intensities near 250 td. Another phenomenon, which distinguishes X- and Y-cells is that Y-cells have much larger second order kernels, even for centre responses. On the average second order kernels, obtained by stimulation by spots (15 min. of arc) or by diffuse stimuli, are four times larger for Y-cells than for X-cells. For the centre mechanism this is explained by the larger responsivity of Y-cells, compared to X-cells, which leads to a more pronounced response rectification in the spike generating mechanism of Y-cells. Especially when the surround stimulus is not modulated the centre of Y-cells is very responsive to small spot intensity modulations.

When the surround is stimulated the responsivity of Y-cells to small spots in the centre decreases, as is expressed in the decrease of size of the first order kernel (Fig.3.3). This decrease of the size of the first order kernel is accompanied by a shortening of response latency, which is never observed in X-cells. This decrease in response latency is compatible with the reduction in phase lag of the response, as found by Shapley and Victor (1978). They demonstrated, that the frequency selective gain attenuation was closely related to the decrease of phase lag, which made them to take the decrease of phase lag as a measure of nonlinear behaviour.

The model in Fig.3.1 is obviously only a first step to explain qualitatively the stimulus-response relations of LGN Y-cells. The model

ascribes the origin of the additive nonlinear responses and of the signals, which cause the multiplicative frequency-selective gain control, to one nonlinear mechanism. This is obviously rather speculative. However, for the sake of simplicity it is a justified way until the model is falsified by new data on the temporal and spatial characteristics of the mechanism, which generates the frequency selective gain control. Moreover, it should be noted, that the model in Fig.3.1 cannot explain all response properties of LGN Y-cells. The absence of an increase of mean firing rate with drifting sine wave gratings is compatible with a complete low-pass attenuation of the filter L_2 in the sandwich model. This conflicts with the experimental result that the second order frequency kernel is not zero for the frequencies $(-f,f)$.

The second order kernels, obtained by stimulation of the surround, reveal information on the nonlinear mechanism in the receptive field, which gives the additive response contributions. Shapley and Victor (1979) demonstrated that the nonlinear mechanism is for the greater part characterized by the second order kernel and to a lesser extent by third or fourth order nonlinear response contributions, which is plausible since clear second order, but no large higher harmonics are generated with counterphase gratings. To what extent these kernels characterize this nonlinear mechanism in LGN Y-cells could not be tested by response prediction since large annuli as used in these experiments also stimulate the linear surround mechanism and thereby involve the multiplicative action of the nonlinear mechanism on the responses from the linear surround mechanism. Since this multiplicative action could not be characterized by the Wiener kernels, a discrepancy between predicted and measured responses for surround stimulation has to be expected.

The peak temporal frequency of the nonlinear mechanism near 5 Hz, which was found both with the GWN crosscorrelation method and with counterphase modulated sine wave gratings, is in the range of peak frequencies (1-8 Hz) as found by Victor and Shapley (1979a) for several spatial frequencies in the same luminance range. In agreement with results of Derrington et al. (1979) in cat retinal ganglion cells and of Lehmkuhle et al. (1980) in cat LGN units, we also found that the nonlinear mechanism, which generates the second order harmonic responses has higher spatial and lower temporal resolution than the linear systems in Y-cells.

Enroth-Cugell and Lennie (1975) have reported the difficulty to

isolate surround responses in retinal ganglion Y-cells. We had the same difficulty in LGN Y-cells (Fig.3.2 and 3.3). The existence of a surround mechanism is clear from the low-frequency attenuation in the spatial transfer function in Y-cells (Fig.3.8E). However, only after adaptation of the centre mechanism a centre-antagonistic first order surround kernel could be obtained, which was somewhat delayed with respect to the centre kernel, but which further had a rather similar time course, just as in X-cells. However, also with adaptation of the centre the predicted responses to intensity increments were much more transient than was predicted by the Wiener kernels, probably by the multiplicative action by the nonlinear mechanism. Whether or not the summation of the responses of the linear centre and surround mechanism is linear could not be decided, because stimulation of the linear surround mechanism also elicited responses from the nonlinear mechanism, which modifies the responses of the linear mechanism in a nonlinear way and by that makes an accurate investigation into the nature of the combination of centre and linear surround responses very difficult.

As already suggested by Jakiela (1978) and by Victor and Shapley (1979), the subsystems in the model in Figure 3.1 can be related to anatomical structures. Werblin (1972) has shown that in mudpuppy the rotation of a concentric windmill affects the responses of amacrine and ganglion cells, but not of bipolar cells. Moreover, Werblin (1977) demonstrated, that in mudpuppy the relatively slow, sustained light responses in bipolar cells are converted into rapid, transient activity in on-off ganglion cells by the activity from amacrine cells. This suggests that the linear centre and surround responses are present in bipolar cells and are modified at the transition to the ganglion cell by activity from amacrine cells, which may be part of the nonlinear mechanism. This identification of anatomical structures with functional subsystems in Y-cells locates the relevant information processing in the retinal net-work leaving room for speculation on the information transfer in LGN Y-cells.

3.5. References

Barlow,H.B., Derrington,A.M., Harris,L.R. and Lennie,P. (1977), The effects of remote retinal stimulation on the responses of cat retinal ganglion cells. J.Physiol.Lond., 269, 177-194.

De Monasterio,F.M. (1978a), Properties of concentrically organized X
and Y ganglion cells of macaque retina. J.Neurophysiol., 41,
1394-1417.

De Monasterio,F.M. (1978b), Center and surround mechanisms of opponent-
color X and Y ganglion cells of the retina of macaques. J.Neuro-
physiol., 41, 1418-1434.

Derrington,A.M., Lennie,P. and Wright,M.J. (1979), The mechanism of
peripherally evoked responses in retinal ganglion cells. J.Physiol.
Lond.,289, 299-310.

De Valois,R.L., Snodderly,D.M., Yund,E.W. and Hepler,N.K. (1977), Sens.
Processes, 1, 244-259.

Dreher,B., Fukada,Y. and Rodieck,R.W. (1976), Identification, classifi-
cation and anatomical segregation of cells with X-like and Y-like
properties in the lateral geniculate nucleus of old-world primates.
J.Physiol.Lond., 258, 433-452.

Enroth-Cugell,C. and Robson,J.G. (1966), The contrast sensitivity of
retinal ganglion cells of the cat. J.Physiol.Lond., 187, 517-552.

Enroth-Cugell,C. and Lennie,P. (1975), The control of retinal ganglion
cell discharge by receptive field surrounds. J.Physiol.Lond., 247,
551-578.

Hochstein,S. and Shapley,R.M. (1976a), Quantitative analysis of retinal
ganglion cell classifications. J.Physiol.Lond., 262, 237-264.

Hochstein, S. and Shapley,R.M. (1976b), Linear and nonlinear spatial
subunits in Y cat retinal ganglion cells. J.Physiol.Lond., 262,
265-284.

Jakiela,H.G. (1978), The effect of retinal image motion on the responsive-
ness of retinal ganglion cells in the cat. Thesis. University of
Illinois, U.S.A.

Kratz,K.E., Webb,S.V. and Sherman,S.M. (1978), Electrophysiological
classification of X- and Y-cells in the cat's lateral geniculate
nucleus. Vision Res., 18, 489-492.

Krüger,J. and Fischer,B. (1973), Strong periphery effect in cat retinal
ganglion cells. Excitatory responses in on- and off-centre neurones
to single grid displacements. Exp.Brain Res.,18, 316-318.

Lee,Y.W. and Schetzen,M. (1965), Measurement of the Wiener kernels of a
non-linear system by cross-correlation. J.Int.Control, 2, 237-254.

Lehmkuhle,S., Kratz,K.E., Mangel,S.C. and Sherman,S.M. (1980), Spatial
and temporal sensitivity of X- and Y-cells in the dorsal lateral
geniculate nucleus in the cat. J.Neurophysiol., 43, 520-541.

Maffei,L., Cervetto,L. and Fiorentini,A. (1970), Transfer characteristics
of excitation and inhibition in cat retinal ganglion cells. J.
Neurophysiol.,23, 276-284.

Marmarelis,P.Z. and Naka,K-I.(1974), Identification of multi-input
biological systems. IEEE Trans. on Biomed. Eng. Vol. BME-21,
88-101.

Marmarelis,P.Z. and Marmarelis,V.Z. (1978), Analysis of physiological
systems. Plenum Press, New York, 1978.

Ratliff,F., Knight,B.W., Toyoda,J.-I. and Hartline,H.K. (1967), Enhance-
ment of flicker by lateral inhibition. Science, 158, 392-393.

Shapley,R.M. and Hochstein,S. (1975), Visual spatial summation in two
classes of geniculate cells. Nature, 256, 411-413.

Shapley,R.M. and Victor,J.D. (1978), The effect of contrast on the transfer
properties of cat retinal ganglion cells. J.Physiol.Lond., 285,
275-298.

Shapley,R.M. and Victor,J.D. (1979), Nonlinear spatial summation and the
contrast gain control of cat retinal ganglion cells. J.Physiol.Lond.,
290, 141-161.

So,Y.T. and Shapley,R.M. (1979), Spatial properties of X and Y cells in
the lateral geniculate nucleus of the cat and conduction velocities
of their inputs. Exp.Brain Res., 36, 533-550.

Swerup,C. (1978), On the choice of noise for the analysis of the
peripheral auditory system. Biol.Cybernetics, 29, 97-104.

Thibos,L.N. and Werblin,F.S. (1978a),The response properties of the steady
antagonistic surround in the mudpuppy retina. J.Physiol., 278,
79-99.

Thibos,L.N. and Werblin,F.S. (1978b),The properties of surround antagonism
elicited by spinning windmill patterns in the mudpuppy retina. J.
Physiol., 278, 101-116.

Victor,J.D. and Shapley,R.M. (1979a), Receptive field mechanisms of cat
X and Y retinal ganglion cells. J.Gen.Physiol., 74, 275-298.

Victor,J.D. and Shapley,R.M. (1979b), The nonlinear pathway of Y ganglion
cells in the cat retina. J.Gen.Physiol., 74,671-689.

Victor,J. and Shapley,R. (1980), A method of nonlinear analysis in the
frequency domain. Biophys.J., <u>29</u>, 459-484.

Werblin,F.S. (1972), Lateral interactions at inner plexiform layer of
vertebrate retina: antagonistic responses to change. Science, <u>175</u>,
1008-1010.

Werblin,F.S. (1977), Regenerative amacrine cell depolarisation and
formation of on-off ganglion cell response. J.Physiol.Lond., <u>264</u>,
767-785.

Wunk,D.F. and Werblin, F.S. (1979), Synoptic inputs to the ganglion
cells in the tiger salamander retina. J.Gen.Physiol., <u>73</u>, 265-286.

C H A P T E R   4

SAMENVATTING

Het doel van dit onderzoek was een algemene karakterisering te geven
van neuronen, die een rol spelen bij de informatieverwerking in het
visuele systeem zó, dat de responsies van deze neuronen op velerlei
stimuli begrepen kunnen worden op grond van enige fundamentele eigen-
schappen.

Het licht,dat als functie van plaats en tijd op de retina valt,
wordt geabsorbeerd door een viertal typen receptoren, namelijk drie
typen kegeltjes en de staafjes, waarbij de electrische spanning van de
receptor verandert afhankelijk van het aantal geabsorbeerde quanten. Na
een complexe signaalverwerking in de retina gaat een gedeelte van de in-
formatie naar het Corpus Geniculatum Laterale (CGL), dat op zijn beurt
naar de visuele cortex projecteert.

Het object van deze studie wordt gevormd door de neuronen in het
CGL van de rhesus aap. Op grond van de al dan niet lineaire sommatie van
visuele informatie in het 'centre' en de 'surround' van het receptieve
veld kunnen deze neuronen geklassificeerd worden in 2 typen: X en Y.
Hoofdstuk 1 en 2 van dit proefschrift hebben betrekking op X-cellen (met
lineaire spatiële sommatie), terwijl het derde hoofdstuk betrekking heeft
op de eigenschappen van Y-cellen (met niet-lineaire spatiële sommatie).

De temporele eigenschappen van X-cellen blijken af te hangen van de
spectrale samenstelling van de stimulus en veranderen geleidelijk met
verandering in golflengte van het licht. 'Centre' en 'surround' hebben elk
een verschillende spectrale gevoeligheid, hetgeen een gevolg is van het
feit, dat de 'centre'- en 'surround'-responsie bepaald worden door ver-
schillende kegelmechanismen. Aangezien de spectrale gevoeligheden van de
receptormechanismen elkaar overlappen, is het niet mogelijk slechts één

receptormechanisme te stimuleren. Daar echter de responsie van de cel
gelijk blijkt te zijn aan de lineaire optelling van de responsies van
'centre' en 'surround', hetgeen ook een lineaire sommatie van de responsie-
bijdragen van de kegelmechanismen impliceert, en aangezien de spectrale
gevoeligheid van de receptormechanismen bekend is, kon met behulp van
een multipele lineaire regressie het tijdsverloop van de individuele
kegelmechanismen bepaald worden. De drie kegelmechanismen blijken nage-
noeg identieke temporele eigenschappen te hebben. Tussen neuronen
onderling varieert slechts het teken van de responsie, de sterkte ervan
en het tijdsinterval tussen stimulus en responsie. Bovendien blijkt het
neurale systeem, waaronder hier begrepen is de absorptie van lichtquanten
door de receptoren, de informatieverwerking in de retina tot en met de
verwerking door CGL neuronen, zich, afgezien van gelijkrichting, lineair
te gedragen binnen een intensiteitsbereik van 0.5 logunit, aangezien de
responsie op stapvormige intensiteitsveranderingen gelijk is aan de
convolutie van de stimulus met de eerste orde kruiscorrelatiefunctie,
welke voor een lineair systeem gelijk is aan de impulsresponsie. Deze
resultaten konden gecontroleerd en bevestigd worden voor het rode en
groene kegelmechanisme met behulp van de spectrale compensatie-methode,
waarbij twee stimuli met verschillende spectrale samenstelling zodanig in
tegenfase worden gemoduleerd, dat de responsie van het neuron afkomstig
is van slechts één kegelmechanisme.

Aangezien het temporeel verloop van de responsiebijdragen van de 3
kegelmechanismen voor alle X-cellen nagenoeg identiek is, is het gedrag
van een neuron volledig bepaald, indien het teken, de sterkte en de tijds-
vertraging van de responsiebijdragen bekend zijn. In het tweede hoofdstuk
worden deze parameters voor een aantal neuronen gegeven en worden de res-
ponsies op in kleur en helderheid gemoduleerde stimuli voorspeld met
behulp van deze parameters. Tengevolge van het verschil in latentietijd van
de responsies van de kegelmechanismen, die via 'centre' en 'surround' aan
de celrespons bijdragen, vertoont de overdrachtsfunctie van het neuron
bij kleurmodulatie minder laagfrequente afsnijding en meer hoogfrequente
afsnijding dan de overdrachtsfunctie voor helderheidsmodulatie. Het ver-
schil tussen de overdrachtsfuncties is evenwel betrekkelijk klein. Hoewel
het gedrag van deze neuronen kwalitatief in overeenstemming is met psycho-
fysisch gemeten resultaten, is er een kwantitatief verschil met de psycho-
fysica, omdat de psychofysisch gemeten afsnijfrequentie aan de hoogfre-

quente kant van de overdrachtsfunctie veel lager ligt dan de afsnij-
frequentie van deze neuronen bij kleurmodulatie.

In het derde hoofdstuk wordt ingegaan op de eigenschappen van Y-
cellen. Deze eigenschappen zijn onderzocht met behulp van de kruiscorre-
latie methode met witte ruis als stimulus. Bij niet al te complexe systemen
is het mogelijk uit de resultaten, verkregen met deze methode, de eigen-
schappen van de subsystemen in een model te bepalen. Het 'centre'-
mechanisme in Y-cellen blijkt zich lineair te gedragen. Behalve het
'centre'-mechanisme bestaat het receptief veld van Y-cellen uit een
lineair en een niet-lineair 'surround'-mechanisme. Stimulatie van het
niet-lineaire mechanisme leidt tot 2e orde harmonische responsies van het
neuron en tot een frequentie-selectieve verandering van de responsies van
de lineaire systemen: de temporeel laagfrequente responsies worden ver-
zwakt. De resultaten van de kruiscorrelatiemethode leiden tot een karak-
terisering van de lineaire en niet-lineaire mechanismen. Echter, de
alineaire interactie tussen lineaire en niet-lineaire systemen kon niet
volledig met deze methode worden gekarakteriseerd.

Ik ben geboren op 18 december 1952 te Breda. Aan het 'Onze-Lieve-Vrouwe'-
lyceum te Breda heb ik mijn gymnasium β opleiding gevolgd, welke in 1971
werd afgerond. In september 1971 ben ik natuurkunde gaan studeren aan de
Katholieke Universiteit Nijmegen. Na het kandidaatsexamen in maart 1974
heb ik mijn afstudeeronderzoek verricht op het laboratorium voor Medische
Fysica en Biofysica onder leiding van dr.P.I.M.Johannesma aan de in-
formatieverwerking in het auditieve systeem van de kat. Vanaf augustus
1976 ben ik als wetenschappelijk medewerker verbonden aan het laboratorium
voor Medische Fysica en Biofysica te Nijmegen in het kader van een
promotie-onderzoek in dienst van de Nederlandse Organisatie voor Zuiver
Wetenschappelijk Onderzoek. Hier heb ik onderzoek verricht aan de visuele
informatieverwerking door hersencellen in het Corpus Geniculatum Laterale
van de rhesus aap. Sinds 1 augustus 1980 ben ik als wetenschappelijk mede-
werker verbonden aan het laboratorium voor Medische Fysica aan de Rijks-
universiteit Utrecht.

1. Het resultaat van Gouras en Zrenner, dat de overdrachtsfunctie van de kleur-opponente neuronen bij kleurmodulatie minder laagfrequente en meer hoogfrequente afsnijding heeft dan bij helderheidsmodulatie, is slechts kwalitatief in overeenstemming met psychofysische metingen. Er ligt een kwantitatieve discrepantie in de hoogfrequente afsnijfrequentie van de psychofysische en neuraal gemeten overdrachtsfuncties.

> P.Gouras en E.Zrenner, Science, <u>205</u>,
> 587-589, 1979.
> Dit proefschrift.

2. De conclusie van Creutzfeldt, Lee and Elepfandt, dat de responsies van de drie kegelmechanismen niet lineair optellen in kleur-opponente neuronen in het CGL van de rhesus aap volgt niet dwingend uit hun experimentele resultaten. Daar de temporele eigenschappen van X-cellen variëren als functie van de golflengte van het licht, mogen de piekresponsies op bewegende lichtspleten van verschillende golflengte niet worden gebruikt als maat voor de gevoeligheid van het neuron bij verschillende golflengten.

> O.D.Creutzfeldt, B.B.Lee en A.Elepfandt,
> Exp.Brain Res., <u>35</u>, 527-545, 1979
> B.B.Lee, O.D.Creutzfeldt en A.Elepfandt,
> Exp.Brain Res., <u>35</u>, 547-557, 1979

3. De bewering van Victor en Shapley, dat de 'sum of sinusoids'-methode een betere signaal-ruis verhouding geeft bij de karakterisering van systeemeigenschappen, dan de kruiscorrelatie-methode met behulp van gaussisch witte ruis, welke leidt tot de Wiener kernels, is niet correct. De 'sum of sinusoids'-methode veronderstelt een geleidelijke verandering van de systeemeigenschappen als functie van de frequentie. Deze veronderstelling staat toe de Wiener kernels te "smoothen",waarna een gelijke signaal-ruis verhouding verkregen wordt.

> J.D.Victor, Proc.Natl.Acad.Sci., USA,
> <u>76</u>, 996-998,1979

4. De benaming 'contrast gain control' door Shapley en Victor voor het verschijnsel, dat de overdrachtsfunctie van de lineaire subsystemen in

het receptieve veld van Y-cellen verandert bij toename van het contrast van de stimulus is misleidend.

R.M.Shapley en J.D.Victor, J.Physiol.,
285, 275-298,1978

5. Het is zeer verwonderlijk, dat de temporele eigenschappen van kleur-opponente neuronen in het CGL, dat deel uitmaakt van de enige tot nu toe bekende neurale baan met informatie over de kleur van visuele beelden, wel overeenkomen met psychofysische metingen voor helderheidsmodulatie, maar niet voor kleurmodulatie.

H.Spekreijse, D.van Norren, T.J.T.P.van
den Berg, Proc.Natl.Acad.Sci., USA, 68,
2802-2805, 1971.
Dit proefschrift.

6. De 'amplitude transition function', zoals gepresenteerd door Becker en Jürgens staat niet toe de karakteristieken te bepalen van het systeem dat berekent waarheen een saccade gemaakt moet worden, aangezien de 'amplitude transition function' verkregen is door gegevens van sacca-dische responsies op verschillende stimuli bij elkaar te nemen en dus alleen de gemiddelde responsie weergeeft op een aantal verschillende stimuli.

W.Becker en R.Jürgens, Vision Res., 19,
967-983, 1979

7. Het schaarser worden van de financiële middelen voor wetenschappelijk onderzoek, gepaard met een gewijzigde prioriteitenstelling, waarbij een groter gewicht wordt toegekend aan toegepast en maatschappelijk relevant onderzoek, kan een bedreiging gaan vormen voor het zuiver wetenschappe-lijk onderzoek.

8. De problemen met betrekking tot de belangen van minderheden bij de besluitvormingsprocedure in de huidige organisatiestructuur van de westerse samenleving,vormen een ernstige bedreiging voor de verhoudingen tussen leden van de samenleving, waardoor enige fundamentele democra-tische verworvenheden in gevaar kunnen komen.

Nijmegen, 11 september 1980   Stan Gielen